International Meteor Organization

METEOR SHOWER WORKBOOK 2014



Edited by
Jürgen Rendtel

.

Cover photo: Image of the 2007 Geminids composed from 113 frames exposed December 12–15 from Ludanyhalaszi, Hungary (image: Erno Berkö, Hungary)

Meteor shower workbook 2014

ISBN 978-2-87355-027-1

Printed in Belgium

©2014 International Meteor Organization

METEOR SHOWER WORKBOOK 2014

Edited by
Jürgen Rendtel

With contributions from

Rainer Arlt, David J. Asher, Jeffrey Brower, Audrius Dubietis, Esko Lyytinen, Alastair McBeath, Robert H. McNaught, Sirko Molau, Jürgen Rendtel, Paul Roggemans, Jérémie Vaubaillon, Cis Verbeeck,

International Meteor Organization
Potsdam, 2014

Table of contents

Preface ... 3
Foreword ... 5

Chapter 1: Meteor showers: designation and general information ... 7
Meteor shower descriptions ... 7

Chapter 2: Shower data ... 9
Working list ... 9
Antihelion source ... 13
Quadrantids (010 QUA) ... 14
α-Centaurids (102 ACE) ... 18
γ-Normids (118 GNO) ... 19
Lyrids (006 LYR) ... 20
π-Puppids (137 PPU) ... 22
η-Aquariids (031 ETA) ... 23
η-Lyrids (145 ELY) ... 25
June Bootids (170 JBO) ... 26
α-Capricornids (001 CAP) ... 28
Southern δ-Aquariids (005 SDA) ... 30
Piscis Austrinids (183 PAU) ... 31
Perseids (007 PER) ... 32
κ-Cygnids (012 KCG) ... 37
Aurigids (206 AUR) ... 38
September ε-Perseids (208 SPE) ... 40
Draconids (009 DRA) ... 42
δ-Aurigids (224 DAU) ... 45
ε-Geminids (023 EGE) ... 46
Orionids (008 ORI) ... 47
Leonis Minorids (022 LMI) ... 49
Taurids (017 NTA, 002 STA) ... 50
Leonids (013 LEO) ... 54
α-Monocerotids (246 AMO) ... 58
Phoenicids (254 PHO) ... 60
Puppid-Velids (301 PUP) ... 61
Monocerotids (019 MON) ... 63
σ-Hydrids (016 HYD) ... 65
Geminids (004 GEM) ... 66
December Leonis Minorids (032 DLM) ... 69
Comae Berenicids (020 COM) ... 70
Ursids (015 URS) ... 71

Chapter 3: Daytime showers ... 73
Observing possibilities ... 73
List of daytime showers ... 74

Appendix:
Extreme events of the past $\approx$ 50 years ... 79
Glossary and Journal abbreviations ... 81

Preface

All previous editions of the *Handbook for Visual Meteor Observers* (1995) and the *Handbook for Meteor Observers* (first published in 2008) included information about observing techniques and meteor showers. The 1995 edition was written before the series of Leonid outbursts. At that time, the series of Perseid peaks was still in progress. Next we recorded the outbursts of the June-Bootids (1998), the α-Monocerotids (1995) and the Aurigids (2007). The 2008 Handbook edition was just printed when the September ε-Perseids peaked, followed by interesting displays of the Draconids in 2011 and 2012, again of the September ε-Perseids in 2013 and the recent activity of the Camelopardalids associated with comet 209P/LINEAR on 2014 May 24. The 2008 Handbook was reprinted twice, in 2009 and 2011, with updates in the shower section particularly in the 2011 edition. Since we will continuously find new results, this part of the Handbook will need updates on a regular basis, of course, not replacing the well-known annual *Meteor Shower Calendar.*

The shower descriptions always reflect the current knowledge based on recent observations and their analyses while the description of the observing techniques changes only over longer timescales. Therefore we now separated the contents into two parts: one devoted to the observing techniques and this *Workbook* containing the shower information.

In the last decade, changes of the observing techniques allowed us to tackle open questions which were difficult to solve when the amount of data was not sufficient. Comprehensive analyses of video data improved our knowledge about minor sources and outer regions of major showers. At the same time, the IAU established a meteor shower data base and shower designations became unambiguous. As a consequence, the shower descriptions in the workbook includes the respective references and sources and will be a quasi-periodic shower manual loosely correlated with the three-year period of the official IAU shower nomenclature update.

Many people—as listed at the front page—helped and contributed. Without their work this workbook would not have been possible. I am particularly grateful to David Asher for his contributions concerning various subjects and his detailed comments. Rainer Arlt worked on many shower data for the previous edition which have been updated. Nevertheless, I felt – during the process of writing the different chapters – that things must remain incomplete. This is a typical situation in science, as we summarize the current knowledge as of today, knowing that projects and publications are underway with exciting new results. As in the previous editions of the Handbook, the references were placed into the chapters and sections rather than into a long list at the end of the book. The data stored in the IMO's *Visual Meteor Data Base*, VMDB, covering more than 25 years now, were used to calculate average activity profiles for most of the showers. Results obtained from the fast growing amount of video meteor data which are published in the IMO Journal *WGN* on a regular basis added to the provided information. For the first time, a chapter on daytime showers is added. It is very likely that further analyses of radar and radio forward scatter data will require considerable modifications soon. I look forward to see such new results of this less known meteoroid population.

I hope that this workbook will encourage meteor workers all over the world to further extend and improve their work, to learn more about the phenomena they are observing, and, above all, to participate in the continually growing international efforts in meteor science. Consequently, the workbook will need updates soon, but with the "two-part solution" we may follow the increase of our knowledge about meteors quite closely.

Potsdam, Germany, July 2014

Jürgen Rendtel

Foreword

Jérémie Vaubaillon

It is my pleasure and an honour to write a few words for this "meteor shower workbook 2014", for many reasons. The first is, as a member of the international meteor organization, to take an active part in this worldwide, long-lasting effort and enjoy as well as increase our knowledge of the meteor showers in general. Second, almost everything I know about meteor observation I learned from the IMO members, during International Meteor Conferences.

This book is the kind w will all refer to many times during the year, in order to answer critical questions such as: is my country best located for the observation of the shower? If not where shall I go? What will be the level of such showers this year? What are the main scientific question to tackle? What can I do in order to help participate to the scientific effort and to answer those questions? What is the best observation strategy? And so on.

The year 2014 will be rich in meteor events, as the reader can discover in this book. In addition to everything mentioned here, we witnessed the birth of a new meteor shower coming from comet 209P/LINEAR (2004 CB) on the 24th May. Another major event is the forecasted meteor "hurricane" at Mars on 19th October, caused by comet C/2013 A1 approaching the planet at a very close distance.

I need to confess that I am always extremely surprised and impressed by those observers spending many hours in the dark, counting the meteors and keeping in mind than they are participating to a world effort. Some might not even witness a major outburst, but still, their data is useful because it tells us about the overall activity of a given shower. As often in research, to observe nothing is nevertheless a result in itself. But of course, the most exciting comes from the observation of meteor outburst or just the regular shower, adding to the overall already existing data recorded for decades now.

Unless a tremendous amount of time, energy and money is spent, there is no way any professional will ever gather the amount of data recorded by the International Meteor Organization, thanks to all of the meteor enthusiasts around the world. Such a world and continuous coverage is probably unique in the world of astronomy, and the collaboration between professionals and amateurs is essential for science to keep going on. In addition to the impressive quantity of data, now available online with a few click, the quality assessments provided by IMO members results in reliable data to be directly used by anyone to conduct research and find new features and new meteor showers. The diversity of the observations demonstrate that anybody can participate, depending on her/his motivation and means.

Last but not least, the live profile of a major shower available directly on the IMO website is a tremendous tool in order to know what is happening on the other side of the world while it is still daylight at home, or, on a more personal note, in order to quickly and effectively verify that a meteor shower prediction is actually correct (or not ...). I will always remember the night of the 8th October 2011, after landing from the 2011 first European Draconids observation campaign, checking online and discovering that the predicted peak actually occurred! It was such an immense relief!

For all these reasons, I cannot express enough my gratitude you towards the IMO members and all the observers around the planet, who patiently and continuously participate to the world effort. To all of you, I wish clear skies!

Chapter 1

Meteor showers: designation and general information

1.1 Meteor shower descriptions

1.1.1 Shower designations

The first recognized radiants were named after the constellation in which the radiant was situated. However, in the 19th century, neither the borders of the constellations were exactly defined nor even the constellations themselves were fixed. Furthermore, during the period of 'radiant hunting' a huge number of radiants needed a designation. This led to the known nomenclature of showers.

Recently, the IAU adopted a system of official meteor shower nomenclature (Jenniskens, 2006), keeping in mind that during discovery the peak time and radiant position are not always known precisely. The general rule is that a meteor shower (and a meteoroid stream) should be named after the then current constellation that contains the radiant, specifically using the possessive Latin form. The possessive Latin name for the constellations end in one of seven declensions:
-ae (e.g., Lyrae),
-is (e.g., Leonis),
-i (e.g., Ophiuchi),
-us (e.g., Doradus),
-ei (e.g., Equulei),
-ium (e.g., Piscium), or
-orum (e.g., Geminorum).

Customary is to replace the final suffix by '-id', or plural '-ids'. Therefore, meteors from Aquarius (Aquarii) are Aquariids, not Aquarids. An exception is made for meteors from the constellation of Hydrus, which will be called "Hydrusids", in order not to confuse with meteors from the constellation of Hydra.

When the constellation name has two parts, only the second declension is to be replaced by 'id'. Hence, meteors from Canes Venatici (Canum Venaticorum) would be 'Canum Venaticids'. When two constellations are grouped together, a bracket is used and both constellation names will have 'id' – hence, Puppids-Velids.

If a higher precision is needed, then the shower is named after the nearest (if in doubt: brightest) star with a Greek letter assigned, as first introduced in the Uranometria atlas by Johann Bayer (1603), or one with a later introduced Roman letter. If in doubt, the radiant position at the time of the peak of the shower (in the year of discovery) should be taken. Hence, the meteors of comet C/1983 H1 IRAS-Araki-Alcock would be named 'η-Lyrids'.

Following existing custom, one may add the name of the month to distinguish among showers from the same constellation. In this case, one could call the shower from comet IRAS-Araki-Alcock the 'May Lyrids', in order to differentiate from the more familiar 'April Lyrids'.

For daytime showers (see Chapter 3), it is custom to add 'Daytime', hence the name for the 'Daytime Arietids' in June as opposed to the Arietids in October.

South and North refer to 'branches' of a shower south and north of the ecliptic plane (strictly the orbital plane of Jupiter), resulting from meteoroids of the same (original) parent body. Because they have nearly the same longitude of perihelion at a given solar longitude (the argument of perihelion and longitude of ascending node both differing by 180 degrees between South and North), the two branches are active over about the same time period.

If the meteoroid stream is encountered at the other node, it is customary to speak of 'twin showers'. The Orionids and η-Aquariids are twin showers, even though they represent dust deposited at different times and now in quite different orbits. As a matter of custom, twin showers and the north and south branches of a stream carry different names. Meteor showers are not to be named after their parent bodies (e.g., Giacobinids, IRAS-Araki-Alcockids). The names of comets tend not to be Latin, making the naming not unique. Also, comet names can change when they get lost and are recovered.

The Task Group for Meteor Shower Nomenclature of the IAU Commission 22 will choose among possible alternative proposed names for newly identified meteor showers, in order to establish a unique name for each meteor shower (e.g., η-Lyrids, not May Lyrids). This should also make sure which shower/stream is described or analysed.

The list of established meteor showers will also be posted at the IAU Meteor Orbit Data Center website: `http://www.astro.sk/~ne/IAUMDC/`. Additionally to the shower name a number is given in the IAU database which we include in our compilation. Hence a shower is

unambiguously designated by the IAU number and code plus the listed name. As an example, the list begins with the α-Capricorninds (001 CAP).

Some constellations 'disappeared' when they were officially defined by the *IAU* in 1925 and 1927. The most famous example is the Quadrans Muralis with the strong shower named the *Quadrantids*.

The lack of exact constellation borders until their definition also causes 'wrong' shower names. Applying the rule given above, we should observe the *Herculids* in April, not the *Lyrids*.

This effect becomes more obvious when individual stars are used to distinguish several radiants:

Shower	Distance to the star at ZHR max.	Appropriate shower name
Southern δ-Aquariids	2°	δ-Aquariids
Northern δ-Aquariids	13°	κ-Aquariids
Southern ι-Aquariids	3°	ι-Aquariids
Northern ι-Aquariids	8°	ξ-Aquariids

Therefore the shower names contain a 'historical component', and surely a change of the names will cause much more confusion than the further use of the traditional designations.

1.1.2 General remarks

Next, we will introduce the individual meteor showers which are suitable for visual observations according to the goal defined in the beginning of this Chapter. This review is by no means complete and contains only a brief summary of observed facts and theoretical research. A more complete description of meteor streams in general can be found in Jenniskens (2006). The aim of this Chapter is to provide you with some background information on meteoroid stream dynamics, evolution and observational features. Reading this part of the book will enable you to develop a clearer picture of a meteoroid stream in the Solar System. The short historical review should stimulate your observational efforts to monitoring meteor shower activity. We hope to use your observations to update further editions of this publication!

1.1.3 On the data

The **radiants** given are derived from visual, photographic, video, and radar meteor observations. We add information about the accuracy and peculiarities with the individual shower descriptions.

Each radiant drifts about 1° per day eastwards. A detailed explanation is given in Chapter 2 of the Meteor Observers Handbook. The geocentric (this is practically the observed) radiant of a meteor stream results from the vectorial addition of the motion of the Earth and the meteoroid. As both vectors change while the Earth crosses the stream, the geocentric radiant changes as well. This change is observed as a drift *parallel to the ecliptic*, i.e., the ecliptic longitude λ of the radiant position increases with time while the ecliptic latitude β remains constant. For certain showers, a drift in β is possible, but generally this component is of the order of 10% of the drift in λ only. This means radiants close to one of the poles of the ecliptic seem to be nearly stationary while those near the ecliptic itself move considerably. The concrete amount of the daily drift depends on the orbit of the meteor stream and the geometrical conditions of its intersection with the Earth's orbit. For a few showers, the radiant drift was determined by photographic or video observations. In most cases, these results were expressed in $\Delta\alpha$ and $\Delta\delta$ rather than in $\Delta\lambda$ and $\Delta\beta$. While the latter expressions are linear at any point of the sky, the former become non-linear in certain regions.

Therefore, the given drifts $\Delta\alpha$ and $\Delta\delta$ were converted into $\Delta\lambda$ and $\Delta\beta$ for the date of maximum. Using the drifts in ecliptic coordinates, the tables for the radiant drift given in this Chapter were computed.

But there are some showers in the *IMO* Working List for which the drift is not known. To obtain a characteristic value of the drift in λ, the observed values for showers that are not too close to one of the ecliptic poles were simply averaged. The average is $\Delta\lambda = 0\overset{\circ}{.}86$ per day with an empirical standard deviation of $\pm 0\overset{\circ}{.}13$, the extreme values being $0\overset{\circ}{.}63$ and $1\overset{\circ}{.}03$. If no drift is given in the characteristics of a shower in, the table of the radiant drift was computed using $\Delta\lambda = 0\overset{\circ}{.}86$ per day and $\Delta\beta = 0$. For the radiant complexes of the Antihelion source and the Puppid-Velids, the drift is overlayed by the activity of subradiants. The centres of these complexes are thus given according to the results of visual or/and video observations without any additional computations.

The enormous amount of data stored in the IMO's VMDB on a continuous basis from 1988 onwards allows us to obtain information about all showers. This includes the population index and the ZHR, but also further data such as the mass index, fluxes and spatial number densities, for both the annual returns and the peculiarities of single outbursts or activity enhancements. We provide an average ZHR profile calculated from the 25 years of data for the annual (mean) returns of the showers introduced in this Chapter. Over a timespan of more than 25 years, we start to see effects of shower evolution in some cases. The ZHR of most showers does not vary greatly from one year to the next, while outbursts or (quasi-)periodic appearance characterize other showers. Hence our ZHR graphs represent the average level. Each future observation contributes to our knowledge. Surprises are always possible, such as the September ε-Perseids in 2008 and 2013 or the Draconids in 2012—so be alert.

Chapter 2

Shower descriptions

2.1 Summary lists

In this Chapter we provide detailed information for a selection of meteor showers. First, we provide two summary tables for the entire year. These are working lists, and as the name indicates: the entries are up to date for March 2014. New observations to which you are invited to contribute, may lead to changes and updates in a later edition of the compilation.

In Table 2.1 we provide the summary data for the showers which are later described in more detail in Chapter 2. The columns list:
Shower name including the IAU number and three-letter code.
Activity period – the time for which reliable information about the detectability exists.
Maximum given in Solar longitude for equinox J2000.0; the date may vary by ±1 day from year to year.
Radiant at maximum in right ascension α and declination δ.
entry-velocity V_∞, i.e. the geocentric encounter velocity.
ZHR – the maximum level for an average return of the shower.

Table 2.2 summarizes the radiant positions of the showers summarized in Table 2.1 in 5-day steps during their activity period. For days between the given dates, the values need to be linearly interpolated.

2.2 Shower data

For each of the described showers we provide synoptic data at the beginning of the subsections. These include:
The **solar longitude** $\lambda_\odot$ refers to equinox J2000.0.
The **date of maximum** has to be computed for each individual year. The dates given here are only approximate and may vary by ±1 day. Detailed information for individual years are provided through the *IMO's* annual Shower Calendar. When observing on other dates than the maximum, please refer to Table 2.2 for the radiant position.
The **entry-velocity** V_∞ is the geocentric encounter velocity augmented with the contribution of the acceleration by the gravity of the Earth.
The **population index** r varies during the the activity period of each shower. Typical values are in the range between $r = 2.0$ to 2.5 near shower maxima. Values in this range should be used for tentative analyses; otherwise r must be determined as a function of time before any activity computation of a meteor shower. Details are described in the sections for each shower.

Table 2.3: Optimum radiant diameters to be assumed for shower association of minor-shower meteors as a function of the distance D between the radiant and the meteor. Detailed explanations are given in Chapter 3 of the *Handbook for Meteor Observers* (Rendtel & Arlt, 2014)

Distance D	Optimum diameter
15°	14°
30°	17°
50°	20°
70°	23°

The **assumed radius** (Table 2.3) to be considered for shower association from visual observations is explained in Chapter 3 of the *Handbook for Meteor Observers* (Rendtel & Arlt, 2014). It is an attempt to compensate the sporadic pollution and the loss of true shower meteors due to errors in the perception of the meteor trail direction (described for plotting errors). Consequently, the given radiant extensions are *not* the real extensions but the extensions to apply for shower association of plotted meteors and which take into account the plotting errors (Koschack, 1991).

The **average orbits** should allow some conclusion about the behaviour of the showers and their relation to other objects. If not noted otherwise, orbital elements of comets are taken from the 16th edition of the 'Catalogue of Cometary Orbits' (Marsden & Williams, 2005).

The **figures of the radiant drift** give the position of the radiant for the activity period, which is also listed in Table 2.2.

We also included a graph of the ZHR for many showers included in the Working List. The data shown here are a reference of the currently available information. It does not mean that the figures are now definitely known. It is the observer's task to collect data which allow to

Table 2.1: Working List of Meteor Showers.

Shower	Code	Activity period –	Maximum $\lambda_\odot$	date	Radiant at max. α	δ	V_∞ km/s	ZHR
Antihelion source	ANT	Dec 10–Sep 10	–	–	see Table 2.2		30	(4)
		ANT not observable during NTA/STA						
Quadrantids	010 QUA	Dec 28–Jan 12	283.°16	Jan 03	230°	+49°	41	120
α-Centaurids	102 ACE	Jan 28–Feb 21	319.°2	Feb 08	210°	−59°	56	6
γ-Normids	118 GNO	Feb 25–Mar 28	353°	Mar 13	239°	−50°	56	4
Lyrids	006 LYR	Apr 16–Apr 25	32.°32	Apr 22	271°	+34°	49	18
π-Puppids	137 PPU	Apr 15–Apr 28	33.°5	Apr 23	110°	−45°	18	var
η-Aquariids	031 ETA	Apr 19–May 28	45.°5	May 05	338°	−01°	66	60
η-Lyrids	145 ELY	May 03–May 12	48.°4	May 08	287°	+44°	44	3
June Bootids	170 JBO	Jun 22–Jul 02	95.°7	Jun 27	224°	+48°	18	var
Piscis Austrinids	183 PAU	Jul 15–Aug 10	125°	Jul 27	341°	−30°	35	4
Southern δ-Aquariids	005 SDA	Jul 12–Aug 19	125°	Jul 27	339°	−16°	41	15
α-Capricornids	001 CAP	Jul 03–Aug 15	127°	Jul 29	307°	−10°	23	4
Perseids	007 PER	Jul 17–Aug 24	140.°0	Aug 12	49°	+58°	59	100
κ-Cygnids	012 KCG	Aug 03–Aug 25	145°	Aug 17	286°	+59°	25	3
Aurigids	206 AUR	Aug 25–Sep 10	158.°6	Aug 31	84°	+42°	66	6
Sep. ε-Perseids	208 SPE	Sep 05–Sep 21	166.°7	Sep 09	48°	+40°	66	5
Draconids	009 DRA	Oct 06–Oct 10	195.°4	Oct 08	262°	+57°	20	var
Southern Taurids	002 STA	Sep 10–Nov 20	197°	Oct 10	32°	+09°	27	5
δ-Aurigids	224 DAU	Oct 10–Oct 18	198°	Oct 12	84°	+44°	67	2
ε-Geminids	023 EGE	Oct 14–Oct 27	205°	Oct 18	102°	+27°	70	3
Orionids	008 ORI	Oct 01–Nov 10	208°	Oct 21	95°	+16°	66	22
Leonis Minorids	022 LMI	Oct 17–Oct 27	211°	Oct 24	162°	+37°	62	2
Northern Taurids	017 NTA	Oct 20–Dec 10	230°	Nov 12	58°	+22°	29	5
Leonids	013 LEO	Nov 06–Nov 30	235.°27	Nov 17	152°	+22°	71	var
α-Monocerotids	246 AMO	Nov 15–Nov 25	239.°32	Nov 21	118°	+01°	65	var
Phoenicids	254 PHO	Nov 28–Dec 09	254.°25	Dec 06	18°	−53°	18	var
Puppid-Velids	301 PUP	Dec 01–Dec 15	(255)	Dec 06	123°	−45°	40	10
Monocerotids	019 MON	Nov 27–Dec 17	257°	Dec 08	100°	+08°	42	2
σ-Hydrids	016 HYD	Dec 03–Dec 15	260°	Dec 11	127°	+02°	58	3
Geminids	004 GEM	Dec 07–Dec 17	262.°2	Dec 13	112°	+33°	35	120
Comae Berenicids	020 COM	Dec 12–Dec 23	264°	Dec 16	175°	+18°	64	3
Dec. Leonis Minorids	032 DLM	Dec 05–Feb 04	268°	Dec 20	161°	+30°	64	5
Ursids	015 URS	Dec 17–Dec 26	270.°7	Dec 22	217°	+76°	33	10

Table 2.2: Radiant positions during the year in α and δ.

Date		ANT		QUA		DLM									
Jan	0	112°	+21°	228°	+50°	172°	+25°								
Jan	5	117°	+20°	231°	+49°	176°	+23°								
Jan	10	122°	+19°	234°	+48°	180°	+21°								
Jan	15	127°	+17°			185°	+19°								
Jan	20	132°	+16°			189°	+17°								
Jan	25	138°	+15°			193°	+15°	ACE							
Jan	30	143°	+13°			198°	+12°	200°	−57°						
Feb	5	149°	+11°			203°	+10°	208°	−59°						
Feb	10	154°	+9°					214°	−60°						
Feb	15	159°	+7°					220°	−62°						
Feb	20	164°	+5°					225°	−63°						
Feb	28	172°	+2°												
Mar	5	177°	0°												
Mar	10	182°	−2°												
Mar	15	187°	−4°												
Mar	20	192°	−6°												
Mar	25	197°	−7°												
Mar	30	202°	−9°												
Apr	5	208°	−11°												
Apr	10	213°	−13°	LYR		PPU									
Apr	15	218°	−15°	263°	+34°	106°	−44°	ETA							
Apr	20	222°	−16°	269°	+34°	109°	−45°	323°	−7°						
Apr	25	227°	−18°	274°	+34°	111°	−45°	328°	−5°						
Apr	30	232°	−19°					332°	−3°	ELY					
May	05	237°	−20°					337°	−1°	283°	+44°				
May	10	242°	−21°					341°	+1°	288°	+44°				
May	15	247°	−22°					345°	+3°	293°	+45°				
May	20	252°	−22°					349°	+5°						
May	25	256°	−23°					353°	+7°						
May	30	262°	−23°												
Jun	5	267°	−23°												
Jun	10	272°	−23°												
Jun	15	276°	−23°												
Jun	20	281°	−23°	JBO											
Jun	25	286°	−22°	223°	+48°										
Jun	30	291°	−21°	225°	+47°	CAP									
Jul	5	296°	−20°			285°	−16°	SDA							
Jul	10	300°	−19°	PER		289°	−15°	325°	−19°	PAU					
Jul	15	305°	−18°	6°	+50°	294°	−14°	329°	−19°	330°	−34				
Jul	20	310°	−17°	11°	+52°	299°	−12°	333°	−18°	334°	−33				
Jul	25	315°	−15°	22°	+53°	303°	−11°	337°	−17°	338°	−31				
Jul	30	319°	−14°	29°	+54°	307°	−10°	340°	−16°	343°	−29	KCG			
Aug	5	325°	−12°	37°	+56°	313°	−8°	345°	−14°	348°	−27	283°	+58°		
Aug	10	330°	−10°	45°	+57°	318°	−6°	349°	−13°	352°	−26	284°	+58°		
Aug	15	335°	−8°	51°	+58°			352°	−12°			285°	+59°		
Aug	20	340°	−7°	57°	+58°	AUR		356°	−11°			286°	+59°		
Aug	25	344°	−5°	63°	+58°	85°	+40°					288°	+60°		
Aug	30	349°	−3°			90°	+39°	SPE				289°	+60°		
Sep	5	355°	−1°	STA		96°	+39°	43°	+40°						
Sep	10	0°	+1°	12°	+3°	102°	+39°	48°	+40°						
Sep	15			15°	+4°			53°	+40°						
Sep	20			18°	+5°			59°	+41°						
Sep	25			21°	+6°										
Sep	30			25°	+7°			ORI							
Oct	5			28°	+8°			85°	+14°	DAU				DRA	
Oct	10	EGE		32°	+9°			88°	+15°	82°	+45°			262°	+54°
Oct	15	99°	+27°	36°	+11°	NTA		91°	+15°	87°	+43°	LMI			
Oct	20	104°	+27°	40°	+12°	38°	+18°	94°	+16°	92°	+41°	158°	+39°		
Oct	25	109°	+27°	43°	+13°	43°	+19°	98°	+16°			163°	+37°		
Oct	30			47°	+14°	47°	+20°	101°	+16°			168°	+35°		
Nov	5			52°	+15°	52°	+21°	105°	+17°	LEO					
Nov	10			56°	+15°	56°	+22°			147°	+24°			AMO	
Nov	15			60°	+16°	61°	+23°			150°	+23°			112°	+2°
Nov	20			64°	+16°	65°	+24°			153°	+21°			116°	+1°
Nov	25					70°	+24°	PHO		156°	+20°	PUP		120°	0°
Nov	30	ANT		GEM		74°	+24°	14°	−52°	159°	+19°	120°	−45°	91°	+8°
Dec	5	85°	+23°	103°	+33°	149°	+37°	18°	−53°	122°	+3°	122°	−45°	96°	+8°
Dec	10	90°	+23°	108°	+33°	153°	+35°	22°	−53°	126°	+2°	125°	−45°	100°	+8°
Dec	15	96°	+23°	113°	+33°	157°	+33°	174°	+19°	130°	+1°	128°	−45°	104°	+8°
Dec	20	101°	+23°	118°	+32°	161°	+31°	177°	+18°	HYD		217°	+76°	MON	
Dec	25	106°	+22°	QUA		166°	+28°	180°	+16°			217°	+74°		
Dec	30	111°	+21°	226°	+50°	170°	+26°	COM				URS			
						DLM									

calculate the values for each return. Moreover, changes can often occur because of the evolution and perturbation of meteoroid streams. The most striking examples are the Orionid returns between 2006 and 2010.

We list **references** and further bibliographic information for each of the described showers. This should help to gather relevant papers easily.

Continuing observations and new analyses will extend our knowledge and understanding of the meteor showers. Hence, all lists and data compilations represent the current status. Several ongoing studies will lead to changes. Most positional data of meteor showers, their radiants and meteoroid orbits are provided by video and radar observations. Analyses based on such data improve and perhaps change our view on the streams. Some showers may be deleted from future compilations, while others have to be added (see, for example, Molau (2007) or the subsequent monthly reports from the video meteor network, regularly published in *WGN*). Of course, we also try to keep the information provided in the Handbook, the annual Meteor Shower Calendar and on the IMO web pages consistent. Finally, we cross-check the data with those provided by the IAU Meteor Data Center.

References

Jenniskens P., 2006: Meteor Showers and their Parent Comets. Cambridge University Press.

Koschack R., 1991: Analysis of visual plotting accuracy and sporadic pollution and consequences for shower association. *WGN* **19,** 225–241.

Molau S., 2007: How good is the IMO working list of meteor showers? A complete analysis of the IMO video meteor database. In: *F.Bettonvil and J.Kac (eds.): Proc. IMC 2006, Roden,* IMO, pp.38–54

Rendtel J., Arlt R., 2014: Handbook for meteor observers. IMO

2.3 Antihelion Source (ANT)

Period	January 1–September 24 November 26–December 31
Maximum	none
Radiant	see radiant ephemeris
$ZHR_{max} \sim 3$	$r = 3.0 \quad V_\infty = 30$ km/s
Parent body	probably large variety of comets in the ecliptic plane

Throughout the entire year, we observe a diffuse source of meteor activity from a point in the sky which is located about opposite to the Sun. The activity is variable over the months. The reason for this antihelion source is the fact that a large number of minor bodies move on orbits crossing the orbit of the Earth. Their origin is in the asteroidal belt. The angle with which they cross the orbit of the Earth is variable, but the addition to the motion of the Earth focuses the radiants on a region near the antihelion point in the sky.

Radiant lists of the last century list a number of individual showers most of which can be identified as parts of the antihelion source. The IAU MDC database `http://www.ta3.sk/IAUC22DB/MDC2007/Roje/` also lists all showers according to their discoveries. The more prominent and to some extent already 'combined' radiants among these are:
δ-Cancrids (095 DCA),
Virginids (050 VIR),
α-Scorpiids (055 ASC),
Scorpiid-Sagittariids (163 SAG),
Northern δ-Aquariids (026 NDA),
Northern and Southern ι-Aquariids (033 NIA, 003 SIA),
Piscids (216 SPI) and
χ-Orionids (014 XOR/256 ORN).
Naturally, there is a lot of overlap in radiant positions and activity data which does not allow to clearly distinguish between the possible sources. Since we are looking for physical data of the showers, we decided to list one continuous source, called Antihelion Source (ANT) thoughout the year. For some time, we had retained the δ-Leonids (029 DLE) because of their lower velocity as compared to the ANT average (20 km/s versus 30 km/s), but the rates were found below the detection limit for years. The α-Capricornids (001 CAP) are distinguishable from the ANT by careful consideration of direction and angular velocity information (see page 28). More important, the Southern and Northern Taurids (002 STA, 017 NTA) dominate the antihelion activity between most of September and mid-December so that visual observers should associate all meteors from the ecliptic sources with only the STA/NTA radiants (details in Section Taurids, page 50).

Table 3.1: Average ephemeris for the Antihelion Source according to video meteor data of 1993–2004.

Date		$\lambda_\odot$	α	δ
Dec	30	278.°12	110.°8	21.°3
Jan	05	284.°49	117.°2	20.°1
Jan	10	289.°59	122.°3	18.°9
Jan	15	294.°69	127.°4	17.°5
Jan	20	299.°78	132.°5	16.°1
Jan	25	304.°86	137.°6	14.°5
Jan	30	309.°94	142.°7	12.°8
Feb	05	316.°03	148.°8	10.°7
Feb	10	321.°10	153.°8	8.°9
Feb	15	326.°15	158.°9	7.°0
Feb	20	331.°20	163.°9	5.°1
Feb	25	336.°23	169.°0	3.°2
Feb	28	339.°24	172.°0	2.°0
Mar	05	344.°26	177.°0	0.°1
Mar	10	349.°26	182.°0	−1.°8
Mar	15	354.°26	187.°0	−3.°7
Mar	20	359.°23	192.°0	−5.°6
Mar	25	4.°19	196.°9	−7.°5
Mar	30	9.°14	201.°9	−9.°3
Apr	05	15.°06	207.°8	−11.°4
Apr	10	20.°00	212.°7	−13.°1
Apr	15	24.°88	217.°6	−14.°7
Apr	20	29.°77	222.°5	−16.°2
Apr	25	34.°64	227.°4	−17.°6
Apr	30	39.°50	232.°2	−18.°9
May	05	44.°36	237.°1	−20.°0
May	10	49.°20	241.°9	−21.°0
May	15	54.°02	246.°7	−21.°9
May	20	58.°84	251.°6	−22.°5
May	25	63.°65	256.°4	−23.°0
May	30	68.°45	261.°2	−23.°4
Jun	05	74.°20	266.°9	−23.°5
Jun	10	78.°98	271.°7	−23.°4
Jun	15	83.°76	276.°5	−23.°2
Jun	20	88.°54	281.°3	−22.°7
Jun	25	93.°30	286.°0	−22.°1
Jun	30	98.°07	290.°8	−21.°3
Jul	05	102.°84	295.°6	−20.°4
Jul	10	107.°61	300.°3	−19.°4
Jul	15	112.°38	305.°1	−18.°2
Jul	20	117.°15	309.°9	−16.°8
Jul	25	121.°92	314.°6	−15.°4
Jul	30	126.°70	319.°4	−13.°9
Aug	05	132.°44	325.°2	−12.°0
Aug	10	137.°23	330.°0	−10.°3
Aug	15	142.°03	334.°8	−8.°4
Aug	20	146.°84	339.°6	−6.°8
Aug	25	151.°65	344.°4	−4.°9
Aug	30	156.°48	349.°2	−3.°1
Sep	05	162.°29	355.°0	−0.°9
Sep	10	167.°14	359.°9	1.°0
TAU break				
Dec	10	257.°76	90.°5	23.°5
Dec	15	262.°85	95.°6	23.°2
Dec	20	267.°93	100.°6	22.°8
Dec	25	273.°02	105.°7	22.°2
Dec	30	278.°12	110.°8	21.°3

2.4 Quadrantids (010 QUA)

2.4.1 Synopsis

Period	December 28 – January 12
Maximum	$\lambda_\odot = 283.^\circ16$ ($\approx$ January 3)
Radiant	$\alpha = 230^\circ$ $\delta = +49^\circ$
$ZHR_{max} = 120$	$r = 2.1$ $V_\infty = 41$ km/s
Parent body	stream belongs to complex with Southern δ-Aquariids and a number of asteroids and comets

Average orbital elements of the stream and 96P/Machholz 1:

Ω	ω	i	e	q	a	P
QUA-stream, Lindblad (1971), phot.						
$282.^\circ4$	$171.^\circ1$	$71.^\circ9$	0.677	0.981 au	3.037 au	5.3 yr
96P/Machholz 1 (2007)						
$94.^\circ55$	$14.^\circ62$	$59.^\circ95$	0.959	0.125 au	3.0 au	5.2 yr
2003 EH_1 (Wiegert & Brown, 2005)						
$282.^\circ9381$	$171.^\circ3687$	$70.^\circ7980$	0.6188	1.1924 au	3.1277 au	

The Quadrantids are effectively observable only from the northern hemisphere (Figure 2.1). The activity is comparable to that of the Perseids and Geminids (Figure 2.2). Although the northern winter nights are long, only the second half of the night provides suitable radiant heights. The radiant reaches its lowest point around 20^hlocal time. At a geographical latitude of 50° N, the radiant climbs above 20° elevation at 0^h10^m local time, while that will happen at 2^h20^m local at a latitude of 30° N. If you observe before midnight, the number of Quadrantids seen may remain very low, even if you correctly picked the time of maximum activity.

The shower peak is of relatively short duration. The full width between half-maximum ZHRs is about 14 hours. The narrow peak makes it probable that one observer will miss the maximum. If, for example, the peak occurs at about 15^h UT, most parts of Europe are in daylight. This moment corresponds to 10^h–11^h local time on North America's east coast, and to about 7^h local time on the west coast, so the peak will occur in daylight from there, too. For Japan, this would correspond to approximately 23^h local time which is 3 hours after the radiant reaches its lowest point, and when it is at less than 5° elevation. For Asia and Eastern Europe, the period would also mark the time when the radiant is at its lowest point. As a result, in this scenario, only observers in Alaska and on Pacific Islands would see the maximum under good conditions. The case we have constructed here is the worst that can happen, yet one thing becomes clear. It is impossible to perform a meaningful analysis of the shower based on observational data from just one location. The compilation of global data is essential for the study of the Quadrantids. A low activity detected from video, visual and radar data begins already on December 28 and extends until January 10 (Molau, 2007).

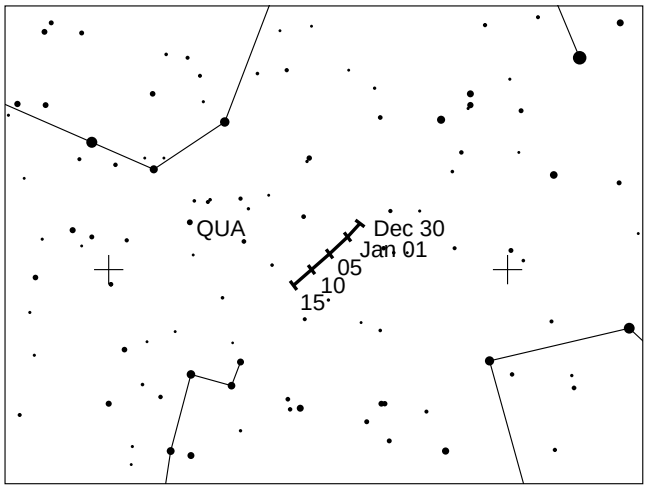


Figure 2.1: Radiant drift of the Quadrantids.

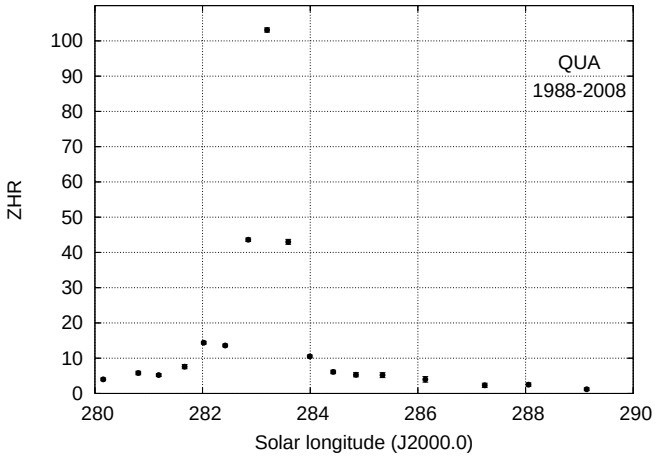


Figure 2.2: ZHR profile of the Quadrantids calculated from visual observations stored in the VMDB covering the period 1988–2008 using the r-profile shown in Figure 2.4. Details near the peak are shown in Figure 2.3.

The activity of the Quadrantids changes rapidly during one night (Figure 2.3), as does the brightness distribution of the meteors (Figure 2.4). Observing reports from the Quadrantid maximum should be broken down into periods of no more than 15 minutes. The same holds for the magnitude distributions, regardless of how small the number of meteors in each bin is.

2.4.2 Research

The first paper on the orbital evolution of the Quadrantids was published by Hamid & Youssef (1963). They found that the orbit was similar to the present one some 4 000 years ago, underwent severe changes in the period in between and returned to about the current orbit again. Wu & Williams (1992) took advantage of the improved computing capabilities to study the long-term evolution of Quadrantid orbits taken from the Meteor Catalogue of the IAU, which comprise about 69 000 photographic and radar meteoroid orbits. They integrated

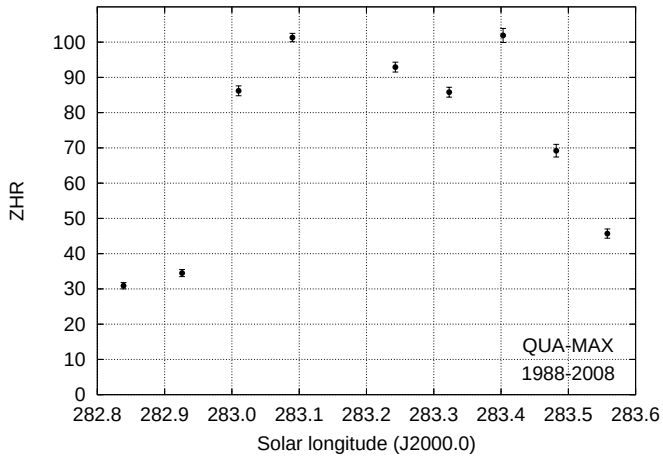


Figure 2.3: ZHR in the maximum period, averaged over the period 1988–2008 as the mean ZHR profile (Figure 2.2). The cross section of the Earth through the stream varies significantly from one encounter to another. The double peak is not a true feature. The width of the peak indicates the range (in solar longitude) of the peaks observed in the 1988–2008 period.

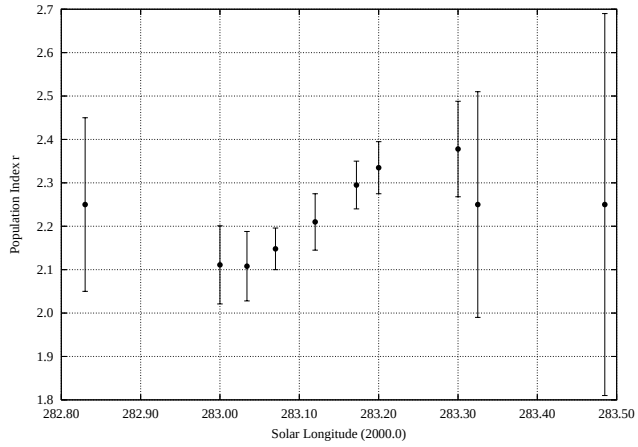


Figure 2.4: Profile of the population index r around the Quadrantid activity maximum in 1992 (Rendtel et al., 1993). Before $282\overset{\circ}{.}0$ and after $284\overset{\circ}{.}0$ we find $r \approx 3.0$.

the motion of 118 meteoroids back in time to 5 000 BC, that is, almost 7 000 years. Five subsets of orbits can be distinguished. Three of them show periodically changing orbital elements. The fourth shows a steady change and the fifth class appears to produce chaotic results. The first subset, containing 21 meteors seems to represent the above orbital evolution estimated by Hamid & Youssef. Even a very long integration over 26 000 years did not show a similarity between the mean orbits of each of the three first subsets at a certain time in the past. Hence, the computations did not indicate a common origin and ejection time of these Quadrantid particles.

Surprisingly, the orbital evolution of Comet 96P/Machholz 1 is very similar to the evolution of the Quadrantid orbits (McIntosh, 1990). The comet changes its orbital elements periodically with a 4 000-year period. At present, it has a similar orbit to that of the Quadrantids between AD 0 and 500. The evolution is thus similar to that of the first subset in the paper of Wu & Williams but shifted by roughly 2 000 years. 96P/Machholz 1 was suggested to be the parent of the Quadrantids first by Zausaev & Pushkarev (1989).

A further step in understanding the structure of the Quadrantids and their related objects was proposed by Babadzhanov & Obrubov (1993). They confirmed the same behaviour of orbital evolution for eight meteoroid streams. The most prominent of them are the Southern δ-Aquariids (see page 30) and the daytime Arietids, a prolific radio meteor shower in June. The above-mentioned paper of McIntosh (1990) indeed showed close orbits for the Quadrantids, the δ-Aquariids, the daytime Arietids and comet 96P/Machholz 1 between AD 0 and 500.

A second comet has been suggested to be the parent object of the Quadrantids (Hasegawa, 1979). The orbital evolution of Comet 1491 I (now designated C/1490 Y1) was subsequently investigated by Williams & Wu (1993). The Comet was on an orbit similar to that of the Quadrantids until around AD 1650 when it underwent a severe perturbation by Jupiter kicking the comet on an orbit with an aphelion of more than 20 au. It is not visible from the Earth anymore. The Comet's orbit was integrated backwards to 3 000 BC. A group of 50 particles were assumed to be ejected at that time from the modelled position of the comet and simulated to move through the Solar System until AD 1954. The result was a mean theoretical orbit of the Quadrantids which resembled the observed orbit well. The scatter in the simulated meteoroid orbits was, however, very large.

It was not possible to say which comet is the parent of any of the mentioned meteoroid streams until Jenniskens & Marsden (2003) showed the similarity of the orbits of the minor planet 196256 (2003 EH_1) and those of the Quadrantids. Numerical simulations of particles released from the asteroid indicates that the material of the densest part of the stream was ejected near 1800 (Wiegert & Brown 2005). The computations even seem to show that it was a single, major perihelion outburst of the parent which made the Quadrantids a major shower observed since 1835. The Solar longitude of the Quadrantids slowly shifts to an earlier position, the rate of change being about -0.34 degrees per century (Wiegert & Brown, 2004).

In two recent papers the complex formed of 96P/Machholz 1 and 196256 (2003 EH_1) is analysed. Neslušan, Kaňuchová and Tomko (2013) studied the meteor shower complex of 96P and Neslušan, Hajduková and Jakubík (2013) studied the structure of the meteoroid particle complexes released from 196256 (2003 EH_1). The latter paper also investigates the relationship to 96P/Machholz 1. The model calculations confirm the filamentary structure of the complex. It is found that the 196256 complex is qualitatively identical to the complex of 96P. As already pointed out above, the complex includes six well-established and two minor filaments approaching the Earth's orbit. Four well-known showers (Daytime Arietids 171 ARI), Southern

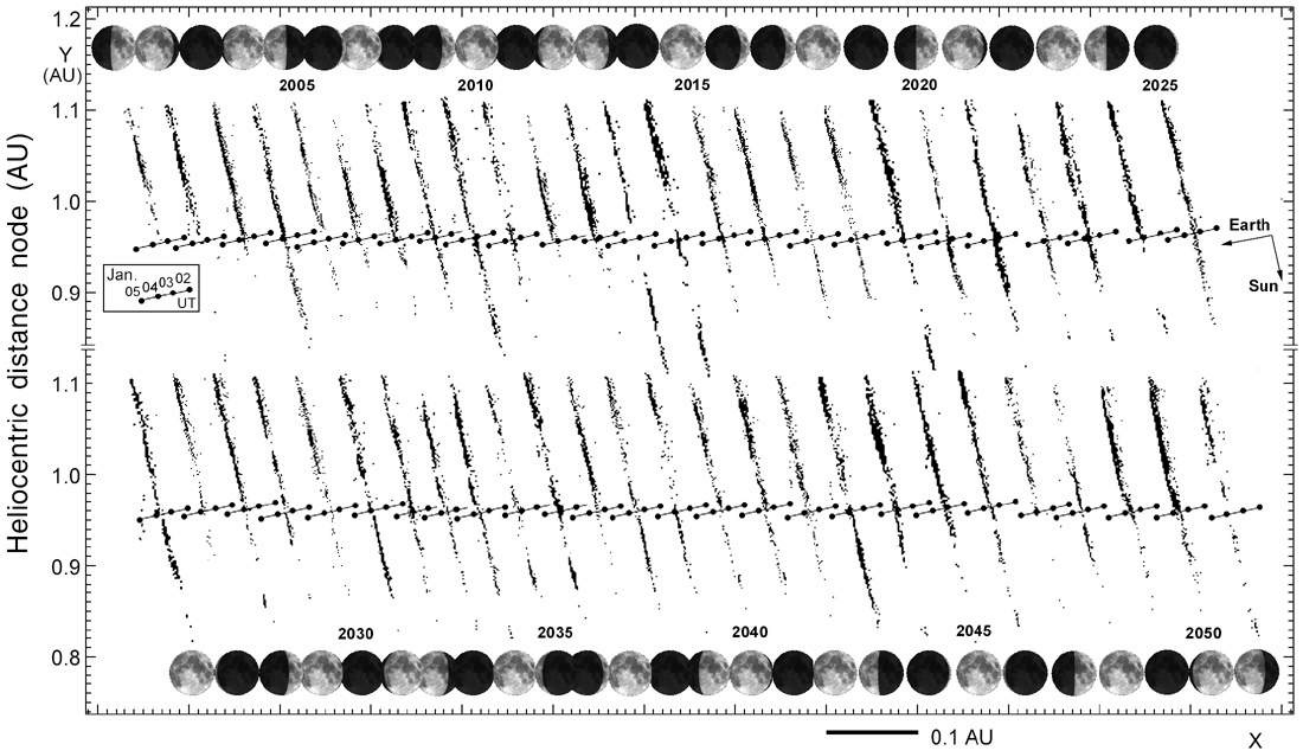


Figure 2.5: Cross sections of the Quadrantid meteoroid stream modelled by Vaubaillon. (Graphics from Jenniskens, 2006, with kind permission).

δ-Aquariids (005 SDA), Quadrantids (010 QUA), and Northern δ-Aquariids (026 NDA, in our compilation being a part of the complex Antihelion Source and are thus not mentioned separately). The modelled filaments corresponding to the Daytime Arietids and Northern and Southern δ-Aquariids constitute the ecliptical component, and those corresponding to the Quadrantids and their southern counterpart (to be detected) constitute the toroidal component of the complex.

Modelling of the meteoroid distribution in the Quadrantid stream by Vaubaillon yielded different density distributions along the annual passages of the Earth through the stream (Figure 2.5).

We observe a number of comets and streams which change their orbital elements periodically in the same range. The phase of evolution of each object is shifted against the other components, whence they appear on very different orbits at the present time, and the associated meteoroid streams show up at different radiant positions and times of the year. But they all appear to belong to one complex of interplanetary matter controlled by Jupiter.

Recent double-station video observations of Quadrantid meteors (Koten et al., 2006) show that the Quadrantid meteoroids are similar to other meteor showers of cometary origin in some aspects, but to the Geminids in others. The intermediate beginning heights of the Quadrantids, their near-independence of beginning heights on mass and the total intensity of Na in spectra show that these meteoroids have suffered a partial loss of volatiles and in this respect must be situated between the Geminids and the Leonids. Orbital evolution modelling indicates that the meteoroids were never closer to the Sun than 0.6 au, which is insufficient for the observed loss of volatiles. Koten et al. propose that the parent 2003 EH_1 is a dormant comet, and that the meteoroids were probably ejected from the surface layers.

References

Babadzhanov P.B., Obrubov Yu.V., 1993: Dynamics and relationships between interplanetary bodies: I. Comet Machholz and its meteor showers. In *J. Štohl, I.P. Williams (eds.): Meteoroids and their parent bodies*. Slovak Acad. Sci., Bratislava, 49–52.

Hamid S.E., Youssef M.N., 1963: A short note on the origin and age of the Quadrantids. *Smithson. Contr. Astrophys.* **7,** 309–311.

Hasegawa I., 1979: Orbits of ancient and medieval comets. *Publ. Astron. Soc. Japan* **31,** 257–270.

Jenniskens P., 2006: Meteor Showers and their Parent Comets. Cambr. University Press.

Jenniskens P., Marsden B., 2003: 2003 EH1 and the Quadrantids. IAUC 8252.

Koten P., Borovička J., Spurný P., Evans S., Štork R., Elliott A., 2006: Double station and spectroscopic observations of the Quadrantid meteor shower and the implications for its parent body. *MNRAS* **366,** 1367–1372.

Lindblad B.A., 1971: A computerized stream search among 2401 photographic meteor orbits. *Smiths. Contr. Astrophys.* **12,** 14–24.

McIntosh B.A., Šimek M., 1984: Quadrantid meteor shower: A quarter-century of radar observations. *BAC* **35,** 14–28.

McIntosh B.A., 1990: Comet P/Machholz and the Quadrantid meteor stream. *Icarus* **86,** 299–304.

Molau S., 2007: How good is the IMO working list of meteor showers? A complete analysis of the IMO video meteor database. In: *F.Bettonvil and J.Kac (eds.): Proc. IMC 2006, Roden,* IMO, pp.38–54

Neslušan L., Kaňuchová Z., Tomko D., 2013: The meteor-shower complex of 96P/Machholz revisited. *Astron. Astrophys.* **551,** id.A87, 14 pp. (DOI: 10.1051/0004-6361/201220299.

Neslušan L., Hajduková, jr. M., Jakubík M., 2013: Meteor-shower complex of asteroid 2003 EH1 compared with that of comet 96P/Machholz. *Astron. Astrophys.* **560,** id.A47, 10 pp. (DOI: 10.1051/0004-6361/201322228.

Rendtel J., Koschack R., Arlt R., 1993: The 1992 Quadrantid meteor shower. *WGN* **21,** 97–109.

Wiegert P., Brown P., 2004: The core of the Quadrantid meteoroid stream is two hundred years old. *EMP* **95,** 81–88.

Wiegert P., Brown P., 2005: The Quadrantid meteoroid complex. *Icarus* **179,** 139–157.

Williams I.P., Wu Z., 1993: The Quadrantid meteoroid stream and Comet 1491 I. *MNRAS* **264,** 659–664.

Williams I.P., Ryabova G.O., Baturin A.P., Chernitsov A.M., 2004: The parent of the Quadrantid meteoroid stream and asteroid 2003 EH1. *MNRAS* **355,** 1171–1181.

Wu Z., Williams I.P., 1992: On the Quadrantid meteoroid stream complex. *MNRAS* **259,** 617–628.

Zausaev A.F., Pushkarev A.N., 1989: The orbital evolution of the Quadrantid meteor stream during 4 000 years (AD 1950 to 2050 BC). *Bull. Inst. Astrofiz.* **80,** 18–24.

2.5 α-Centaurids (102 ACE)

2.5.1 Synopsis

Period	January 28–February 21	
Maximum	$\lambda_\odot = 319\overset{\circ}{.}2$ ($\approx$ February 7)	
Radiant	$\alpha = 210°$	$\delta = -59°$
$ZHR_{max} = 6$	$r = 3.0$	$V_\infty = 56$ km/s
Parent body	unknown	

Average orbital elements of the stream:

Ω	ω	i	e	q	a	P
ACE-stream, Kronk (1988), phot.						
$139\overset{\circ}{.}5$	$357\overset{\circ}{.}3$	$108\overset{\circ}{.}3$	1.0	0.99 au	∞	–
ACE-stream, Gartrell & Elford (1975), radar						
146°	344°	$105\overset{\circ}{.}0$	0.61	0.97 au	2.5 au	3.9 yr

Meteors of this shower can only be observed from the southern hemisphere (Figure 2.7). For most of its activity period, the shower provides 1 to 3 meteors per hour, but around maximum, rates may rise up to 5. Occasionally, enhanced α-Centaurid rates were observed. Such enhancements were short-lived, lasting no more than two or three hours.

Hoffmeister (1948) listed a radiant near the α-Centaurids with a rather low reliability, derived from his observations in southern Africa during the mid 1930s. He did not think it significant enough to include in his lists of southern hemisphere streams. Following the 1930s' observations no further record of the shower occurs until the early 1970s when Morgan (New Zealand), Skelsey (Sydney, Australia) and Buhagiar (Perth, Australia) detected it again. All their records indicated that the shower was producing 4 to 5 meteors per hour at maximum, and that the shower was rich in bright meteors.

The first observation was made on 1974 February 8–9: Buhagiar and Skelsey recorded some 12–15 meteors per hour. Following this display, regular watches were maintained on the α-Centaurids every year, but it was not until 1980 that an enhanced display was noted again. In the early evening hours of February 8–9, the people of Western Australia were able to witness a very short, spectacular display from this stream (Kronk, 1988). At the time, three experienced observers were out monitoring the sky, and it was largely due to their diligence that an accurate picture of the display was obtained. Glen Blencowe, Neil Freckelton and Craig Willoughby from Australia recorded 14, 11 and 9 meteors per hour, respectively, from 12^h10^m to 13^h10^m UT in dark skies. As this was just after twilight, it is impossible to tell how long the display had been going on during daylight hours. However, after just the one hour, the rates dropped off markedly, until only a couple of meteors per hour were recorded.

The data stored in the IMO's VMDB produce the ZHR profile shown in Figure 2.6 with a maximum of about 6 near $\lambda_\odot = 319°$. The graph considers all data from 1988 to 2007 with the radiant more than 20° above the horizon and a standard ZHR correction.

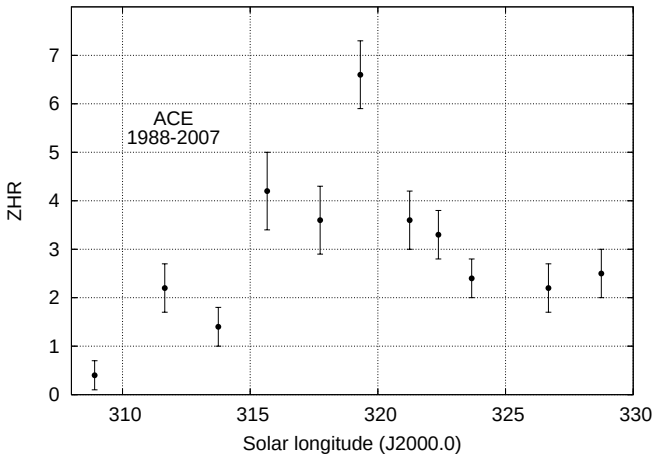


Figure 2.6: Activity of the α-Centaurids derived from visual observations stored in the VMDB covering the period 1988–2007 using a constant $r = 2.0$ over the activity period.

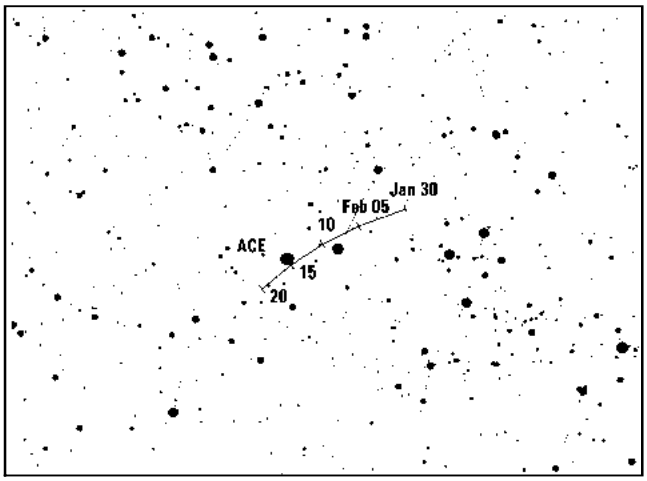


Figure 2.7: Radiant drift of the α-Centaurids.

References

Gartrell G., Elford W.G., 1975: Southern hemisphere meteor stream determinations. *Australian Journal of Physics* **28,** 591–620.

Hoffmeister C., 1948: Meteorströme. J.A. Barth, Leipzig.

Kronk G., 1988: Meteor Showers. A Descriptive Catalog. Enslow, Hillside, New Jersey.

2.6 γ-Normids (118 GNO)

2.6.1 Synopsis

Period	February 25–March 22	
Maximum	$\lambda_\odot = 353°$	(≈ March 13)
Radiant	$\alpha = 239°$	$\delta = -51°$
$ZHR_{max} = 4$	$r = 2.4$	$V_\infty = 56$ km/s
Parent body	unknown	

Only little information is available for this southern shower. The earliest reference is an analysis of Australian radar data (Gartrell & Elford, 1975). The radiant and activity period in the optical region are poorly documented. An analysis of 2005 data (Trigo-Rodríguez et al., 2005) shows a maximum close to $\lambda_\odot = 350°$, i.e., about three days before the previously assumed time. Rates seem to vary slightly from one year to the next with peak ZHRs reported between 2 and 6 with a probable median ZHR of 2–3. An analysis of the entire data set stored in the VMDB shows a smooth profile (Figure 2.9). All rates shown here are calculated with a population index $r = 2.4$ and a zenith coefficient $\gamma = 1.0$.

In a systematic search among video meteors recorded from three Australian camera stations (Molau & Kerr, 2014) between 2001 and 2012 the shower is not clearly detected. Similar to the situation described above, the video analysis yields a shower between March 23 and 28. The reference longitude is about 11° later in the recent video data (353° for the entry in the meteor database, 4° for the new analysis). While the declination of the radiant fits well, the right ascension is about 15° distant. The result obtained already in an earlier analysis from two cameras of the video network is shown in Figure 2.8. It fits the radiant derived from two data sets of visual plotting observations (Arlt & Rendtel, 2006). However, the currently available positional data are not yet sufficient for final conclusions about the reliability of the radiant and the activity of a shower at that position.

Further, the orbital databases do not supply support for this minor shower which makes it the weakest candidate in the shower list. However, we leave it in our Working List with the urgent request for detailed observations. The radiant position shown in Figure 2.6 is fitted with the location derived from the recent video and visual data.

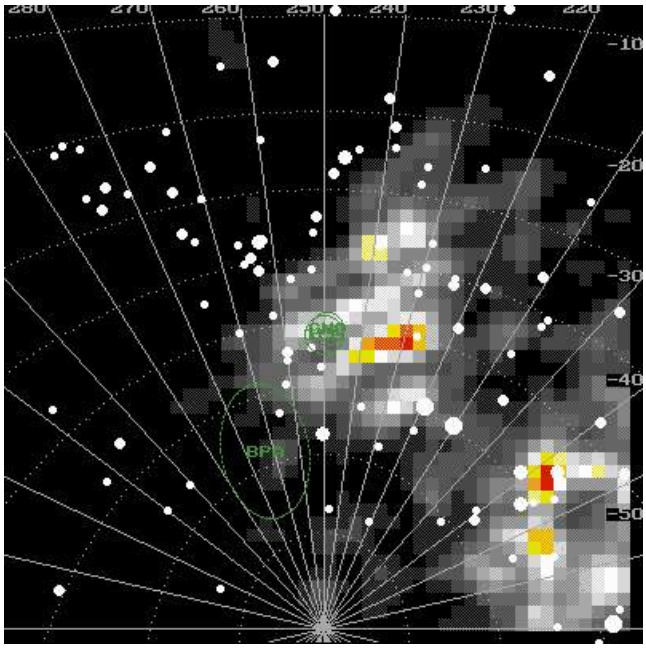


Figure 2.8: Radiant area of the γ-Normids from video observations.

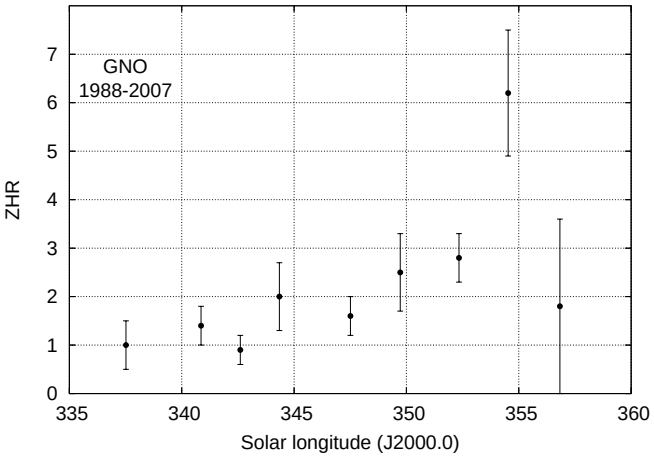


Figure 2.9: Activity of the γ-Normids from visual observations stored in the VMDB covering the period 1988–2007 using a constant $r = 2.4$ over the activity period. The zenith correction included the standard sine term (no zenith coefficient $\gamma > 1.0$) and allowed only intervals with a radiant elevation of $\geq 20°$.

References

Arlt R., Rendtel J., 2006: A new Working List of meteor showers. *WGN* **36,** 77–84.

Gartrell G., Elford W. G., 1975: Southern hemisphere meteor stream determinations. *Australian Journal of Physics* **28,** 591–620.

Molau S., Kerr S., 2014: Meteor showers of the southern hemisphere. *WGN* **42,** submitted.

Trigo-Rodríguez J. M., Balderas P., Moyano R., Bianchi V., Javora I., 2005: LIADA results of the 2005 γ-Normids. *WGN* **33,** 87–89.

2.7 Lyrids (006 LYR)

2.7.1 Synopsis

Period	April 16–25	
Maximum	$\lambda_\odot = 32\,^\circ\!.32$ ($\approx$ April 22)	
Radiant	$\alpha = 271\,^\circ\!.4$	$\delta = +33\,^\circ\!.6$
$\mathrm{ZHR_{max}} = 18$	$r = 2.1$	$V_\infty = 49$ km/s
Parent body	Comet C/1861 G1 (Thatcher)	

Average orbital elements of the stream and C/1861 G1:

Ω	ω	i	e	q	a	P
LYR, Lindblad (1987)						
$31\,^\circ\!.7$	$214\,^\circ\!.3$	$79\,^\circ\!.0$	0.968	0.919 au	28 au	164 yr
C/1861 G1						
$31\,^\circ\!.87$	$213\,^\circ\!.4$	$79\,^\circ\!.8$	0.983	0.921 au	55 au	415 yr

During the evening hours, the radiant (Figure 2.10) will be found low on the horizon in northern latitudes and even below the horizon at more southerly latitudes. It is more favourably placed in the second part of the night. The radiant is positioned near κ Lyrae, between Lyra and Hercules, and not near Vega (α Lyrae) as is sometimes assumed.

Rates will stay rather low over most of the time, as the Lyrids are effectively a minor shower of moderate activity before and after their maximum. Only during the short maximum do Lyrids attract attention with 15 to 20 Lyrids an hour. The maximum activity can thus be easily missed, and observers may tend to conclude that Lyrid production was very low.

The Lyrid shower is the oldest meteor shower to be found in ancient records. It was first observed and recorded in China more than 2000 years ago. Observations of high meteor activity in 687 BC, 15 BC were associated with the Lyrid shower by Zhuang (1977). Dall'Olmo (1978) linked observations in 1040, 1096, 1122 and 1123 to the Lyrids. In 1803, the Lyrids provided a spectacular display when a single observer noted 167 meteors in 15 minutes (Fisher, 1931)! This outburst happened almost 60 years before the parent comet reached its perihelion. However, the Lyrids were not recognized as an annual shower until 1835, by Arago (Quételet, 1861). In most years, the hourly rates were low, sometimes with the maximum rates concentrated in a narrow peak in several years, but apparently without any obvious periodicity.

Another remarkable Lyrid return was witnessed in 1982 from North America (Adams, 1982; Spalding, 1982). European observers recorded a low activity during their nighttime on April 22. Shortly thereafter American observers recorded 3 to 5 Lyrids per minute. This exceptional rate lasted only one hour. Counting Lyrids over five minute intervals showed a spike-like peak at around $6^\mathrm{h}50^\mathrm{m}$ UT in the hourly rate profile, corresponding to a ZHR of 90.

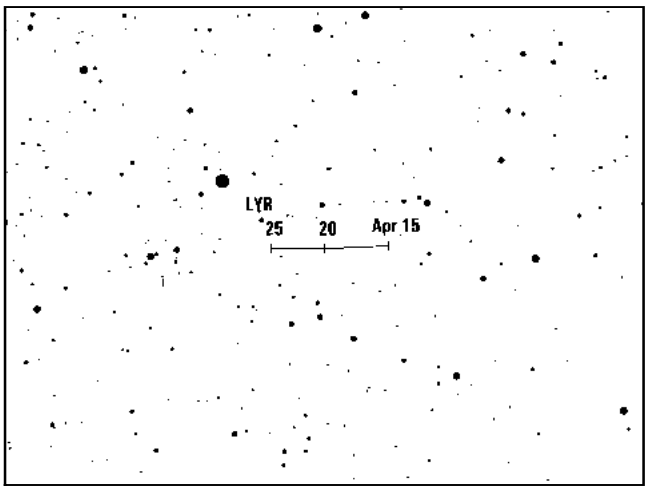


Figure 2.10: Radiant drift of the Lyrids.

2.7.2 Research

Recent studies of the Lyrid activity and population index were presented by Dubietis & Arlt (2001) and Rendtel & Arlt (2007). The population index is very typically between $r = 2.0$ and 2.2 during the day near the maximum. We obtained maximum ZHR-averages between 14 and 23 (a very low average ZHR of 12 for the poorly defined profile of 1990; the peak time seems missing in the data, and we do not consider that year's results for our conclusions). Typical full widths at half maximum lie between $1\,^\circ\!.1$ and $1\,^\circ\!.4$. The regular maximum of the Lyrids thus covers more than one day. The striking exceptions are 1993 (sharp peak) and 2000 (broad maximum). Those years coincide with the highest maximum ZHR and the second-lowest ZHR, respectively.

No systematic trend of ZHRs and peak width is found, and we conclude that the Lyrids exhibit a fairly stable annual activity profile of ZHRs 15–20, at solar longitudes $32\,^\circ\!.05$–$32\,^\circ\!.45$. The shower parameter which suffers from strongest variations is the FWHM ranging from well over half a day to 2.5 days.

Brief summaries of recent publications:

Arter & Williams (1997a) find a ring structure for the Lyrid nodal distribution, in which the Lyrid filament moves around with a $\approx$ 12-yr period.

Arter & Williams (1997b) investigated the mean Lyrid orbit. From measured Poynting-Robertson effect they deduce an age of 1.5×10^6 years.

From the prominence of a ring structure and the number of Lyrids present when the Comet is at aphelion, an upper and lower limit of the ejection velocity of 25–150 m/s is determined by Arter & Williams (2002).

Enhanced activity is predicted from model calculations of Lyytinen & Jenniskens (2003). The expected peaks are due on 2040 April 22, $00^\mathrm{h}25^\mathrm{m}$ UT, -0.00022 AU, and 2041 April 22, $08^\mathrm{h}40^\mathrm{m}$ UT, -0.00025 AU. Both should be composed mainly of faint meteors.

Table 2.4: Overview of results obtained for the Lyrid meteor shower from 1988 to 2013. The quantity of $r^{(\max)}$ is an estimate of the population index near the activity maximum. $N_{\rm obs}$ is the number of observing periods defining the peak time and activity level; it is not the total number of observations in the respective activity graph.

Year	$r^{(\max)}$	$\mathrm{ZHR}_{\max}$	$\lambda_\odot^{(\max)}$ (J2000.0)	$N_{\rm obs}$	Gaps and comments
1988	2.2 ± 0.1	21.3 ± 2.8	32.°3	7	None
1990	2.3 ± 0.1	(12.5 ± 1.4)	(32.°1)	6	32.°21–32.°46
1991/92	(2.2 ± 0.2)	16.4 ± 2.1	32.°0	10	Combined
1993	2.1 ± 0.1	22.9 ± 1.6	32.°35	15	None
1994	2.0 ± 0.1	17.3 ± 1.3	32.°1	11	32.°22–32.°44
1995	2.2 ± 0.1	14.0 ± 0.6	32.°45	75	32.°06–32.°30
1996	2.0 ± 0.1	17.8 ± 1.5	32.°4	15	None
1997	2.6 ± 0.4	–	–	–	–
1998	2.1 ± 0.1	18.2 ± 2.5	32.°4	7	None
1999	2.0 ± 0.1	20.8 ± 2.3	32.°15	15	31.°9–32.°1
2000	2.3 ± 0.1	15.6 ± 1.6	32.°05	28	None; full moon
2003	2.2	19.0 ± 2.0	32.°32		Constant r
2006	2.2	19.8 ± 3.5	32.°28	29	Full moon; constant r
2007	2.2 ± 0.1	20.4 ± 1.1	32.°31	47	31.°85–32.°15
2009	2.1	15 ± 2	32.°24	25	Constant r
2010	2.1	20 ± 4	32.°49	10	Constant r
2011	2.1	20 ± 2	32.°32	27	Constant r
2012	2.1	25 ± 3	32.°19	13	Constant r
2013	2.1	20 ± 4	32.°17	9	Constant r

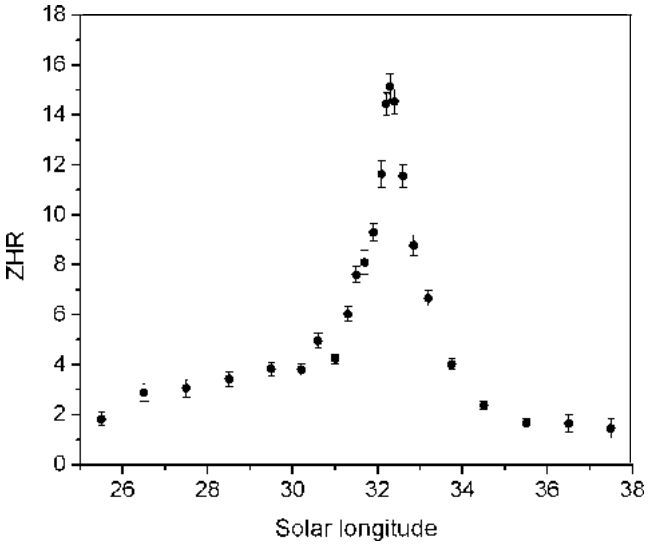


Figure 2.11: Average activity profile of the Lyrids derived from observations of 1988–2000. Increasing the resolution of the binning, the maximum can actually be driven a little higher to $\mathrm{ZHR}_{\max} = 18 \pm 1$ before noise fluctuations start to dominate (Dubietis & Arlt 2001).

References

Adams M.T., 1982: An exceptional return of the April Lyrids. *Meteor News* No. 58, 1–6.

Arter T.R., Williams I.P., 1997a: Periodic behaviour of the April Lyrids. *MNRAS* **286,** 163–172.

Arter T.R., Williams I.P., 1997b: The mean orbit of the April Lyrids. *MNRAS* **289,** 721–728.

Arter T.R., Williams I.P., 2002: Meteoroid ejection velocities deduced from a study of the April Lyrid meteor shower. *MNRAS* **329,** 175–180.

Dall'Olmo U., 1978: Meteors, meteor showers and meteorites in the middle ages: from European medieval sources.. *J. Hist. Astr.* **9,** 123–134.

Dubietis A., Arlt R., 2001: Thirteen years of Lyrids from 1988–2000. *WGN* **29,** 119–133.

Fisher W.J., 1931: Records of the Lyrid meteor shower of 1803. *Pop. Astr.* **39,** 256–263.

Lindblad B.A., 1987: Physics and orbits of meteoroids. In: *The Evolution of the Small Bodies of the Solar System*, Soc. Italiana di Fisica, Bologna.

Lyytinen E., Jenniskens P., 2003: Meteor outbursts from long period comet dust trails. *Icarus* **162,** 443–452.

Quételet A., 1861: Sur la Physique du globe, des étoiles filantes, aperçu historique (In French, On the physics of the globe, the shooting stars, historical review).

Rendtel J., Arlt R., 2007: The Lyrid meteor shower in 2006 and 2007. *WGN* **35,** 74–78.

Spalding G., 1982: 1982 Lyrid outburst. *JBAA* **92,** 272.

Zhuang, T.-S., 1977: Ancient Chinese records of meteor showers. *Chinese Astr.* **1,** 197–220.

2.8 π-Puppids (137 PPU)

2.8.1 Synopsis

Period	April 15–28
Maximum	$\lambda_\odot = 33\overset{\circ}{.}5$ ($\approx$ April 23)
Radiant	$\alpha = 110°$ $\delta = -45°$
$\mathrm{ZHR_{max}} = \mathit{variable}$	$r = 2.0$ $V_\infty = 18$ km/s
Parent body	26P/Grigg-Skjellerup

Orbital elements of the stream and 26P:

Ω	ω	i	e	q	a	P
PPU, Jenniskens (2006)						
$33\overset{\circ}{.}64$	359°	21°		1.00 au	2.97 au	
26P/Grigg-Skjellerup						
$213\overset{\circ}{.}31$	$359\overset{\circ}{.}33$	$21\overset{\circ}{.}09$	0.664	0.997 au	2.96 au	5.11 yr

The radiant can be effectively observed only from the southern hemisphere in the evening hours, at elevations of over 70° on a latitude of 30° S (Figure 2.12). It sets shortly after midnight.

The π-Puppids beautifully illustrate the surprising nature of new periodic streams, that is, showers that have become observable only recently. In the case of such young streams the meteoroids are clustered close to their parent comet, so we only see activity from them when the comet is nearby. With the π-Puppids, the comet returns to perihelion every five years, which is when we have the best chance to see some. It is possible that these meteors will in the future become observable in the intermediate years between successive perihelion passages.

In 1964, Jupiter slightly disturbed the Comet's orbit, reducing its minimum distance to the Earth's orbit to as little as 640 000 km (Sitarski, 1964). A possible meteor display was predicted for 1967, but observational results proved negative. In 1972, there were new attempts to find some associated meteor activity. About April 23, the Earth passed close to the Comet's orbit, but only very low rates were recorded, while radar observations in New Zealand showed an activity level of only 70% of the usual sporadic background (Baggaley, 1973).

Major observing campaigns were planned for the Comet's return in 1977. In the USA and Brazil, observers got very low rates. The Australians and New Zealanders, however, were blessed with a much richer display. Several meteors were photographed and some fireballs reported in New Zealand. In Australia, maximum activity was observed at $\lambda_\odot = 33\overset{\circ}{.}53$ with an hourly rate of 75 (Lindblad, 1987). The unusual meteor activity even caught the attention of the public, which means that it must have been remarkable.

Australian observers saw another π-Puppid return in 1982 (Wood, 1982). The maximum was sharp, with a peak ZHR of 23 at April $23^{\mathrm{h}}49^{\mathrm{m}}$ UT. This was lower than in 1977, but the main maximum may have been missed. Rates on adjacent nights were less than 2 per hour.

The 1977 maximum was located at $\lambda_\odot = 33\overset{\circ}{.}2$. Maximum activity in 1982 and 1983 occurred at $33\overset{\circ}{.}3$, which is the time at which the Earth passed through the

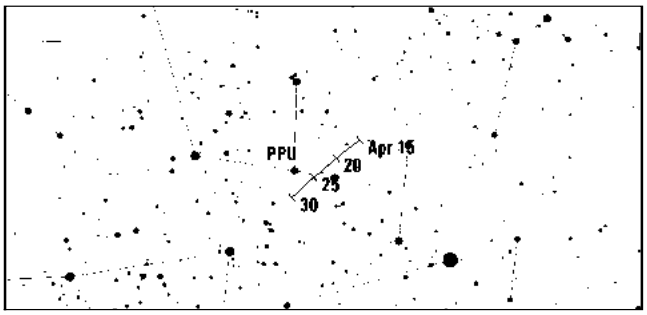


Figure 2.12: Radiant drift of the π-Puppids.

Comet's orbital plane. It follows that the debris is gradually being dispersed along the Comet's orbit, but is still very much confined to its orbital plane. In 1992 and 1993, maximum ZHRs were about 4 at $\lambda_\odot = 33\overset{\circ}{.}7$ and $\lambda_\odot = 33\overset{\circ}{.}4$, respectively. It is evident that continued observation of π-Puppid meteors over the next few years will provide unique information on the rate at which cometary material is dispersed to become a meteoroid stream.

In view of the extremely low velocity of the π-Puppid meteors, the observed 1977 peak hourly rate of 75 is quite remarkable. Members of the π-Puppid shower are 3.8 magnitudes fainter than Perseid meteors of comparable masses. If the observed visual rate was scaled up to a velocity of 60 km/s and if we assumed r-values between 2.0–2.9, we arrive at a ZHR of some 1 000–4 000 meteors per hour (Lindblad, 1987).

2.8.2 Research

Messenger (2002) predicted a return of the π-Puppids which should be observable by radio methods. These meteoroids were assumed to be only small particles (20 to 100 microns) which were ejected from 1967 to 1997.

Vaubaillon & Colas (2005) simulated the dynamics of the stream. Its evolution is dominated by close encounters with Jupiter. In the case of the π-Puppids, the effect is so great that it can cause the stream to split into several parts and form gaps. The difference in period of each part leads to the possibility of a meteor outburst on Earth while the parent body is at aphelion. Observations described above are linked to streams ejected in the 19th and 20th century. Sometimes there are overlaps between several streams ejected at different perihelion passages of the parent body, affecting the time of maximum meteor activity. In the 1972 and 2003 cases, only radio observations are available, but the predicted or post-predicted radio-outbursts have not been confirmed.

References

Baggaley W.J., 1973: Observations of meteors associated with Comet Grigg-Skjellerup. *The Observatory* **93,** 23–26.

Jenniskens P., 2006: Meteor showers and their parent comets. Cambridge Univ. Press.

Lindblad B.A., 1987: The meteor stream associated with comet P/Grigg-Skjellerup. *A & A* **187,** 931–932.

Messenger S., 2002: Opportunities for the stratospheric collection of dust from short-period comets. *Meteoritics & Plan. Sci.* **37,** 1491–1506.

Sitarski G., 1964: The motion of comet Grigg-Skjellerup after its approach to Jupiter in 1964. *Acta Astronomica* **14,** 25–37.

Vaubaillon J., Colas, F., 2005: Demonstration of gaps due to Jupiter in meteoroid streams. What happened with the 2003 Pi-Puppids?. *A & A* **431,** 1139–1144.

Wood J., 1982: Grigg-Skjellerupiden 1982. *WGN* **10,** 156–159 (In Dutch).

2.9 η-Aquariids (031 ETA)

2.9.1 Synopsis

Period	April 19–May 28	
Maximum	$\lambda_\odot = 45\overset{\circ}{.}5$ ($\approx$ May 5)	
Radiant	$\alpha = 338°$	$\delta = -1°$
$\mathrm{ZHR}_{\max} = 60$	$r = 2.4$	$V_\infty = 66$ km/s
Parent body	1P/Halley	

Orbital elements of the stream and 1P/Halley:

Ω	ω	i	e	q	a	P
ETA, Shigeno et al. (1997), video						
$44\overset{\circ}{.}9$	$96\overset{\circ}{.}6$	$164\overset{\circ}{.}0$	0.944	0.575 au	10.3 au	33 yr
1P/Halley						
$58\overset{\circ}{.}8$	$111\overset{\circ}{.}8$	$162\overset{\circ}{.}2$	0.967	0.582 au	18.2 au	77 yr

The η-Aquariids remain almost unknown in northern latitudes, while it is one of the highlights for southern hemisphere meteor observers. The radiant (Figure 2.14) reaches only low elevation above the eastern horizon by dawn for observers at northern latitudes (north of 45° N). Here, low elevation *and* twilight cause a small observable number of shower meteors. The shower is only favourable for southern observers. The ZHR profile is broad, yielding high rates for several days as shown in Figure 2.13.

The η-Aquariids appear in old Chinese annals from the eighth century and belong to the most prominent showers from the 10th to the 14th centuries (Ahn, 2003). The first European record of η-Aquariids comes from the period 1868 to 1870, when Italian observations, analyzed several years later by Denning (1883), allowed the determination of a radiant at $\alpha = 335°$, $\delta = -9°$. Denning discovered the association between this shower and Comet 1P/Halley in 1900, although many astronomers had made this suggestion since 1868 in various articles. Denning predicted an increase in activity at the next return of the Comet in 1910, although we have no evidence that η-Aquariid activity was any higher than normal around that perihelion passage time of 1P/Halley. The Comet produces another meteor shower, the Orionids, which is described at page 47. Both the meteoroids of the η-Aquariids and the Orionids are quite far from the orbit of their parent and thus we do not see freshly ejected meteoroids close to the perihelion passage of the Comet (Babadzhanov et al., 1987; McIntosh & Jones, 1988; Ryabova, 2003). The modelled stream shows a complex structure of layers and currently observable η-Aquariids should have been released from the Comet not later than 837 AD (Ryabova, 2003).

2.9.2 Research

Since 1975 the η-Aquariids have been observed carefully in almost every year. In the broad maximum the ZHR reaches 50–80, and a minor activity can be traced until end-May (Cooper, 1996; Rendtel, 1997; Dubietis, 2003). The average population index r is found in the range

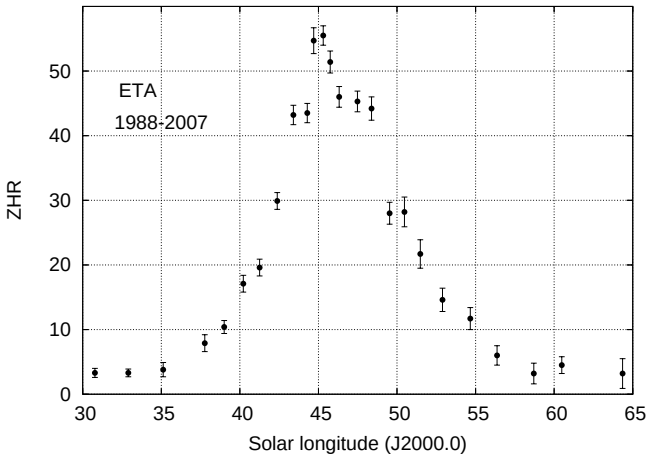


Figure 2.13: Activity of the η-Aquariids from visual observations stored in the VMDB covering the period 1988–2007 using a constant $r = 2.4$ over the activity period. The zenith correction included the standard sine term (no zenith coefficient $\gamma > 1.0$) and allowed only intervals with a radiant elevation of $\geq 20°$.

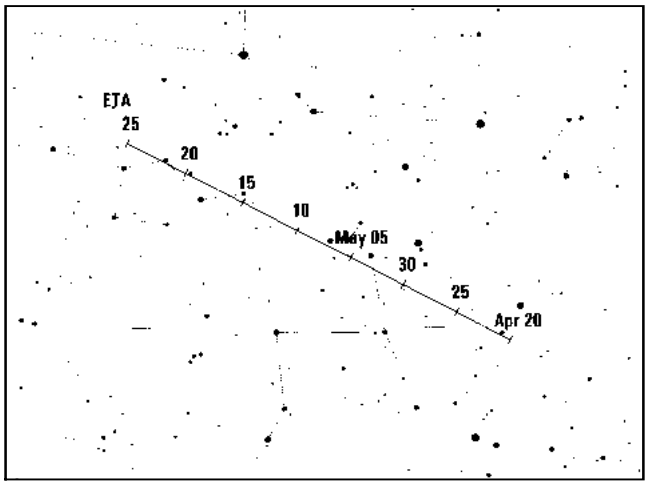


Figure 2.14: Radiant drift of the η-Aquariids.

2.2–2.5 (Dubietis, 2003), but is slightly lower near the rate maximum (e.g. $r \approx 2.0$ was found in 1997; Rendtel, 1997).

Jenniskens (2006; p. 305) suggests a profile composed of two components. The narrow one peaks at $\lambda_\odot$=44.°4, but was found only in the 1993–1997 data while it did not occur in the 1986–1992 data. He notes that the position of Jupiter could be the reason for the small difference in the rate profiles.

In 2013, the maximum ZHR exceeded the average level of about 70 significantly and for a long time. The preliminary analysis provided by the live graph of the *IMO* (see `http://www.imo.net/live/eta-aquariids2013/`) assuming a constant $r = 2.4$ yielded ZHR > 70 between $\lambda_\odot = 44.°49$ and $46.°83$ corresponding to 2013 May 05, 0^h UT and May 07, 10^h UT (i.e. almost 2.4 days. An explanation was presented by Mikiya Sato (Sato & Watanabe, 2014), showing that the meteoroids are from very old ejection from the parent 1P/Halley and are trapped probably in resonances to Jupiter's orbit (similar to the Orionids observed between 2007 and 2010). The peak ZHR assuming the ETA standard $r = 2.4$ reached 135 ± 16 at $\lambda_\odot = 45.°56 \pm 0.°05$. As there were reports about a considerable amount of bright ETA shower meteors, the true value of the population index may have been lower. Applying $r = 2.1$ yields a ZHR of 120 instead, not changing the result. The 2014 return of the shower showed the average ZHR of about 50 again which is in agreement with the Sato's model calculation.

References

Ahn S-H., 2003: Meteors and showers a millenium ago. *MNRAS* **343,** 1095–1100.

Babadzhanov P.B., Obrubov J.V., Pushkarev A.N., Hajuk A., 1987: On the formation of meteor showers of comet Halley. *Bull. Astr. Inst. Czechosl.* **38,** 367–371.

Cooper T., 1996: A decade of visual η-Aquarid meteor observations. *WGN* **24,** 157–161.

Denning W.F., 1883: The Aquarids of April 29 to May 3. *MNRAS* **43,** 111–114.

Dubietis A., 2003: Long-term activity of meteor showers from Comet 1P/Halley. *WGN* **31,** 43–48.

Jenniskens P., 2006: Meteor Showers and their Parent Comets. Cambridge University Press.

McIntosh B.A., Jones J., 1988: The Halley comet meteor stream – numerical modelling of its dynamic evolution. *MNRAS* **235,** 673–693.

Rendtel J., 1997: The η-Aquarid meteor shower in 1997. *WGN* **25,** 153–156.

Ryabova G.O., 2003: The comet Halley meteoroid stream: just one more model. *MNRAS* **341,** 739–746.

Sato M., Watanabe J., 2013: Forecast of enhanced activity of eta-Aquariids in 2013, in: T.J. Jopek, F.J.M. Rietmeijer, J. Watanabe, I.P. Williams (eds.), Meteoroids 2013, Proc. Int. Conf. Poznań, Poland, 213–216

Shigeno Y., Toda M., Shioi H., 1997: Double station observations of the η-Aquarids. *WGN* **25,** 217–221.

2.10 η-Lyrids (145 ELY)

2.10.1 Synopsis

Period	May 3-12
Maximum	$\lambda_\odot = 48\overset{\circ}{.}4$ ($\approx$ May 8)
Radiant	$\alpha = 287°$ $\delta = +44°$
$ZHR_{max} = 3$	$r = 3.0$ $V_\infty = 44$ km/s
Parent body	C/1983 H1 (IRAS-Araki-Alcock)

Orbital elements of the stream and C/1983 H1:

Ω	ω	i	e	q	a	P
ELY, Jenniskens (2006)						
$45\overset{\circ}{.}7$	$190\overset{\circ}{.}0$	$79\overset{\circ}{.}4$		0.995 au	6.03 au	
C/1983 H1						
$49\overset{\circ}{.}10$	$192\overset{\circ}{.}85$	$73\overset{\circ}{.}25$	0.990	0.991 au	98.1 au	

This shower which is associated with Comet C/1983 H1 (IRAS-Araki-Alcock). It was introduced to the Working List although it appears to be only a weak source. The radiant position found from recent IMO video data gives a radiant centred at $\alpha = 290°$, $\delta = +42°$ (Figure 2.15). Careful visual or telescopic plotting will be needed to separate any potential η-Lyrids from the sporadics.

Comet C/1983 H1 (IRAS-Araki-Alcock) is a well studied object, and meteor activity from that parent has been significant though not very high. A comprehensive set of video meteors shows the radiant very clearly. Since nearly all the video meteors are in the visual range of brightnesses, the radiant is also a good representation of what visual observations would obtain, less accurately though. Ohtsuka (1991) reported about five orbits in the IAU orbital database which were associated with the Comet. These orbits give a radiant position of about $\alpha = 289°$, $\delta = +43\overset{\circ}{.}2$ centered around a solar longitude of $\lambda_\odot = 49\overset{\circ}{.}6$. The closest approach to the orbit of C/1983 H1 is $\lambda_\odot = 48\overset{\circ}{.}4$ with a theoretical radiant position of $\alpha = 288\overset{\circ}{.}0$, $\delta = 44\overset{\circ}{.}0$ and a geocentric velocity of $v_g = 43.8$ km/s. Bearing in mind that the difference in reference dates for the observational and the theoretical estimates is about one day, the results agree very well.

For the Shower List, we adopt an activity period of May 3–12 as was done by Kronk (1988). There are several methods of how to compute the possible evolution of meteoroid particles to approach Earth, without actually following the motion of individual particles. The methods compiled by Neslušan et al. (1998) yield a time of probable maximum activity at $\lambda_\odot = 48\overset{\circ}{.}4$ or roughly May 9. The encounter velocity of the particles including the gravity of the Earth is 44 km/s. A daily motion of the radiant of 1° per day is assumed for the ephemeris.

The η-Lyrids may be an interesting meteoroid source as both orbital elements and parent are available. The shower should not be confused with the τ-Herculids theoretically generated from the disintegrated Comet 73P/Schwassmann-Wachmann 3, but not exhibiting significant meteor numbers hitherto (Arlt & Vaubaillon, 2006).

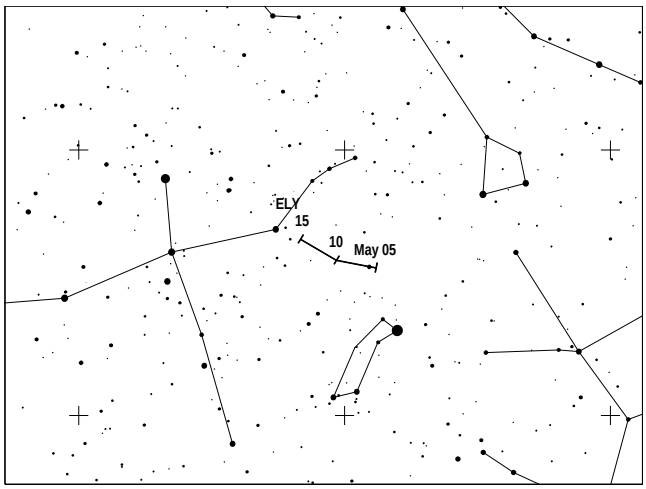


Figure 2.15: Radiant drift of the η-Lyrids.

References

Arlt R., Vaubaillon J., 2006: The meteors from 73P/Schwassmann-Wachmann 3 in 1930 and 2006. *WGN* **34,** 15–18.

Jenniskens P., 2006: Meteor Showers and their Parent Comets. Cambridge University Press.

Kronk G., 1988: Meteor Showers: A Descriptive Catalog. Enslow Publ., Hillside, New Jersey.

Neslušan L., Svoreň J., Porubčan V., 1998: A computer program for calculation of a theoretical meteor-stream radiant. *A & A* **331,** 411–413.

Ohtsuka K., 1991: Lyrid meteor stream associated with Comet Iras-Araki 1983 VII. In: *A.C. Levasseur-Regourd and H. Hasegawa (eds.): Origin and Evolution of Interplanetary Dust*, page 315. Kluwer.

2.11 June Bootids (170 JBO)

2.11.1 Synopsis

Period	June 22–July 2
Maximum	$\lambda_\odot = 95\overset{\circ}{.}7$ ($\approx$ June 27)
Radiant	$\alpha = 224°$ $\delta = +48°$
$\mathrm{ZHR_{max}} = \textit{variable}$	$r = 2.2$ $V_\infty = 18$ km/s
Parent body	7P/Pons-Winnecke

Orbital elements of the stream and 7P/Pons-Winnecke:

Ω	ω	i	e	q	a	P
JBO, Jenniskens (2006)						
$96\overset{\circ}{.}05$	$183\overset{\circ}{.}65$	$18\overset{\circ}{.}4$		1.016 au	3.3 au	
7P/Pons-Winnecke						
$93\overset{\circ}{.}45$	$172\overset{\circ}{.}29$	$22\overset{\circ}{.}28$	0.634	1.258 au		6.38 yr

This shower was reinstated on the Working List after its unexpected return of 1998 (Arlt et al., 1999), when ZHRs of 50–100+ were visible for more than half a day. Another outburst of similar length, but with lower ZHRs of $\approx 20 - 50$ was observed on 2004 June 23. This occurred outside the usually assumed activity period, *earlier than* any June Bootids previously had been recorded.

The activity period is an issue with this shower, since the maximum on June 27 follows the beginning of the period, June 26, very closely. Dust trail predictions have delivered peak dates as early as June 22. That case may have been exceptional but, nevertheless, we list the activity of the June Bootids from June 22 to July 2 (Arlt & Rendtel, 2006). Even if this activity period is overestimated, pollution by sporadic meteors is not very likely because of the high elongation of the radiant from the apex and the peculiar velocity of the shower. The radiant (Figure 2.16) is well above the horizon for most observers in the northern hemisphere, although twilight is a problem for latitudes north of about 50°. Rates are close to the detection limit in years with no enhancements (Seifert, 1998; Arlt, 2000; Rendtel, 2002).

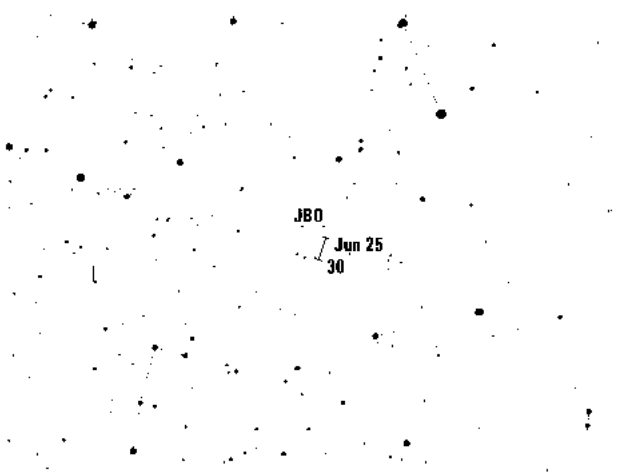


Figure 2.16: Radiant drift of the June Bootids.

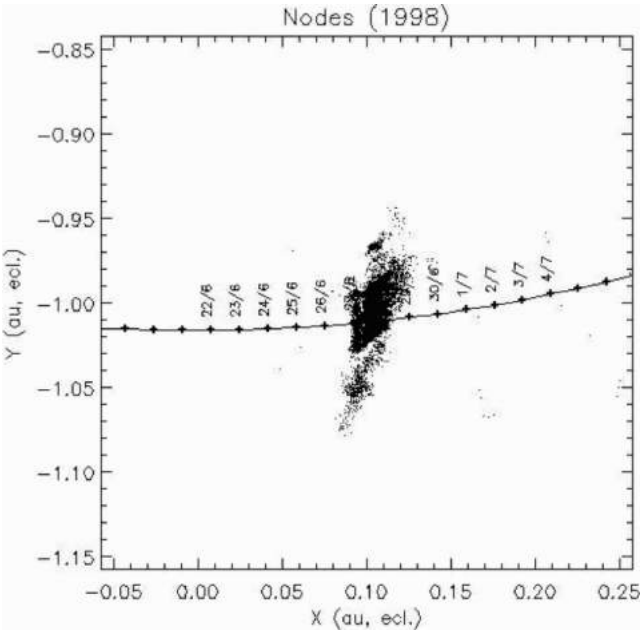


Figure 2.17: Distribution of nodes of particle orbits producing the 1998 June Bootid outburst (model calculations by J. Vaubaillon).

2.11.2 Research

Prior to 1998, three more probable returns with enhanced rates had been recorded, in 1916, 1921, and 1927. The outbursts of 1916 and 1998 were analysed and modelled in detail by Asher & Emel'yanenko (2002), following the work of Reznikov (1983). Particles responsible for the 1998 outburst were ejected from the parent comet, 7P/Pons-Winnecke at its 1825 return. Then, a substantial portion of the meteoroids remained in a 2:1 resonance with Jupiter (Figure 2.17). The comet's perihelion distance undergoes variations which periodically take it on an Earth-crossing orbit.

Another result was obtained by Tanigawa & Hashimoto (2000). They associate the 1998 outburst with meteoroids released from the parent comet in 1819 and 1869 and perturbed into Earth-colliding orbits by Jupiter.

Each meteoroid orbit is a modification of the parent's orbit due to ejection velocity and direction. The model calculations of Asher and Emel'yanenko (2002) are consistent with an ejection velocity of 10–20 m/s for meteoroids to reach the 2:1 resonance. The discussion of particle ejection from comets using different models has yielded different results over the past years, but it seems that low values of some tens of m/s are currently favoured. Assuming that a significant number of June Bootid meteoroids is still in the 2:1 resonance another June Bootid activity increase in 2004 was expected (Figure 2.18) and indeed occurred (Figure 2.19)—after 0.5 orbital periods of Jupiter, with the 1998 outburst time falling on June 27, 01 UT. An attempt to combine the 1921 and 1927 observations of increased June Bootid rates with the major events in 1916 and 1998, led to the chance of enhanced rates on 2003 June 27, 19 UT, which in fact did not materialize.

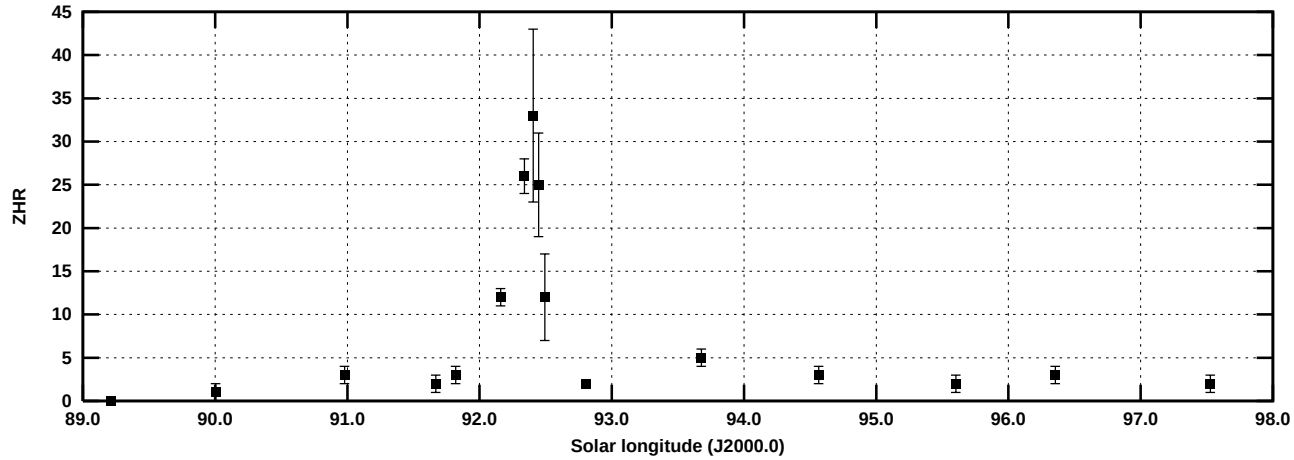


Figure 2.19: Activity profile of the 2004 June Bootids from visual observations.

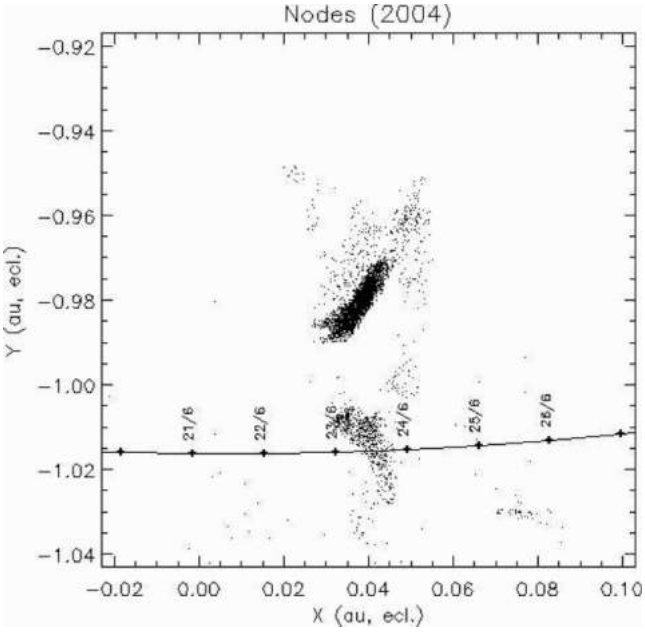


Figure 2.18: Distribution of orbital nodes of particles ejected in 1813–1875 producing the 2004 June Bootid outburst (J. Vaubaillon).

In 2004, enhanced rates were expected and observed (Okamoto et al., 2005). A maximum ZHR of 30±10 was found at 2004 June 23, $14^{\mathrm{h}}50^{\mathrm{m}}$ UT ±60 min with a full width at half-maximum of about 7 hours (Vaubaillon et al., 2005). The population index was found as $r = 2.49 \pm 0.15$.

References

Arlt R., 2000: The analysis of a weak meteor shower: the June Bootids 2000. *WGN* **28,** 98–108.

Arlt R., Rendtel J., 2006: A new Working List of meteor showers. *WGN* **36,** 77–84.

Arlt R., Rendtel J., Brown P., Velkov V., Hocking W.K., Jones J., 1999: The 1998 Outburst and History of the June Bootid Meteor Shower. *MNRAS* **308,** 887–896.

Asher D.J., Emel'yanenko V.V., 2002: The origin of the June Bootid outburst in 1998 and determination of cometary ejection velocities. *MNRAS* **331,** 126–132.

Jenniskens P., 2006: Meteor showers and their parent comets. Cambridge Univ. Press.

Okamoto S., Ueda M., Fujiwara Y., Uehara S., 2005: TV Observation of the 2004 June Bootid Meteors. *WGN* **33,** 105–107.

Rendtel J., 2002: June Bootid Observations in 2002. *WGN* **30,** 85–86.

Reznikov E.A., 1983: The origin of the Bootid meteor stream (in Russian). *Trudy Kazan. Gor. Astron. Obs.* **47,** 131–136.

Seifert H., 1998: The June Bootids in 1995 and 1997. *WGN* **26,** 267.

Tanigawa T., Hashimoto T., 2000: The origin of the 1998 June Bootid meteor shower. *Earth, Moon, and Planets* **88,** 27–33.

Vaubaillon J., Arlt R., Shanov S., Dubrovski S., Sato M., 2005: The 2004 June Bootid meteor shower. *MNRAS* **362,** 1463–1471.

2.12 α-Capricornids (001 CAP)

2.12.1 Synopsis

Period	July 3–August 15
Maximum	$\lambda_\odot = 127°$ ($\approx$ July 29)
Radiant	$\alpha = 307°$ $\delta = -10°$
$\mathrm{ZHR_{max}} = 4$	$r = 2.5$ $V_\infty = 23$ km/s
Parent body	(2101) Adonis or 45P/Honda-Mrkos-Pajdušáková

Orbital elements of the stream and related objects:

Ω	ω	i	e	q	a	P
CAP, Lindblad (1987), phot.						
126.°9	270.°2	7.°3	0.758	0.587 au	2.421 au	3.8 yr
(2101) Adonis						
350.°58	41.°69	1.°36	0.764	0.443 au	1.87 au	2.6 yr
45P/Honda-Mrkos-Pajdušáková						
89.°17	326.°02	4.°2	0.824	0.533 au	3.03 au	5.3 yr

In mid to high northern latitudes the radiant of the α-Capricornids (Figure 2.20) rises relatively little above the horizon. With a maximum ZHR of about 4 (Figure 2.21), the number of observed shower meteors will remain low. At subtropical and tropical latitudes, the radiant will be seen at a much smaller zenith distance, leading to a noticeably richer display. The α-Capricornids often display bright meteors.

While the ZHR level seems to vary little from one year to another, it seems that the 1984 return yielded and a lower population index r and a significantly enhanced ZHR between 8 and 12 (Figure 2.21 (b); Miskotte & Johannink, 2008). Observations from Namibia in 2011 and from La Palma in 2008 (Miskotte & Johannink, 2012) yielded maximum ZHRs of about 6 with an average population index of $r = 2.00$.

Despite the radiant overlap with the Antihelion Source (see Figure 2.20 on page 29), we leave the shower in the Working List, because of the interesting connection with a comet or perhaps asteroids, the good knowledge of orbits, and the prominence in activity curves of the ecliptical activity in July–August. Observers should make a careful distinction between the Capricornids and the Antihelion Source from July 3 to August 15 considering the low velocity of the α-Capricornids.

2.12.2 Research

Hasegawa (2001) suggested the existence of substructures of the stream from data in the IAU database connected with the comets 45P/Honda-Mrkos-Pajdušaková, 72P/Denning-Fujikawa, 141P/Machholz 2, the minor planets (2101) Adonis, (9162) 1987OA, C/1457 L1, and a hypothetical comet whose orbital elements are given. Investigations of the orbital evolution yield connections with meteor showers in July and February (Babadzhanov, 2003).

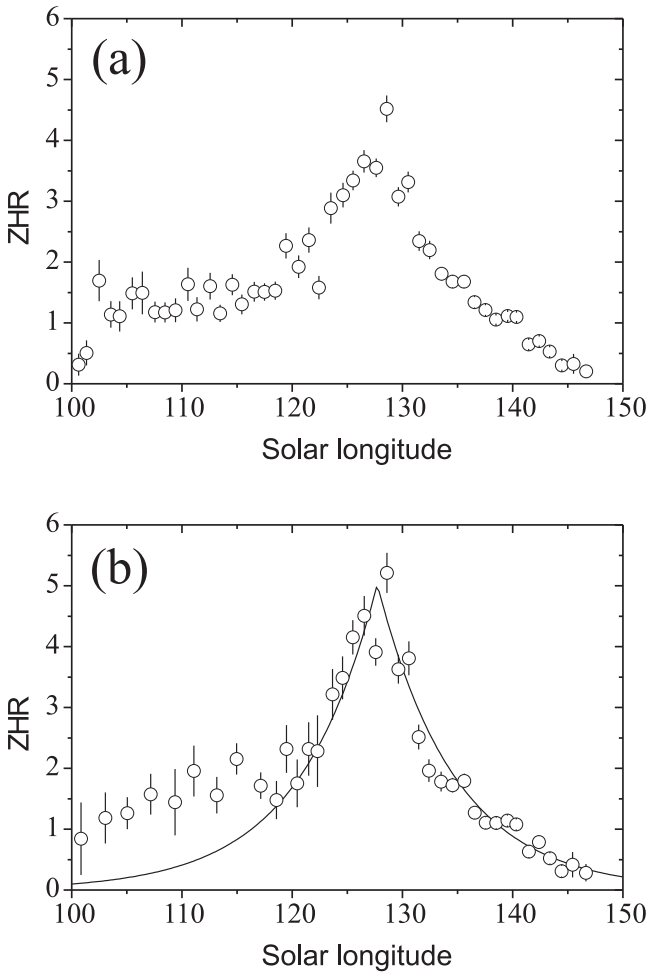


Figure 2.21: Activity profile of the α-Capricornids from observations of 1997–2002.

References

Babadzhanov P.B., 2003: Meteor shower associated with the near-Earth asteroid (2101) Adonis. *A&A* **397,** 319-323.

Hasegawa I., 2001: Parent objects of α Capricornid meteor stream. *In: Proc. Meteoroids 2001*, ESA-SP 495, 55–62.

Lindblad B.A., 1987: Physics and orbits of meteoroids. In: *The Evolution of the Small Bodies of the Solar System*, Soc. Italiana di Fisica, Bologna.

Miskotte K., Johannink C., 2008: The Capricornids in 1984. *WGN* **36,** 37–39.

Miskotte K., Johannink C., 2012: The Capricornids observed from Namibia. *WGN* **40,** 87–89.

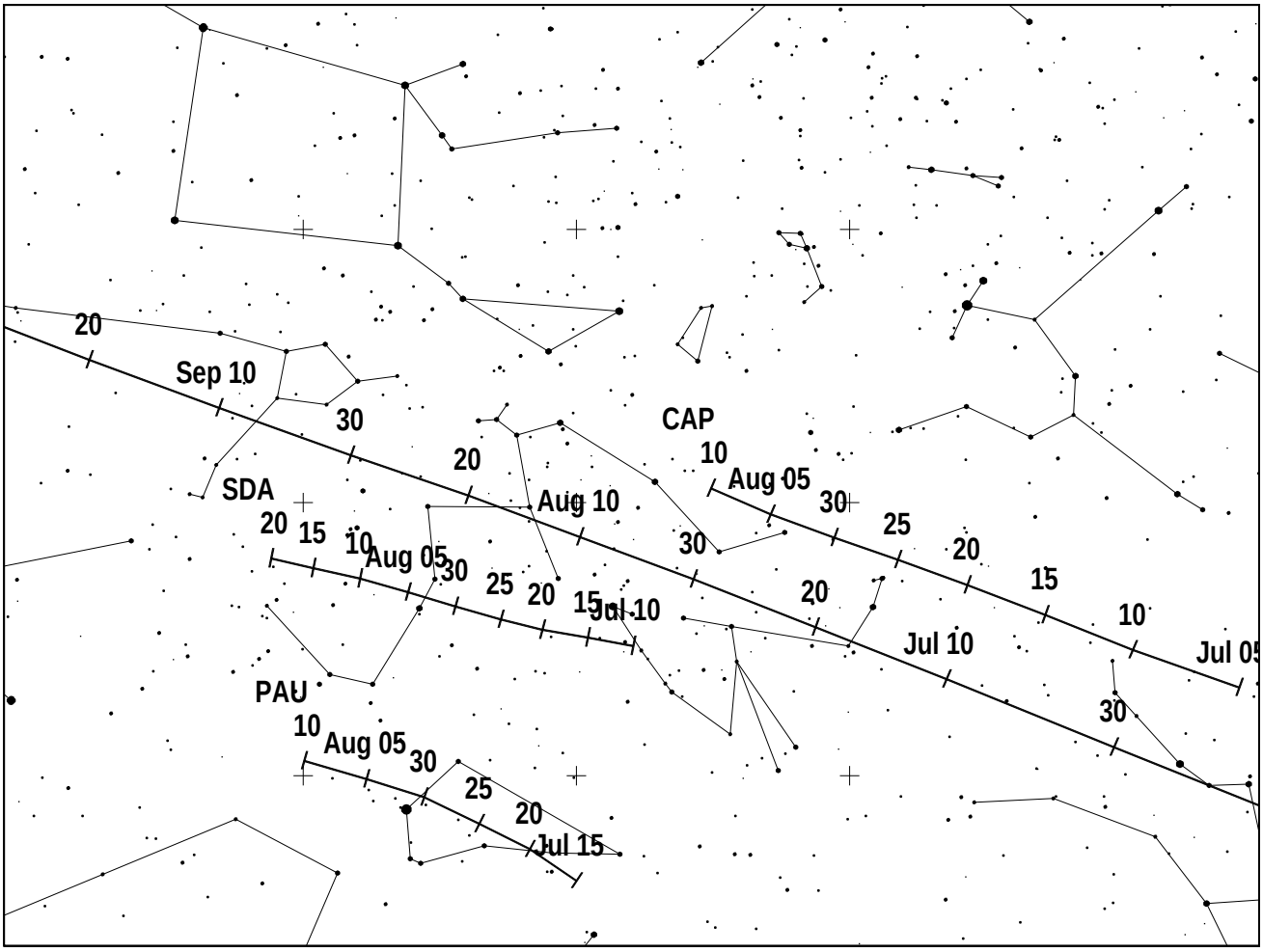


Figure 2.20: Radiant drift of the showers in the Aquarius-Capricornus-region in summer. The radiant of the Antihelion Source also moves through the field. Care needs to be taken when associating meteors to the different sources, considering not only the direction but also the apparent trail length and angular velocity.

2.13 Southern δ-Aquariids(005 SDA)

2.13.1 Synopsis

Period	July 12–August 19
Maximum	$\lambda_\odot = 125°$ (≈ July 28)
Radiant	$\alpha = 339°$ $\delta = -16°$
$ZHR_{max} = 15$	$r = 3.2$ $V_\infty = 41$ km/s
Parent body	stream belongs to complex with Quadrantids and a number of asteroids and comets

Orbital elements of the stream and 96P/Machholz 1:

Ω	ω	i	e	q	a	P
SDA, Lindblad (1987), phot.						
309.°6	149.°5	26.°2	0.967	0.102 au	3.09 au	5.4 yr
Kashcheyev & Lebedinets (1967), radar						
307°	151°	28°	0.96	0.08 au	2.04 au	2.9 yr
96P/Machholz 1 (2007)						
94.°55	14.°62	59.°95	0.959	0.125 au	3.0 au	5.2 yr

Around the maximum of this southern shower, we can observe quite a number of δ-Aquariids. At latitudes north of about 45° the δ-Aquariid radiant (Figure 2.20) never reaches a reasonable elevation above the horizon.

A study of the radiant structure of the various sources in Aquarius (Arlt et al., 1992) involving nearly 5000 meteors from the Aqr-Cap region, based mainly on data obtained from mid-northern locations, showed the Northern δ-Aquariids (now part of the Antihelion Source as shown in Figure 2.20 on page 29) between July 21 and August 11. The Southern δ-Aquariids only occurred distinctly on July 30 at $\alpha = 340°$ and $\delta = -14°$, which is almost the date of their maximum. The activity over the entire period given in the list is shown in Figure 2.22. It can be detected until August 7 by visual means. A recent analysis of video data allows to detect the shower reliably until August 24 (Molau & Rendtel, 2009).

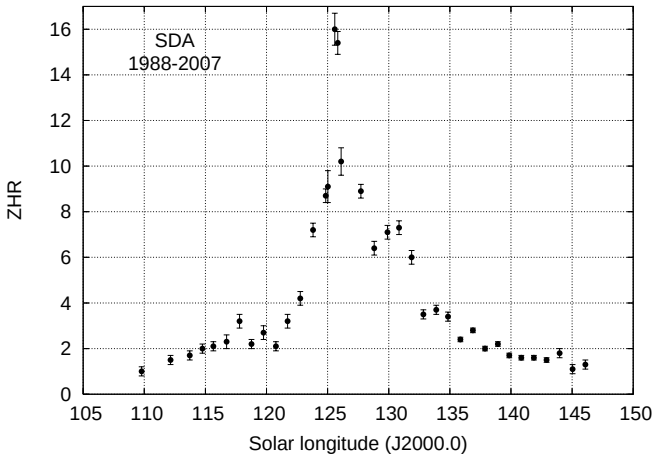


Figure 2.22: Activity of the δ-Aquariids from visual observations stored in the VMDB covering the period 1988-2007 using a constant $r = 3.2$ over the activity period. The zenith correction included the standard sine term (no zenith coefficient $\gamma > 1.0$) and allowed only intervals with a radiant elevation of $\geq 20°$.

2.13.2 Research

Model calculations of the evolution of the Southern δ-Aquariids indicated a possible relationship between the current δ-Aquariids and the past orbital elements of the Quadrantids. Details are given in the Quadrantid section.

Still another remarkable relationship with the δ-Aquariids has been found. The Arietids, a daylight shower in June, display their maximum activity on June 1 with a radiant near $\alpha = 38°$ and $\delta = +15°$. After perihelion passage, this stream encounters the Earth's orbit again on July 28 with a predicted radiant at $\alpha = 336°$ and $\delta = -11°$, exactly coincident with the δ-Aquariid radiant! This clearly demonstrates the relationship (Almond, 1951).

Ceplecha (1983) classified the δ-Aquariid meteoroids in class B, which means that they may originate from the nucleus of a small comet. As the δ-Aquariid stream is involved in the orbital complex of the Quadrantids, it is also connected to 96P/Machholz 1 or possibly Comet C/1490 Y1 = 1491 I (McIntosh, 1990). However, it is not evident whether the meteoroids of the δ-Aquariid stream were ejected from the nucleus of either of these comets. Another class B meteoroid stream associated with a known parent body is the Geminid stream, which is related to the asteroid 3200 Phaethon.

Double-station video observations (Shigeno et al., 1999) yielded a radiant motion of $\alpha = 339.°31 + 0.75(\lambda_\odot - 125.°0)$, $\delta = -16.85 + 0.22(\lambda_\odot - 125.°0)$. This is fairly close to the *IMO* radiant drift used hitherto (cf. Figure 2.20).

References

Almond M., 1951: The summer daytime meteor streams of 1949 and 1950. III. Computation of the orbits. *MNRAS* **110,** 37–44.

Arlt R., Koschack R., Rendtel J., 1992: Results of the IMO Aquarid project. *WGN* **20,** 114–135.

Ceplecha Z., 1983: New aspects in the classification of meteoroids. In: *C.I. Lagerkvist, H. Rickman (eds.), Proceedings of Asteroids, Comets, Meteors*, Univ. of Uppsala, 435–438.

Kashcheyev B.L., Lebedinets V.N., 1967: Radar studies of meteors. *Smithson. Contr. Astrophys.* **11,** 183–199.

Lindblad B.A., 1987: Physics and orbits of meteoroids. In *M. Fulchignoni & L. Kresák (eds.): The evolution of the small bodies of the Solar System.* Soc. Italiana di Fisica, Bologna, 229–251.

McIntosh B.A., 1990: Comet P/Machholz and the Quadrantid meteor stream. *Icarus* **86,** 299–304.

Molau S., Rendtel J., 2009: A Comprehensive list of meteor showers obtained from 10 years of observations

with the IMO Video Meteor Network. *WGN* **37,** 98–121.

Shigeno Y., Shigeno T., Shioi H., 1999: Double-station TV meteor observations of the α-Capricornids and Aquarids in late July. *WGN* **27,** 202–205.

2.14 Piscis Austrinids (183 PAU)

Period	July 15–August 10	
Maximum	$\lambda_\odot = 125°$ ($\approx$ July 27)	
Radiant	$\alpha = 341°$	$\delta = -30°$
$ZHR_{max} = 4$	$r = 3.2$	$V_\infty = 35$ km/s
Parent body	unknown	

Orbital elements of the stream:

Ω	ω	i	e	q	a	P
PAU, Kashcheyev & Lebedinets (1967), radar						
303.°9	132.°6	37.°5	0.24	0.84 au	1.0 au	1.0 yr
303°	114°	45°	0.96	0.17 au	4.31 au	8.9 yr

The Piscis Austrinids are visible from July 15 to August 10. As this period, together with their maximum, almost coincides with the δ-Aquariids, observations of this shower are often neglected in favour of its more northerly neighbour (Figure 2.20). The ZHR-graph (Figure 2.23) shows a low rate. Hence the Piscis Austrinids produce 1 or 2 meteors per hour rising to some 3 to 5 per hour at maximum for observers in southern latitudes for most of their period of activity. Observers at more northern locations will see only very few shower meteors of this southern radiant (Figure 2.20).

The shower is on the various lists already from 1865 onwards (Herschel, 1866; Denning, 1899). From 1910 to 1940, the Piscis Austrinids were given close scrutiny by members of the Western Australian Astronomical Society. Hoffmeister (1948) remarked that a distinct Piscis Austrinid shower was not evident, and that it might only be the southernmost branch of the Aquariid scatter field. McIntosh (1935), in a comprehensive radiant study, identified some 7 sub-showers, each of which had their own particular maximum between July 17 and August 13.

Radio-echo meteor observations at Christchurch, New Zealand (Ellyett & Roth, 1955) showed a radiant probably linked to the Piscis Austrinids at $\alpha = 328°$ and $\delta = -27°$ between 1953 July 21 and 26. The shower was not mentioned until 1960 when Kashcheyev & Lebedinets (1967) carried out extensive radio observations. They detected 32 meteors with similar orbits between July 16 and August 13 which we can associate with the Piscis Austrinids. They found a maximum on July 26 ($\lambda_\odot = 123°$) with a radiant at $\alpha = 340°$ and $\delta = -26°$.

In the 1960s and 1970s, visual observers from Australia and New Zealand determined the date of maximum to be July 28, with maximum ZHRs of about 4 in 1977 and 1979 (Kronk, 1988).

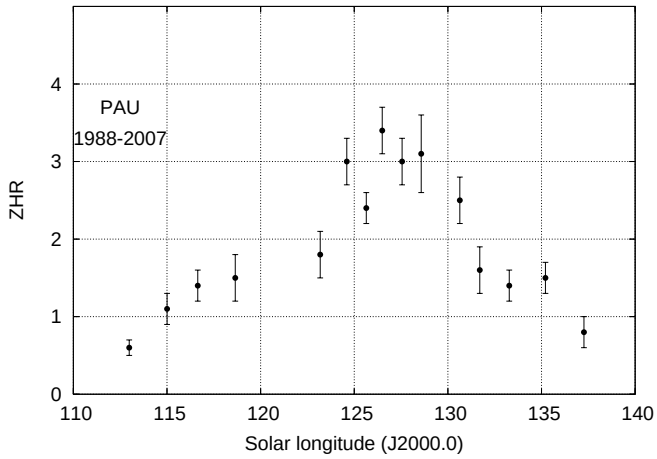


Figure 2.23: Activity of the Piscis Austrinids from visual observations stored in the VMDB covering the period 1988–2007 using a constant $r = 3.2$ over the activity period. The zenith correction included the standard sine term (no zenith coefficient $\gamma > 1.0$) and allowed only intervals with a radiant elevation of $\geq 20°$.

References

Denning W.F., 1899: General catalogue of the radiant points of meteoric showers and of fireballs and shooting stars observed at more than one station. *Mem. Roy. Astr. Soc.* **53,** 202–292.

Ellyett C.D., Roth K.W., 1955: The radar determination of meteor showers in the shouthern hemisphere. *Austr. J. Phys.* **8,** 390–401.

Herschel A.S., 1866: Radiant points of shooting stars. *MNRAS* **26,** 51–53.

Hoffmeister C., 1948: Meteorströme. J.A. Barth, Leipzig.

Kashcheyev B.L., Lebedinets V.N., 1967: Radar studies of meteors. *Smithson. Contr. Astrophys.* **11,** 183–199.

Kronk G., 1988: Meteor Showers. A Descriptive Catalog. Enslow, Hillside, New Jersey.

McIntosh R.A., 1935: An index to southern meteor showers. *MNRAS* **95,** 709–718.

2.15 Perseids (007 PER)

2.15.1 Synopsis

Period	July 17–August 24
Maximum	$\lambda_\odot = 140\,^\circ\!.0$ ($\approx$ August 12)
Radiant	$\alpha = 49^\circ$ $\delta = +58^\circ$
$\mathrm{ZHR_{max}} = 100$	$r = 2.2$ $V_\infty = 59$ km/s
Parent body	109P/Swift-Tuttle

Orbital elements of the stream and 109P/Swift-Tuttle:

Ω	ω	i	e	q	a	P
PER, Lindblad & Porubčan (1994), phot.						
$139\,^\circ\!.61$	$150\,^\circ\!.53$	$113\,^\circ\!.27$	0.996	0.948 au	81 au	730 yr
PER, Kashcheyev & Lebedinets (1967, radar, mean)						
136°	151°	113°	0.91	0.95 au	11.0 au	36 yr
109P/Swift-Tuttle						
$139\,^\circ\!.44$	$153\,^\circ\!.00$	$113\,^\circ\!.43$	0.964	0.958 au	27 au	135 yr

When a novice amateur astronomer talks about meteors, the shower most likely to be mentioned is the Perseids. Indeed the Perseid meteor shower is the singlemost popular regular meteor display for observers at the present time.

Whatever the phase of the Moon, there is always part of the activity period observable without moonlight. The radiant (Figure 2.24) rises from a low elevation in the evening hours to a small zenith distance by the end of the night, but Perseids are unobservable from southern latitudes. In subtropical areas, the radiant can only be observed after midnight.

The activity level remains low in the outer regions of the stream, as is evident from the ZHR profile shown in Figure 2.26, calculated from data covering the period 1988–2008. Hence the method for minor shower observations should be applied. The Perseids can be regarded as a major shower only in the interval 137°–143°.

The ZHR profile is skew with a steeper decrease after the maximum period. The impression of a possible ZHR sub-maximum a few days before the maximum is obviously imposed by the decreasing r combined with the continuous ZHR rise. The profile of the population index r, also calculated from the 1988–2008 data (Figure 2.25), shows four distinct features:
(i) a low $r = 2.1 - 2.2$ at the activity start;
(ii) a significant maximum of $r = 2.46$ at $\lambda_\odot = 122\,^\circ\!.3$ (July 25);
(iii) $r < 2.0$ in the immediate peak period (different for each return);
(iv) steady increase of r after the maximum, reaching $r = 2.6$ at the end of the activity period.

The Perseids have been observed for at least 2000 years now. The first information on them came from the Far East (Zhuang, 1977). Clearly, the Perseid stream has a very stable, highly inclined orbit which protects it from strong planetary perturbations.

In the period 1864–1866, Schiaparelli (1871) proved by calculations of the Perseid orbit that this stream

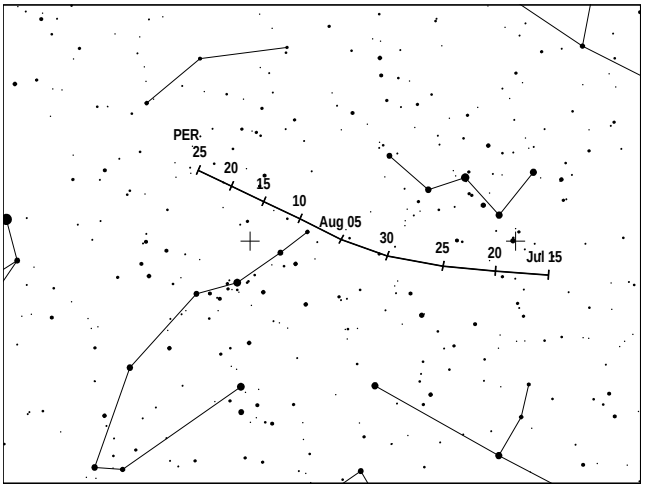


Figure 2.24: Radiant drift of the Perseids, according to recent positional data (Arlt, 2003).

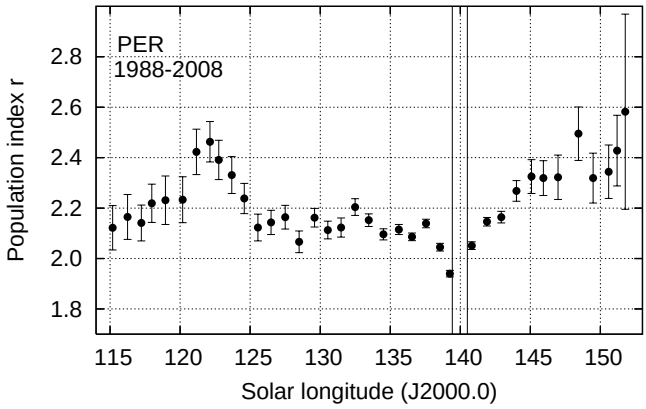


Figure 2.25: Profile of the population index for the entire activity period, except the immediate peak ($139\,^\circ\!.4$–$140\,^\circ\!.5$) of the Perseids, derived from data collected between 1988 and 2008. The profile is smooth and shows an average of $r \approx 2.2$ with a prominent maximum near $\lambda_\odot = 122^\circ$ (July 25), while a steady decrease towards and after the peak period is found.

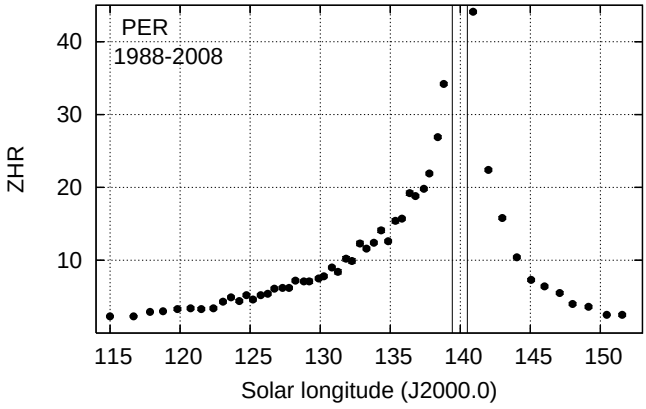


Figure 2.26: Perseid ZHR Profile for the entire activity period, except the immediate peak ($139\,^\circ\!.4$–$140\,^\circ\!.5$), derived from data collected between 1988 and 2008, using the r-profile shown in Figure 2.25.

shared the orbit of Comet 1862 III (109P/Swift-Tuttle). This was the first proven association between a meteor shower and a comet.

Since that time, Perseids have been observed in virtually every year. Variable maximum rates have been reported in the first half of this century. At that time, no global data sets were used to determine maximum activity. The actual peak may have been missed by the observer reporting the rates as it appeared during day-time.

At the end of the 1970s, Perseid rates showed signs of an increase, culminating in 1980 when the ZHR reached 180. Observers in the Swiss Alps counted up to 14 Perseids in one minute on 1980 August 12, between $1^{\rm h}$ and $2^{\rm h}$ UT (Simmons, 1981). These exceptional rates were related to the expected return of Comet Swift-Tuttle. However, the comet was finally recovered only in 1992. The rich return of 1980 was confirmed by observers at several other sites, although the ZHR level of 180 may not be entirely accurate. Even so, revised results do indicate an above average activity level for the 1980 return. However, we cannot qualify this as an exceptionally strong return, and there was certainly no meteor storm as some people suggested.

In the rate profile for the 1988 Perseids obtained from global observational data, a small new peak was found which preceded the 'normal' peak by about 12 hours (Roggemans, 1989). This peak reappeared in the 1989 analysis (Koschack & Roggemans, 1991).

In 1991 this 'new' maximum caused exceptional activity with a peak ZHR of 350 at $\lambda_\odot = 139\,^\circ\!.58$, which was observed in Japan and the Far East. The detailed analysis of the outburst period showed that the r value did not significantly vary during the outburst (Koschack et al., 1993).

The recurrence of the outburst was expected in 1992 at $22^{\rm h}$ UT. In fact, it occurred about 2.5 hours earlier, at $\lambda_\odot = 139\,^\circ\!.50$ (Koschack et al., 1993). This is exactly the nodal longitude of Comet 109P/Swift-Tuttle.

The Perseid's parent comet was re-discovered after the 1992 Perseid outburst by Kiuchi on 1992 September 26 (Marsden, 1992). Although the Comet was quite bright in 1862 (about +2 mag), the determination of its orbit was not very certain. Furthermore, no earlier apparition of 109P/Swift-Tuttle seemed to have been observed. However, Marsden (1973) reported a possible link with Comet Kegler of 1737. If these were successive apparitions of one comet, the orbital period should have been significantly longer than the 120 years derived from the 1862 observations. This has indeed been confirmed by the rediscovery of 109P/Swift-Tuttle. Marsden (1992) points out that a precise linkage of comet observations, even at only two apparitions, is not possible without involving large nongravitational forces.

The 1993 return of the shower received at lot of attention from the general public, as some predictions suggested the possibility of higher activity than in 1991 and 1992. Even NASA delayed the launch of the Space Shuttle 'Discovery' due to the danger posed by meteoroidal debris from the Perseid stream (Brown, 1993). Based on the 1992 data, the 1993 peak was predicted

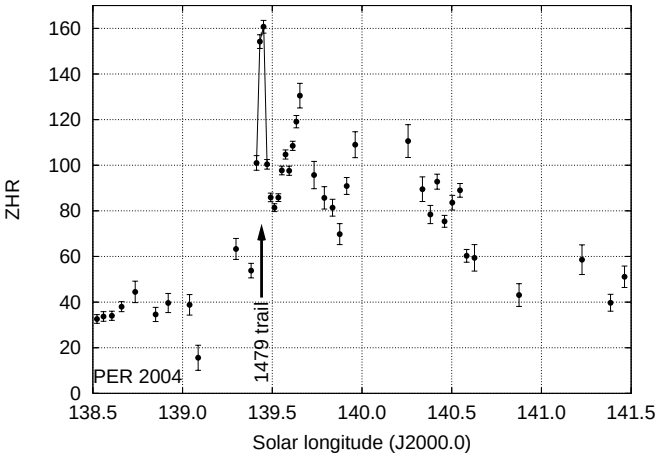


Figure 2.27: ZHR profile of the 2004 Perseids with the peak of the 1-revolution trail at $\lambda_\odot = 139\,^\circ\!.44$ (Rendtel, 2008).

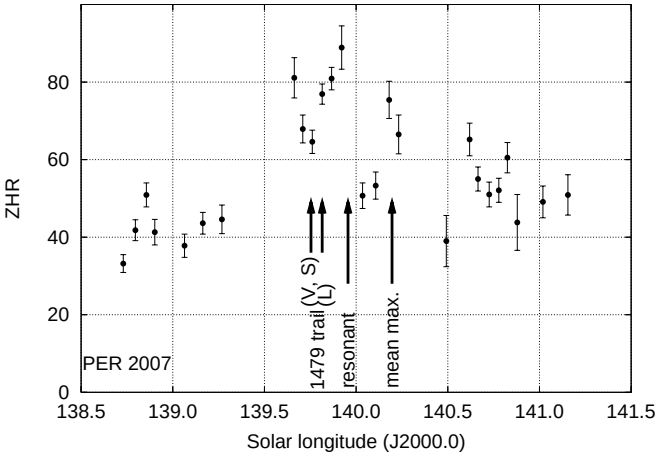


Figure 2.28: ZHR profile of the 2007 Perseids with the mean maximum and peaks which may be associated with the 1-revolution trail (predictions of L–Lyytinen, V–Vaubaillon, S–Sato), and with resonant meteoroids. (Rendtel, 2008).

for $1^{\rm h}$ UT on August 12. It occurred about 2.5 hours later at $\lambda_\odot = 139\,^\circ\!.535$ with a peak ZHR of about 300 (Rendtel, 1993). This analysis revealed a population index r of the order of $1.8 - 2.0$ around the outburst, and hence lower than in 1991, when $r \approx 2.1$.

Meteoroids were ejected from the comet over many revolutions and have been transferred into differing orbits by planetary perturbations and non-gravitational effects such as the Poynting-Robertson Effect.

Therefore, we find different components contributing the entire activity of a given shower:
(i) meteoroids from different ejection periods which have seen many perturbations over time and hence can cross the Earth's orbit at different positions;
(ii) meteoroids in dust trails formed not too many orbital periods ago and—although perturbed as well—still in a reasonably small band at least when approaching their perihelia close to the Earth's orbit;

Table 2.5: The relatively broad 'traditional' (or mean) Perseid maximum with a ZHR in the range between 75 and about 120 occurs at $\lambda_\odot = 140\,^\circ\!.1 \pm 0\,^\circ\!.1$ (J2000). Additional peaks related to dust trails or stream filaments have been observed in many years. Positions and peak ZHRs are summarized below.

Year	Mean maximum		Filament peak		References
	$\lambda_\odot$	$\mathrm{ZHR_{max}}$	$\lambda_\odot$	$\mathrm{ZHR_{max}}$	
1988	$140\,^\circ\!.08 \pm 0\,^\circ\!.04$	106±22	$139\,^\circ\!.78 \pm 0\,^\circ\!.03$	86± 4	Brown & Rendtel, 1996; Roggemans, 1989
1989	$139\,^\circ\!.80 \pm 0\,^\circ\!.09$	94± 6	$139\,^\circ\!.56 \pm 0\,^\circ\!.03$	102±10	Brown & Rendtel, 1996; Koschack & Roggemans, 1991
1990	$140\,^\circ\!.54 \pm 0\,^\circ\!.2$	81±61	$139\,^\circ\!.55 \pm 0\,^\circ\!.05$	75±10	Brown & Rendtel, 1996
1991	$139\,^\circ\!.94 \pm 0\,^\circ\!.04$	97± 2	$139\,^\circ\!.55 \pm 0\,^\circ\!.03$	284±63	Brown & Rendtel, 1996
1992	$140\,^\circ\!.13 \pm 0\,^\circ\!.2$	84±34	$139\,^\circ\!.48 \pm 0\,^\circ\!.02$	220±22	Brown & Rendtel, 1996
1993	$139\,^\circ\!.91 \pm 0\,^\circ\!.04$	98± 5	$139\,^\circ\!.53 \pm 0\,^\circ\!.01$	264±17	Brown & Rendtel, 1996
1994	$139\,^\circ\!.84 \pm 0\,^\circ\!.04$	86± 2	$139\,^\circ\!.59 \pm 0\,^\circ\!.01$	238±17	Brown & Rendtel, 1996
1995	$139\,^\circ\!.90 \pm 0\,^\circ\!.15$	65±20	$139\,^\circ\!.62 \pm 0\,^\circ\!.05$	171±30	Rendtel & Arlt, 1996
1996	$140\,^\circ\!.08 \pm 0\,^\circ\!.04$	85±10	$139\,^\circ\!.66 \pm 0\,^\circ\!.03$	121±17	Rendtel & Arlt, 1996
1997	$140\,^\circ\!.03 \pm 0\,^\circ\!.03$	94± 2	$139\,^\circ\!.71 \pm 0\,^\circ\!.01$	137± 5	Arlt, 1998
1998	$140\,^\circ\!.10 \pm 0\,^\circ\!.02$	74± 3	$139\,^\circ\!.75 \pm 0\,^\circ\!.03$	110±20	Arlt, 1999
1999	$139\,^\circ\!.9 \pm 0\,^\circ\!.02$	87± 6	$139\,^\circ\!.80 \pm 0\,^\circ\!.01$	104± 4	Rendtel & Arlt, 1999
2000	$139\,^\circ\!.97 \pm 0\,^\circ\!.02$	97± 3	none	—	Arlt & Händel, 2000; Rendtel, 2008
2001	$139\,^\circ\!.8 \pm 0\,^\circ\!.2$	71± 8	none	—	Rendtel, 2008
2002	$140\,^\circ\!.11 \pm 0\,^\circ\!.06$	74± 3	$139\,^\circ\!.82 \pm 0\,^\circ\!.04$	110± 8	Arlt & Buchmann, 2002; Rendtel, 2008
2003	$140\,^\circ\!.1 \pm 0\,^\circ\!.2$	64± 7	none	—	Rendtel, 2008
2004	$140\,^\circ\!.15 \pm 0\,^\circ\!.20$	115±10	$139\,^\circ\!.44 \pm 0\,^\circ\!.01$	160± 4	Rendtel, 2008
			$139\,^\circ\!.65 \pm 0\,^\circ\!.05$	130± 7	Rendtel, 2008
2005	$140\,^\circ\!.2 \pm 0\,^\circ\!.1$	76± 3	$139\,^\circ\!.75 \pm 0\,^\circ\!.05$	86± 5	Rendtel, 2008
2006	$140\,^\circ\!.29 \pm 0\,^\circ\!.10$	57± 7	none	—	Rendtel, 2008
2007	$140\,^\circ\!.25 \pm 0\,^\circ\!.05$	67± 8	$139\,^\circ\!.86 \pm 0\,^\circ\!.03$	78± 5	Rendtel, 2008
			$139\,^\circ\!.86 \pm 0\,^\circ\!.03$	88± 6	Rendtel, 2008
2008	$139\,^\circ\!.8 \pm 0\,^\circ\!.2$	80± 5	$140\,^\circ\!.55 \pm 0\,^\circ\!.05$	120± 5	IMO preliminary analysis (`www.imo.net`)
2009	$139\,^\circ\!.95 \pm 0\,^\circ\!.2$	150±11	none	—	IMO preliminary analysis (`www.imo.net`)
2010	$139\,^\circ\!.8 \pm 0\,^\circ\!.2$	88± 5	none	—	IMO preliminary analysis (`www.imo.net`)
2011	$140\,^\circ\!.0 \pm 0\,^\circ\!.4$	58± 4	none	—	IMO preliminary analysis (`www.imo.net`)
2012	$140\,^\circ\!.15 \pm 0\,^\circ\!.2$	122± 8	none	—	IMO preliminary analysis (`www.imo.net`)
2013	$139\,^\circ\!.8 \pm 0\,^\circ\!.2$	112±11	none	—	IMO preliminary analysis (`www.imo.net`)

(iii) older dust accumulated and kept in mean-motion resonances with Jupiter, called a filament (Jenniskens et al., 1998).

The mean maxima and additional peaks observed from 1988 onwards are listed in Table 2.5. Examples of recent returns with peaks caused by filaments and trails are shown in Figures 2.27 and 2.28 for the Perseid returns in 2004 and 2007, respectively (Rendtel, 2008).

Harris et al. (1995) integrated the motion of the parent comet backwards in time over a period of 270 000 years. They calculated the resulting distribution of the orbital nodes of the ejected meteoroids. According to the simulation, the Earth passes only the inner part of the stream whereas the densest part of the stream is not crossed by the Earth.

The population index has been found to vary during the Perseid's activity period. Pre-maximum values are around $r \approx 2.2$, but near the maximum r slightly decreases (2.0–2.1), and after maximum there is a steady increase until the sporadic level of $r \approx 3.0$ is reached at the end of the shower's activity period (Koschack & Roggemans, 1991; Koschack et al., 1993). These figures illustrate that mass-sorting has taken place within the stream, with smaller particles concentrated in the outer regions. As r is the most basic value for any analysis (Koschack & Rendtel, 1990) it is very important to obtain a complete and reliable r profile for the whole activity period, which in turn requires accurate magnitude distributions for each night. This requires magnitude and rate data for intervals shorter than one hour in the near-peak periods.

The Perseid data in the Working List are almost constant over the years. Recently, we adapted the radiant motion which was studied by Arlt (2003). The positions of August 10 and later are taken from that paper, while earlier position have been recomputed with a larger set of video meteors and longer, overlapping intervals in order to produce a smooth ephemeris of the radiant. The positions were also compared with the photographic results by Svoreň and Kaňuchová (2005) based on the most recent version of the IAU orbital database. We found fairly good agreement, especially on the fact the radiant does not lie below $\delta = +40°$ or even below $\delta = +30°$ in July and early July, respectively. Radiant positions in the central part of Andromeda have often been reported from visual data, but cannot be deduced from video and photographic data.

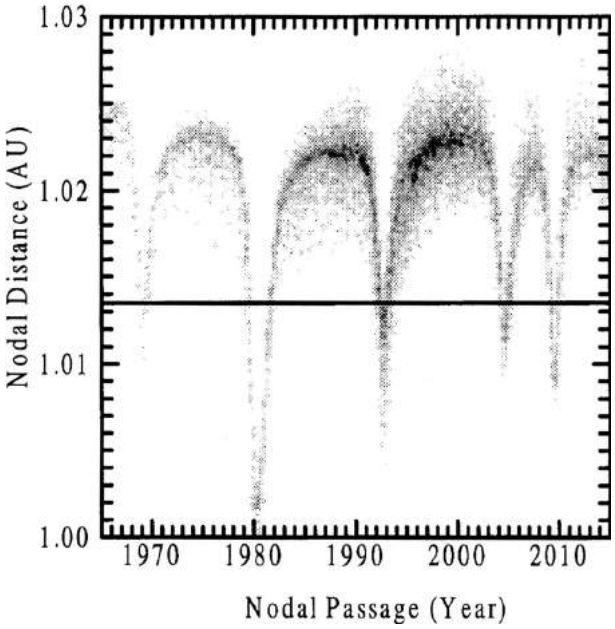


Figure 2.29: Distribution of orbital nodes of individual particles in the Perseid meteoroid stream.

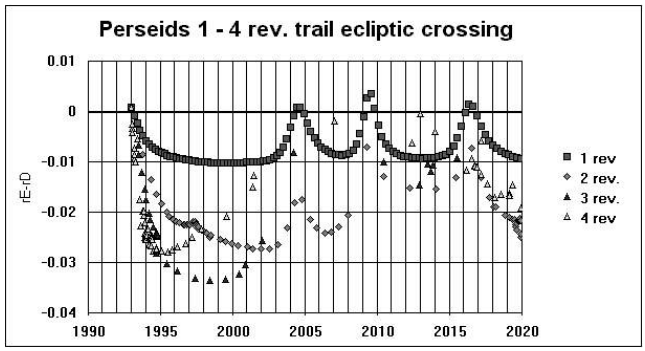


Figure 2.30: The ecliptic crossing of 1-to-4-revolution meteor trails. In the calculations, the original particle density is the same for 1-to-3-rev. trails. For the 4-revolution trail, the density is four times bigger. For the 1 revolution trail, the number of visible meteors is expected to start to decline more than about 10 years behind the comet. Prospects for a good shower from the 1-revolution trail were clearly best in 2004. The vertical line marks the start of the year. Visible Perseid meteors occur at about 0.61 of the way through each year.

2.15.2 Perseids in the next years

In the year 2028, the Earth will pass within about −0.0004 au of the 4-revolution trail from the year 1479, with a mean anomaly factor of about 0.15 (Figure 2.30). Lyytinen expects this to produce a real storm over the U.S., although under unfavourable moonlight conditions (`www.sci.fi/ fmbb/astro/perseids.htm`).
The same is found by Maslov
(`feraj.narod.ru/Radiants/Predictions/ 1901-2100eng/Perseids1901-2100predeng.html`).
who points out that in this year the Earth will encounter a part of the stream which was perturbed by Jupiter. He estimates the peak ZHR to be about 250–300. Slightly enhanced rates may also occur in the adjacent years.

Earlier, in 2015, there will be a close encounter with the 1-revolution trail. Model calculations by Esko Lyytinen and Jeremie Vaubaillon indicate enhanced rates. Vaubaillon's prediction shown in Figure 2.31 hints at the period 2015 August 12.8–13.3 UT. Since there will also meteoroids of the 2-revolution trail relatively close to the Earth's orbit in 2016, rates may exceed the average in that year between August 11.9 and 12.6 UT.

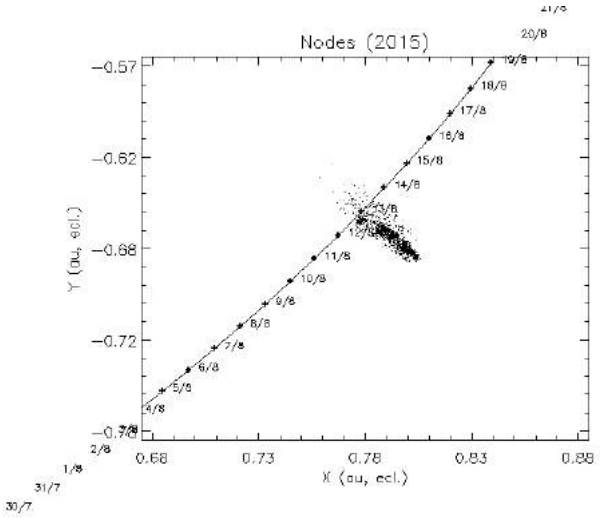


Figure 2.31: In 2015 the Earth is expected to encounter part of a denser dust trail of comet 109P/Swift-Tuttle. (see `http://www.imcce.fr/langues/en/ephemerides/phenomenes/meteor/predictions_request.php?shower=Perseids`

References

Arlt R., 1998: Global analysis of the 1997 Perseids. *WGN* **26,** 61–71.

Arlt R., 1999: Global analysis of the 1998 Perseid meteor shower. *WGN* **27,** 237–249.

Arlt R., 2003: Radiant ephemeris for the Perseid meteorshower. *WGN* **31,** 19–28.

Arlt R., Buchmann A., 2002: Global analysis of the 2002 Perseids. *WGN* **30,** 232–243.

Arlt R., Händel I., 2000: The 'new' peak failed: first analysis of the 2000 Perseids. *WGN* **28,** 166–171.

Brown P., 1993: Space Shuttle 'Discovery' is delayed by the 1993 Perseids. *WGN* **21,** 218.

Brown P., Rendtel J., 1996: The Perseid meteoroid stream: characterization of recent activity from visual observations. *Icarus* **124,** 414–428.

Harris N.W., Yau K.K.C., Hughes D.W., 1995: The true extent of the nodal distribution of the Perseid meteoroid stream. *MNRAS* **273,** 999–1015.

Jenniskens P., Betlem H., de Lignie M., Ter Kuile C., van Vliet M.C.A., van 't Leven J., Koop M., Morales E., Rice T., 1998: On the unusual activity of the Perseid meteor shower (1989-96) and the dust trail of comet 109P/Swift-Tuttle. *MNRAS* **301,** 941–954.

Jenniskens P., Sato I., Lyytinen E., Vaubaillon J., 2007: Perseid Meteors 2007. Central Bureau Electronic Telegrams, Nr. 1019.

Kashcheyev B.L., Lebedinets V.N., 1967: Radar studies of meteors. *Smiths. Contr. Astrophys.* **11,** 183–199.

Koschack R., Rendtel J., 1990: Determination of spatial number density and mass index from visual meteor observations. *WGN* **18,** 44–58, 118–140, 212 (errata).

Koschack R., Roggemans P., 1991: The 1989 Perseid meteor stream. *WGN* **19,** 87–98.

Koschack R., Arlt R., Rendtel J., 1993: Global analysis of the 1991 and 1992 Perseids. *WGN* **21,** 152–167.

Lindblad B.A., Porubčan V., 1994: The activity and orbit of the Perseid meteor stream. *Planet. Space. Sci.* **42,** 117–122.

Lyytinen E., Van Flandern T., 2004: Perseid one-revolution outburst in 2004. *WGN* **32,** 51–53.

Marsden B.G., 1992: The rediscovery of P/Swift-Tuttle. *WGN* **20,** 204–205.

Marsden B.G., 1973: The next return of the comet of the Perseid meteors. *AJ* **78,** 654–662.

Rendtel J., 1993: Perseids 1993: A first analysis of global data. *WGN* **21,** 235–239.

Rendtel J., 2008: Filament and dust trail encounters and the mean Perseid maximum 2000–2007. *WGN* **36,** 68–76.

Rendtel J., Arlt R., 1996: Perseids 1995 and 1996–an analysis of global data. *WGN* **24,** 141–147.

Rendtel J., Arlt R., 1999: First results of the 1999 Perseid meteor shower. *WGN* **27,** 250–255.

Roggemans P., Macek M., Parviäinen P., Rendtel J., McLeod N., Castilla G., 1983: Perseid results 1983. *WGN* **11,** 174–188.

Roggemans P., 1989: The Perseid meteor stream in 1988: a double maximum. *WGN* **17,** 127–137.

Schiaparelli G.V., 1871: Entwurf einer astronomischen Theorie der Sternschnuppen. Nahmer, Stettin, pp. 196–229 (In German, Draft of an astronomical theory of shooting-stars).

Simmons K., 1981: The 1980 Perseid shower. *Meteor News* **52,** 1–3.

Svoreň J., Kaňuchová Z., 2005: Perseids – the list of photographic orbits. *Contrib. Astron. Obs. Skalnaté Pleso* **35,** 199–220.

Wu Z., Williams I.P., 1993: The Perseid meteor shower at the current time. *MNRAS* **264,** 980–990.

Zhuang T.-S., 1977: Ancient Chinese records of meteor showers. *Chinese Astronomy* **1,** 197–220.

2.16 κ-Cygnids (012 KCG)

2.16.1 Synopsis

Period	August 03–25	
Maximum	$\lambda_\odot = 145°$	(≈ August 17)
Radiant	$\alpha = 286°$	$\delta = +59°$
$ZHR_{max} = 3$	$r = 3.0$	$V_\infty = 25$ km/s
Parent body	unknown	

Orbital elements of the stream

Ω	ω	i	e	q	a	P
KCG, Lindblad (1987), phot.						
147.°7	199.°8	38.°2	0.769	1.04 au	4.50 au	9.5 yr
KCG, Gavajdová (1994), fireballs						
142.°0	197.°7	33.°0	0.718	0.99 au	3.51 au	6.6 yr

The shower radiant (Figure 2.32) is high in the sky for mid-northern latitudes. Therefore essentially all shower meteors appear slow because they are either close to the radiant, or low in the sky (and thus far away from the observer). Despite the high position in the sky for most northern hemisphere observers, the number of shower meteors remains low; ZHRs reach just 2.5 about a week after the Perseid maximum (Figure 2.33).

Occasionally bright κ-Cygnid fireballs are recorded, but no periodicity has been proven. The bulk of κ-Cygnids are medium bright to faint meteors. Despite the long period of its visibility, the low hourly rates and the very limited data on the shower leave a lot of questions open about the nature and evolution of this meteoroid stream. Video meteor observations indicate that the activity can be traced even after the end date given here (Molau, 2007).

There have been rumours about a suspected periodicity of 6.6 years in appearances of unusually bright κ-Cygnid fireballs. Indeed, several fireballs have been observed from the κ-Cygnid radiant but no periodicity has been proven. The bulk of κ-Cygnids are medium bright to faint meteors, all with a noticeably low angular velocity, but it cannot truly be called a fireball shower. The long period of its visibility, the low hourly rates and the very limited data on the shower leave a lot of questions open about the nature and evolution of this meteoroid stream.

2.16.2 Research

Since the meteoroids are significantly dispersed in node, radiant and speed, the shower was considered to be old. In 1993, increased rates were observed, indicating that at least some dust is concentrated in trailets. Jenniskens & Vaubaillon (2008) report that Minor Planet 2008 ED_{69} fits the orbital dynamics to account for the κ-Cygnids. With one node near Jupiter's orbit, the perihelion distance q, the longitude of perihelion ω and the node Ω quickly change over time, but in a way that keeps dust concentrated over a long time.

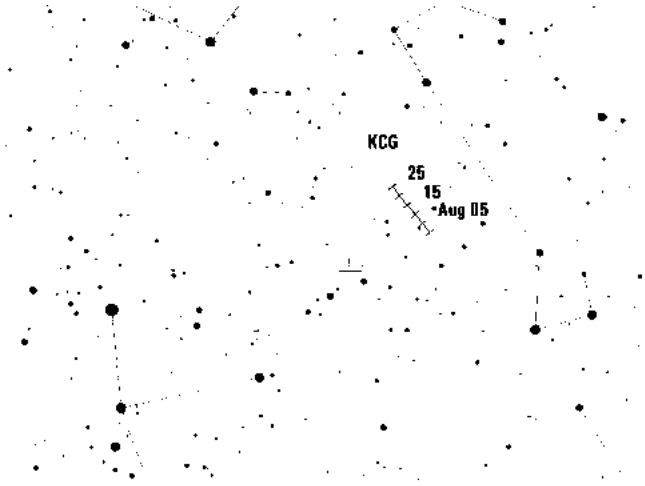


Figure 2.32: Radiant drift of the κ-Cygnids.

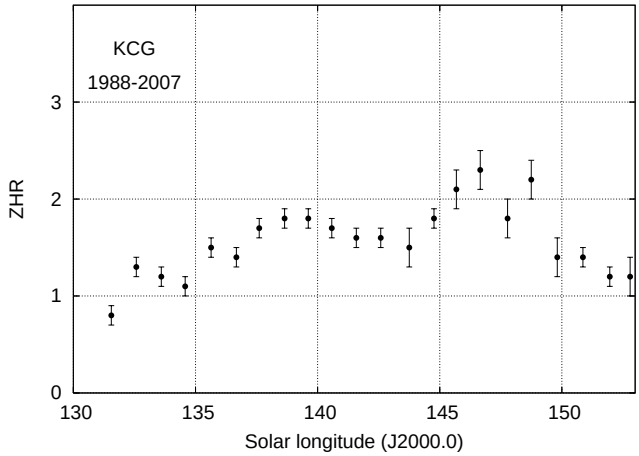


Figure 2.33: Activity of the κ-Cygnids from visual observations stored in the VMDB covering the period 1988–2007 using a constant $r = 3.0$ over the activity period. The zenith correction included the standard sine term (no zenith coefficient $\gamma > 1.0$) and allowed only intervals with a radiant elevation of $\geq 20°$.

References

Gavajdová M., 1994: On the population of very bright meteors in meteor streams. *Contr. Astr. Obs. Skalnaté Pleso* **24,** Slovak Acad. Sci., Tatranská Lomnica.

Jenniskens P., Vaubaillon J., 2008: Minor planet 2008 ED69 and the Kappa Cygnid meteor shower. *Astron. J.* **136,** 725–730.

Lindblad B.A., 1987: Physics and orbits of meteoroids. In: *The Evolution of the Small Bodies of the Solar System*, Soc. Italiana di Fisica, Bologna.

Molau S., 2007: How good is the IMO working list of meteor showers? A complete analysis of the IMO video meteor database. In: *F.Bettonvil and J.Kac (eds.): Proc. IMC 2006,* IMO, pp. 38–54

2.17 Aurigids (206 AUR)

2.17.1 Synopsis

Period	August 25 – September 08
Maximum	$\lambda_\odot = 158°$ ($\approx$ August 31)
Radiant	$\alpha = 84°$ $\delta = +42°$
$ZHR_{max} = 6$	$r = 2.5$ $V_\infty = 66$ km/s
Parent body	C/1911 N1

Orbital elements of the stream and Comet C/1911 N1 (Kiess)

Ω	ω	i	e	q	a
AUR, Kronk (1988), parabolic orbit assumed					
158.°7	126.°7	149.°0	(1.0)	0.807	∞
C/1911 N1					
158.°67	110.°37	148.°4	0.996	0.684 au	

The first valuable reports on the Aurigids (sometimes also called α-Aurigids) date back to a rather strong return in 1935. Teichgraeber and Hoffmeister (1936) in Sonneberg, as well as Vrátnik, Vlček and Štěpánek in Prague, observed enhanced meteor activity in the morning hours of 1935 September 1 from a radiant at $\alpha = 86°$, $\delta = 40.°5$ (1925.0), with a difference in position from the two sites of only 2° in declination. Neither Denning's catalog of radiants nor observations carried out in Germany during years previous to 1935 gave any hints of an earlier appearance of meteors from this radiant or region. Since no limiting magnitude was given, it is not possible to calculate a modern ZHR, but the hourly rates corrected only for the zenith distance of the radiant were as high as 26 in Germany and 29 for the Prague team.

A first calculation of the orbit by Guth (1936) showed a quite close coincidence between the parabolic elements of the meteoroid stream and Comet Kiess 1911 II. This comet has an orbital period of about 2500 years, so the existence of a more or less permanent shower from this source may seem surprising. The April Lyrids, however, are also connected to a rather long period comet and produce an annual meteor shower. The annual Aurigid activity reaches a ZHR of about 10 (Dubietis & Arlt 2002). Figure 2.35 gives the average ZHR profile calculated for the period 1988–2006.

2.17.2 Research

Short lived outbursts have been reported in 1935, 1986, 1994 (Jenniskens, 2006), and 2007. The 2007 outburst was predicted by Lyytinen and Jenniskens (2003) with an update by Jenniskens and Vaubaillon (2007). This activity caused by the long-period comet C/1911 N1 (Kiess) yielded a unique opportunity to study meteoroids from this comet ejected around 83 BC. The predicted peak time was 11:36 UT on 2007 September 1 (Jenniskens and Vaubaillon, 2007).

A detailed analysis of the visual data obtained during the well observed 2007 outburst (Rendtel, 2007) yields a population index of $r = 1.74 \pm 0.08$ from the meteors observed under a sky with a limiting magnitude of at

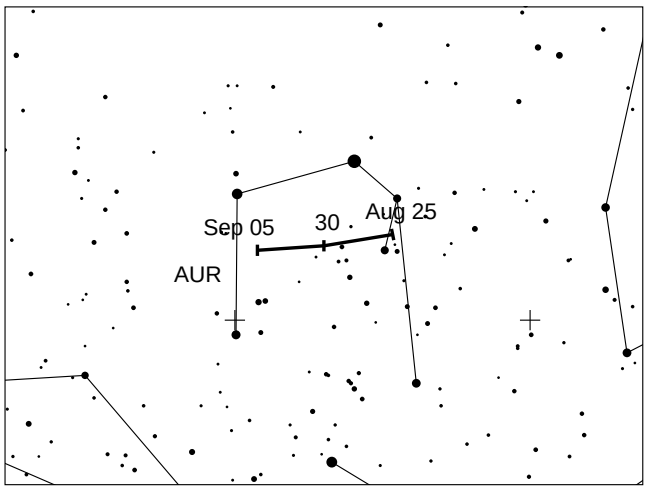


Figure 2.34: Radiant drift of the Aurigids (AUR).

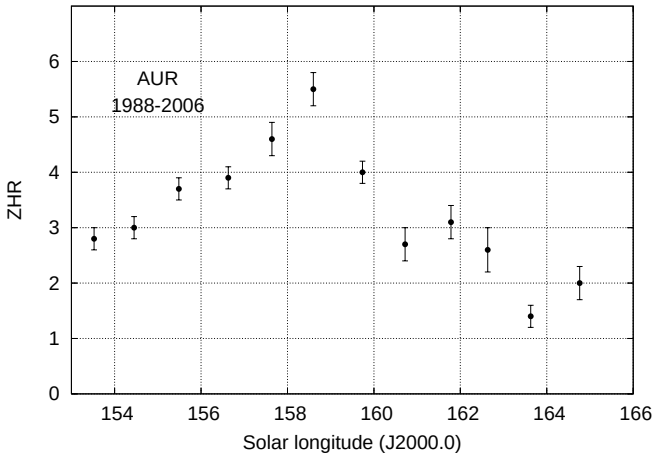


Figure 2.35: Activity of the Aurigids from visual observations stored in the VMDB covering the period 1988-2006 using a constant $r = 3.0$ over the activity period. The zenith correction included the standard sine term (no zenith coefficient $\gamma > 1.0$) and allowed only intervals with a radiant elevation of $\geq 20°$. The 2007 return with the outburst is described in detail.

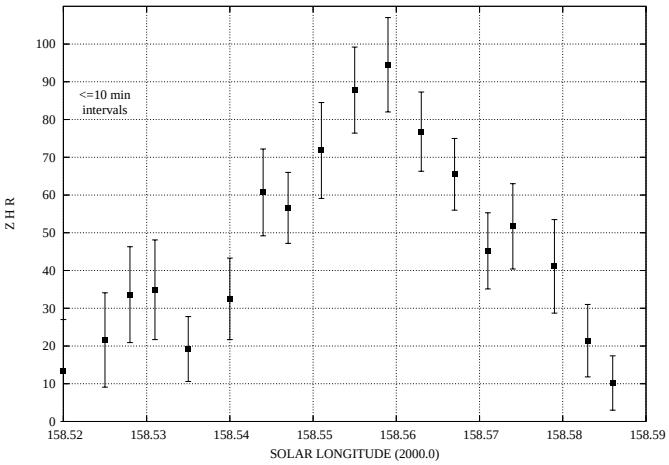


Figure 2.36: Activity profile of the Aurigid outburst observed on 2007 September 1 based on count intervals of maximal 10 min duration (Rendtel 2007).

least +4 mag. The effect of the bright skies due to the moonlight interference is relatively small, indicating that the meteoroid size distribution does not vary over the magnitude interval between −4 and about +3 mag within the error margins.

The calculated peak ZHR depends on the maximum length of the included bins (Rendtel, 2007). Probably the best estimate for the peak time is obtained when the maximum bin length was set to 10 minutes (Figure 2.36). The peak occurred at $\lambda_\odot = 158\overset{\circ}{.}556 \pm 0\overset{\circ}{.}003$, that is 2007 August 01, 11:20 UT. In the ZHR profile we have to consider possible (true) density fluctuations which superpose with statistical effects. The best estimate of the peak rate seems to be the value ZHR $= 132 \pm 26$ derived from 6 minute intervals. Indications of substructures are very weak because of the error limits.

References

Dubietis A., Arlt R., 2002: Annual activity of the alpha Aurigid meteor shower as observed in 1988–2000. *WGN* **30,** 22–31.

Guth V., 1936: Über den Meteorstrom des Kometen 1911 II (Kiess). *Astr. Nachr.* **258,** No. 6170, 27-30 (In German. On the meteor shower of comet Kiess).

Hoffmeister C., 1936: Unerwarteter Meteorstrom. *Astr. Nachr.* **258,** No. 6170, 25-26 (In German. Unexpected meteor shower).

Jenniskens P., 2006: Meteor showers and their parent comets, Cambridge University Press, Cambridge.

Jenniskens P., Vaubaillon J., 2007: Aurigid predictions for 2007 September 1. *WGN* **35,** 30–35.

Kronk G., 1988: Meteor Showers. A Descriptive Catalog. Enslow, Hillside, New Jersey.

Lyytinen E., Jenniskens P., 2003: Meteor outbursts from long-period comet dust trails. *Icarus* **162,** 443–452.

Rendtel J., 2007: Visual observations of the Aurigid peak on 2007 September 1. *WGN* **35,** 108–112.

2.18 September ε–Perseids (208 SPE)

2.18.1 Synopsis

Period	September 5–21
Maximum	$\lambda_\odot = 166\overset{\circ}{.}7$ ($\approx$ September 9)
Radiant	$\alpha = 48°$ $\delta = +40°$
$ZHR_{max} = 5$	$r = 2.50$ $V_\infty = 64$ km/s
Parent body	unknown

Orbital elements of the stream

Ω	ω	i	e	q	a	
Gajvadova, 1994; photographic						
$166\overset{\circ}{.}2$	$242\overset{\circ}{.}6$	$140\overset{\circ}{.}5$	1.031	0.733 au		
Rendtel, 1993; photographic						
168°	$241\overset{\circ}{.}3$	$142\overset{\circ}{.}8$	0.95	0.75 au		15
Welch, 2001; photographic						
$165\overset{\circ}{.}9$	$242\overset{\circ}{.}8$	$138\overset{\circ}{.}9$	1.00	0.74 au		
Gajdoš et al., 2014 (2013 outburst, video)						
$167\overset{\circ}{.}206$	$246\overset{\circ}{.}1$	$139\overset{\circ}{.}1$	0.959	0.714 au		

The radiant listed in the previous editions could not be located by analyses of video data at all (Molau & Rendtel, 2009). Instead, the formerly-little-known September ε–Perseid shower was clearly detected. This radiant was responsible for producing an unexpected outburst of swift, bright meteors on 2008 September 9 (Rendtel & Molau, 2010). The maximum timing listed above was detected from the recent video meteor data analysis and was virtually coincident with the 2008 bright-meteor outburst. Further details are given in section 2.18.2. The value of $r = 2.50$ given in the synopsis Table refers to the average returns.

Another peculiar outburst was observed on 2013 September 9 centered at $167\overset{\circ}{.}200$ (22^h18^m UT). The most surprising fact of the observations was an extremely low value of the population index $r = 1.45\pm0.15$ (Rendtel et al., 2014). Hence the apparent high rate of mainly bright shower meteors was caused by a meteoroid stream with a comparatively low flux density (comparable to that of the α-Capricornids).

Relations to the δ-Aurigids as described in the previous editions of the Handbook based on photographic data published by Drummond (1982) and visual data (Rendtel, 1989, 1992), extrapolating the radiant drift back from early October to the more prominent activity observed in early September. Later investigation of visual and orbital data (Dubietis & Arlt, 2002) suggested that the September ε–Perseids and the δ-Aurigids (see next section) are two separate showers. The strongest argument in favour of two streams is a difference in their (mean) orbits. The activity of the merged showers observed visually yields a period of very low rates clsoe to $\lambda_\odot = 175°$. Hence the activity period of the September Perseids is listed until September 17.

The first record goes back to Denning (1882) who compiled a number of sources from the 1870s obviously describing this shower which he named the September Perseids. The most reliable reports on this source

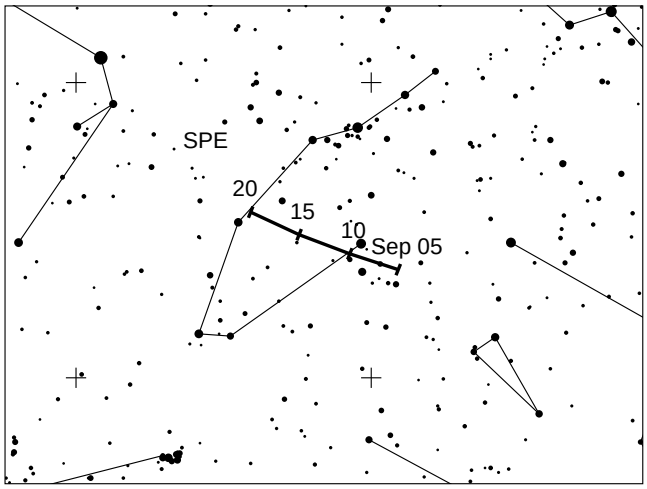


Figure 2.37: Radiant drift of the September ε–Perseids from recent video observations.

come from Hoffmeister's (1948) radiant investigation. He noted the September Perseids on 1936 September 8, but no further observations from this period of the year were obtained during the other years of his study. Nevertheless, the radiant is listed as a permanent shower in his catalog.

This shower is essentially visible from the northern hemisphere. The radiant (Figure 2.37) reaches useful elevations after about 23^h local time. The activity remains low, with some enhancement near $\lambda_\odot = 166\overset{\circ}{.}7$ (September 9) coinciding with the time of the 2008 outburst mentioned above but deviating from the 2013 peak position.

2.18.2 Research

Distinct activity outbursts have been observed in 2008 and 2013. The 2008 event was centered at September 09, 0820 UT (±20min), corresponding to $\lambda_\odot = 166\overset{\circ}{.}907$ and lasted for four hours (Rendtel & Molau, 2010 and refereces therein). The peak ZHR is difficult to estimate since there were no systematic observations carried out close to the peak time. Most likely, the ZHR was in the range of 10. While the ZHR is not unusual, the magnitude of the shower meteors was. A large fraction of the meteors was bright (−8 mag to +4 mag), giving a very low value of the population index r.

The 2013 activity increase was similar to the 2008 return in terms of the unusual magnitude distribution (yielding a very low $r \approx 1.45 \pm 0.15$; Figure 2.38) but had a much shorter duration. Video data show a peak on September 09, 22^h18^m UT (corresponding to $\lambda_\odot = 167\overset{\circ}{.}200$) with a FWHM of about 50 minutes only (Figures 2.39 and 2.40 from Rendtel et al., 2014). Considering the low r, the ZHR and flux was not exceptional. The passage through the respective stream section was mainly manifested in a very different particle population. Seen the rather short duration of the 2013 return, the assumption of resonant meteoroids similar to the 1998 June-Bootids (page 26) or the 2006–2009 Orionids (page 47) is not likely. This is also supported by a model of Lyytinen (presented in Rendtel et al.,

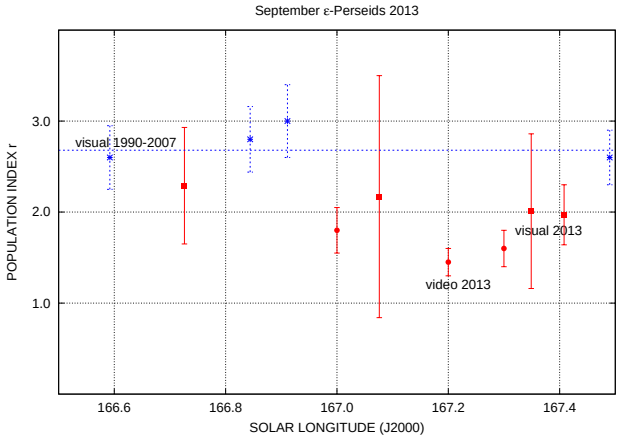


Figure 2.38: Population index profile found for the 2013 SPE return, combining visual (squares) and video data (dots). Asterisks and the dashed line show the average from visual data 1990–2007.

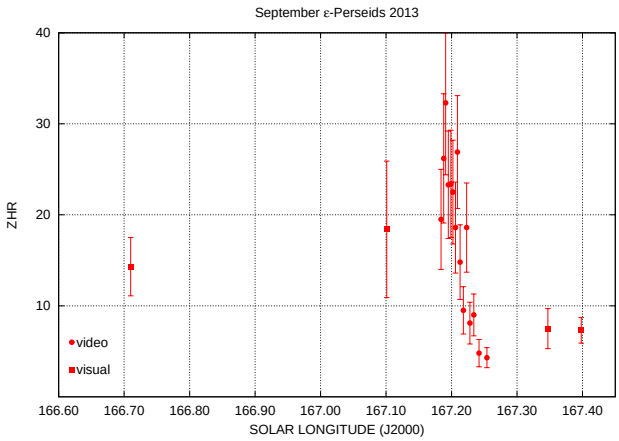


Figure 2.39: Combined ZHR profile based on visual data (squares) and video data (dots), applying r from the 2013 data (peak) and the average (outside the peak)

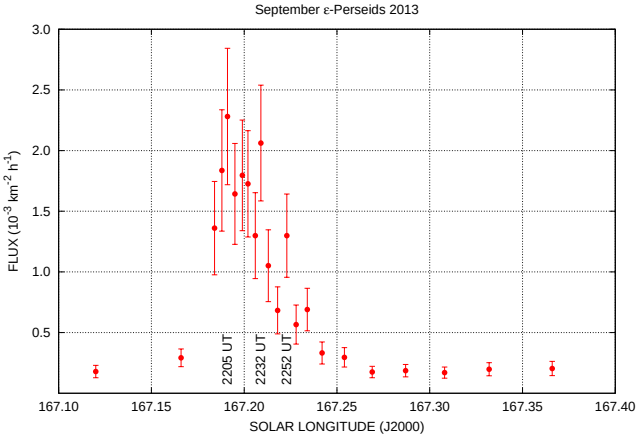


Figure 2.40: Flux determined from the video data of the IMO Video Meteor Network. Details are given in Rendtel et al. (2014).

2014) which shows the 2013 peak time based on the 2008 outburst time and the radiant position and the assumption that the Earth encountered a medium-long period comet orbit, with no indications for peaks in the near future.

The 2013 data (Gajdoš et al., 2014) yield a radiant at $\alpha = 47.^\circ6$, $\delta = +39.^\circ4$ and an average velocity of 64.27 km/s.

The "irregular" peaks of the September ε-Perseids as well as the fact that the Drummond (1982) analysis based on photographic records from the 1960ies may be signs that there is a larger group of medium-to-weak showers at similar orbits which cause recordable rates only at a few occasions. This might also explain the difficulties to establish a consistent image of high-iclination showers in September and October (Rendtel & Molau, 2010).

References and bibliography

Denning W.F., 1882: The September Perseids. *The Observatory* **5,** 262–265.

Drummond J., 1982: A note on the Delta Aurigid meteor stream. *Icarus* **51,** 655–659.

Dubietis A., Arlt R., 2002: The current delta-Aurigid meteor shower. *WGN* **30,** 168–174.

Gajdoš Š, Tóth J., Kornoš L., Koukal J., Piffl R., 2014: The September epsilon Perseids in 2013. *WGN* **42,** 48–56.

Gajvadova M., 1994: On the population index of very bright meteors in meteor streams. *Contr. Astron. Obs. Skalnaté Pleso* **24,** 101–110.

Hoffmeister C., 1948: Die Meteorströme. J.A. Barth, Leipzig, 79–93.

Molau S., Rendtel J., 2009: A comprehensive list of meteor showers obtained from 10 years of observations with the IMO Video Meteor Network. *WGN* **37,** 98–121.

Rendtel J., 1989: Radiants in the Per-Aur Region between August and October. In: *D. Heinlein, D. Koschny (eds.), Proceedings of the IMC Violau 1990*, Veitsbronn, 37–41.

Rendtel J., 1993: Radiants and orbits of δ-Aurigids and September Perseids. In: *D. Očenáš, P. Zimnikoval (eds.), Proceedings of the IMC Smolenice 1992*, Banská Bystrica, 67–73.

Rendtel J., Lyytinen E., Molau S., Barentsen G., 2014: Peculiar activity of the September ε-Perseids on 2013 September 9. *WGN* **42,** 40–47.

Rendtel J., Molau S., 2010: Meteor activity from the Perseus-Auriga region in September and October. *WGN* **38,** 161–166.

Welch P.G., 2001: A new search for streams in meteor data bases and its application. *MNRAS* **328,** 101–111.

2.19 Draconids (009 DRA)

2.19.1 Synopsis

Period	October 6–10
Maximum	$\lambda_\odot = 195\,\overset{\circ}{.}4$ ($\approx$ October 8)
Radiant	$\alpha = 262^\circ$ $\delta = +57^\circ$
ZHR_{max} = var	$r = 3.0$ $V_\infty = 20$ km/s
Parent body	21P/Giacobini-Zinner

Orbital elements of the stream and comet 21P/Giacobini-Zinner

Ω	ω	i	e	q	a	P
Jacchia et al. (1950); photographic						
$196\,\overset{\circ}{.}3$	$171\,\overset{\circ}{.}8$	$30\,\overset{\circ}{.}7$	0.717	0.996 au	3.51 au	6.6 yr
Lindblad (1987); photographic						
$195\,\overset{\circ}{.}5$	$176\,\overset{\circ}{.}9$	$24\,\overset{\circ}{.}6$	0.700	0.999 au	3.33 au	6.08 yr
21P/Giacobini-Zinner						
$195\,\overset{\circ}{.}38$	$172\,\overset{\circ}{.}54$	$31\,\overset{\circ}{.}82$	0.706	1.037 au	3.52 au	6.60 yr

The radiant of the October Draconids (Figure 2.41) is circumpolar for northern latitudes. It is one of the few radiants which is well placed for evening observations. Later in the night, the radiant is very low in the sky or even below the horizon, re-appearing only in the hours before dawn.

The shower's parent comet was discovered by Giacobini from Nice (France) on 1900 December 20. It was rediscovered by Zinner in Bamberg (Germany) on 1913 October 23. Davidson (1915) predicted the possibility of shower activity in 1915. High hopes were raised in 1933 when the Earth would pass the stream's descending node 80 days after the Comet. Reports from Belgium show that the event was spectacular: on October 9 at 19^h UT, several meteors appeared simultaneously, and the hourly rate became remarkable. Maximum activity occurred at 20^h08^m UT, when the (observed) rate was 78 meteors *per minute*. By 21^h UT, the rate had fallen to about 10% of this value. Rates estimated from many European sites varied from one observer to the next between 50 and 450 meteors per minute, since the waxing moon caused rather poor circumstances. The total duration of the event was limited to 4.5 hours.

On 1946 October 9, Canadian meteor workers photographed 204 Draconids in four hours (Jacchia et al., 1950). One exposure contains 29 trails caught in 13 minutes. The cosmic spread of the radiant was just $6'.2$. The geocentric velocity of the meteoroids was found to be as low as 20.43 km/s. The meteors were visible at great heights (between 90 and 98 km on average). The observed decelerations and masses indicated that the Draconid meteoroids were composed of fluffy material which was easily disintegrated in the Earth's atmosphere.

About 17 hours before Full Moon, and with twilight reducing the limiting magnitude during the visual observations, observers at the Skalnaté Pleso observatory found a maximum ZHR of 6800 for 5-minute intervals at 03^h53^m UT (Kresák & Slančiková, 1975).

For this 1946 Draconid return, new radar techniques were tested at Jodrell Bank, England. The radar maximum occurred at 3^h40^m UT with 168 echoes per minute. At 6^h UT, activity had ceased.

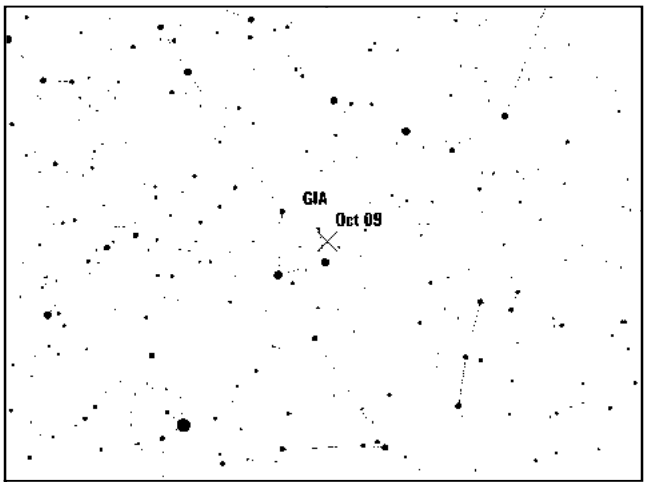


Figure 2.41: Radiant of the Draconids.

The parent comet, 21P/Giacobini-Zinner, has its perihelion near its descending node, and both are close to the orbit of the Earth. Its aphelion lies close to the orbit of Jupiter. In 1958, the Comet was perturbed by Jupiter (closest passage of 0.93 au; Belyayev et al., 1986). From then on, the descending node intersected the ecliptic plane far inside the orbit of the Earth. The comet made another close passage of Jupiter (0.58 au) in 1969. Its orbit was perturbed again, restoring the favorable position of the descending node close to the Earth's orbit. This strengthened the idea of a possible meteor storm in 1972, but rates remained very low.

On 1985 October 8, the highest rates (ZHR of the order of 200–300) were reported for the period 09^h30^m to 10^h00^m UT (Koseki, 1990). Ottawa radar data yield a maximum at 09^h25^m UT ± 5 min (Šimek, 1994). DeMeyere of Belgium got the highest radio (forward scatter) hourly rate around 10^h UT (Steyaert, 1985). Mason of Britain reported a saturated receiver system between 09^h15^m and 09^h55^m UT (Mason, 1985). There have been no reports on rate variations as described for the 1933 and 1946 returns (Jenniskens, 1995; p.223).

Another outburst occurred in 1998 which was correctly predicted by Reznikov (1993). The peak ZHR reached 720 ± 90 (Arlt, 1998). The time derived from forward scatter observations (Bus, 1999) was 1998 October 8, 13^h10^m UT or $\lambda_\odot = 195\,\overset{\circ}{.}075$ with no deviation between the peaks for short reflections and long-duration reflections (> 1 s). Video observations (Fujiwara et al., 2001) yielded a peak at $\lambda_\odot = 195\,\overset{\circ}{.}07$. Details of the profile are discussed by Jenniskens (2006; pp. 333–334).

The most recent return was calculated to occur on 2011 October 8 when several dust trails contribute to a considerable rate between 17^h and 21^h UT (Jenniskens, 2006, p. 678; Vaubaillon et al., 2011). Although all optical observations suffered from moonlight interference from a waxing moon (91% illuminated), the activity with a peak ZHR of 400 at 19^h UT and was well documented (Borovička et al., 2012 and references therein).

Another, not predicted outburst composed of a large fraction of small meteoroids occurred on 2012 October 8, $16^{\rm h}30^{\rm m}$ UT. Due to the different meteoroid size distribution, it was most prominent in radar data. It was reported while the outburst was ongoing (see below in the Research section)..

2.19.2 Research

Suzuki et al. (1999) find a strange elongated distribution of individual radiants, but mass-dependent effects are not visible in the distribution. Beginning and end heights both vary with magnitude, becoming lower/higher for faint meteors: $H_b({\rm km}) = 107.3 - 0.00m_v$ and $H_e({\rm km}) = 84.4 - 1.54m_v$.

Sato (2003) finds the 1926 trail being responsible for the 1998 outburst. The best fitting ejection velocity is +10.8 m/s. The 1966 and 1959 trails caused the 1999 enhanced activity (fitting ejection velocities 60–70 m/s).

General aspects of model calculations are described by Asher & Steel (2012). The 2011 outburst was predicted (Vaubaillon et al., 2011; Maslov, 2011) and occurred exactly at the expected position. Observations revealed also the substructure caused by particles ejected at an earlier occasion (Koten et al., 2014). The main peak was observed on October 8, 20:15 UT ($\lambda_\odot = 195\,\overset{\circ}{.}039$. The maximum ZHR obtained from the live analysis of global visual data with a constant $r = 2.8$ reached 304 ± 10 (`http://www.imo.net/live/draconids2011/`); the profile is almost symmetric and has a FWHM of 60 minutes. Ground based video meteor data of the IMO Video Meteor Network (Molau et al., 2012) essentially yield an identical profile with a peak at 20:10 UT ($\lambda_\odot = 195\,\overset{\circ}{.}036$) and a FWHM of 80 minutes. The peak rate is twice as high as the visual rate, but both are preliminary data based on a fix r-value. The analysis of airborne video data (Koten et al., 2014) yields a mass index of $s = 2.0 \pm 0.1$ (corresponding to $r = 2.5 \pm 0.2$). This would reduce the above mentioned ZHR since the visual observations were affected by bright moonlight. Koten et al. also report that the brightest meteors occurred in the interval 19:30–20:00 UT. Substructures in the rate profile were also reported by Sato (2014).

The activity increase in 2012 happened unexpected and was detected by the Canadian Meteor Orbit Radar (Ye et al., 2013). (Maslov (2011) concluded from his calculations that the chances for a weak display of faint meteors between 15 and 17 UT are low.) Radar observations revealed that the peak flux occurred at approximately 16:40 UT on October 8 with a maximum of $2.4 \pm 0.3{\rm h}^{-1}{\rm km}^{-2}$ (appropriate to meteoroid mass larger than 10^{-7} kg). This is equivalent to a $\mathrm{ZHR}_{\rm max} \approx 9000 \pm 1000$ using 5-minute intervals and a mass distribution index of $s = 1.88 \pm 0.01$ (equivalent to a population index of $r = 2.25 \pm 0.02$). At the same time, the visual ZHR was of the order of 324 ± 66 near 16:50UT ($\lambda_\odot = 195\,\overset{\circ}{.}631$, see `http://www.imo.net/live/draconids2012/`. The descending branch of the outburst was also recorded by cameras of the IMO Video Meteor Network (Molau et al., 2013), confirming a rather low activity in the optical range. Considering the radar data, this outburst is among the strongest Draconid returns since 1946 and the highest flux shower since the 1966 Leonid meteor storm, assuming that a constant power-law distribution holds from radar to visual meteoroid sizes. The weighted mean geocentric radiant in the time interval of 15–19 h UT, 2012 October 8, was $\alpha_g = 262\,\overset{\circ}{.}4 \pm 0\,\overset{\circ}{.}1, \delta_g = 55\,\overset{\circ}{.}7 \pm 0\,\overset{\circ}{.}1$ (J2000.0). The fact that the ZHR derived from visual observation data is much lower is a sign that the magnitude-cumulative number relationship is not a simple power law. Dynamical simulations indicate that the outburst was caused by dust particles released during the 1966 perihelion passage of 21P/Giacobini-Zinner, although there are discrepancies between the modelled and observed timing of the encounter, presumably caused by approaches of the comet to Jupiter during 1966–1972. Based on the results of their dynamical simulation, Ye et al. (2013) predict further possible increased activity of the Draconid meteor shower in 2018, 2019, 2021 and 2025. Maslov (2011) analysed the Draconid evolution and gives a list of future events. Both the predicted peaks of Ye et al. and Maslov are summarized in Table 2.6.

Table 2.6: Possible Draconid outburst predictions of Maslov (2011; M) and Ye et al. (2013; Y).

Year	Peak (UT)	ZHR	Remarks
2014	Oct 6, 20:10	10–15	several trails Oct 7–14, faint meteors (M)
2018	Oct 8, 23–24	10–20	peak activity from 1953 trail (M)
2018	Oct 9, ≈ 00		1953 trail (Y)
2019	Oct 8, 14:45	5–10	close encounter with 1959 trail (M)
2019	Oct 8, ≈ 01		1979 trail (Y)
2021	Oct 193.8		1979 trail (Y)
2023	Oct 8, 12:10	10–20	1887 trail, bright meteors (M)
2025	Oct 8, 05–11	50–60	several trails, submaxima; bright meteors (M)
2025	Oct 8, 15:14	10–40	2012 trail, faint meteors, strong in radar (M)
2025	Oct 194.0		1933 trail (Y)
2030	Oct 8, 21–22	10–20	1817–1859 trails, submaxima, bright meteors (M)

References

Arlt R., 1998: Summary of 1998 Draconid outburst observations. *WGN* **26,** 256–259.

Asher D.J., Steel, D.I., 2012: Draconid meteor storms. In: Proc. IMC 2011, 40–43

Belyayev N.A., Kresák L., Pittich E.M., Pushkarev A.N., 1986: Catalogue of short period comets. Astron. Inst. of the Slovak Acad. of Sciences. Bratislava.

Borovička J., Koten P., Shrbený L., Štork R., Hornoch K., 2012: Radiants, orbits, spectra and deceleration of slected 2011 Draconids. In: M. Gyssens & P.

Roggemans (eds.) Proc. of the IMC 2012, IMO, 2013, pp. 65–69.

Bus E.P., 1999: Results of radio meteor scatter observations for the outburst of the 1998 Draconid meteor shower. *WGN* **27,** 219–220.

Davidson M., 1915: Meteor radiants from debris of comets. *JBAA* **25,** 292–293.

Jacchia L.G., Kopal Z., Millman P.M., 1950: A photographic study of the Draconid meteor shower of 1946. *ApJ* **111,** 104–133.

Jenniskens P., 1995: Meteor stream activity. II. Meteor outbursts. *A&A* **295,** 206–235.

Jenniskens P., 2006: Meteor showers and their parent comets, Cambridge University Press, Cambridge.

Koseki M., 1990: Observations of the 1985 Giacobinids in Japan. *Icarus* **88,** 122–128.

Koten P., Vaubaillon J., Tóth J., Margonis A., Ďuriš F., 2014: Three peaks of 2011 Draconid activity including that connected with pre-1900 material. *Earth, Moon, Planets* **,** DOI 10.1007/s11038-014-9435-9.

Kresák L., Slančiková J., 1975: On the structure of the Giacobinid meteor shower. *BAC* **26,** 327-342.

Lindblad B.A., 1987: Physics and orbits of meteoroids. In *The evolution of the small bodies of the Solar System.* Soc. Italiana di Fisica, Bologna.

Maslov M., 2011: Future Draconid outbursts (2011 – 2100). *WGN* **39,** 64–67.

Mason J., 1985: Draconid meteors 1985. *WGN* **13,** 194–195.

Molau S., Kac J., Berko E., Crivello S., Stomeo E., Igaz A., Barentsen G., Goncalves R., 2012: Results of the IMO Video Meteor Network – October 2011. *WGN* **40,** 41–47.

Molau S., Kac J., Berko E., Crivello S., Stomeo E., Igaz A., Barentsen G., Goncalves R., 2013: Results of the IMO Video Meteor Network – October 2012. *WGN* **41,** 23–30.

Reznikov E.A., 1993: The Giacobini-Zinner comet and Giacobinid meteor stream (in Russian). *Trudy Kazan. Gor. Astron. Obs.* **53,** 80–101.

Sato M., 2003: An investigation into the 1998 and 1999 Giacobinids by meteoroid trajectory modeling. *WGN* **31,** 59–63.

Sato M., Watanabe J., Ohkawa T., 2014: Observation of October Draconids 2011 in Maidanak Observatory and Study of its Peak time, in: T.J. Jopek, F.J.M. Rietmeijer, J. Watanabe, I.P. Williams (eds.), Proc. Meteoroids 2013, Poznan, Poland, submitted.

Šimek M., 1994: The 1985 Giacobinids. Canadian radar observations. *Planet. Space Sci.* **42,** 141–143.

Steyaert C., 1985: Radio observations of the Draconids. *WGN* **13,** 193.

Suzuki S., Akebo T., Yoshida T., Suzuki K., 1999: TV observations of the 1998 Giacobinid outburst. *WGN* **27,** 217–218.

Vaubaillon J., Watanabe J., Sato M., Hori S., Koten P., 2011: The coming 2011 Draconids meteor shower. *WGN* **39,** 59–63.

Ye Q., Wiegert P.A., Brown P.G., Campbell-Brown M.D., Weryk R.J., 2013: The unexpected 2012 Draconid meteor storm. *MNRAS* **437,** 3812–3823.

2.20 δ-Aurigids (224 DAU)

2.20.1 Synopsis

Period	October 10–18
Maximum	$\lambda_\odot = 198°$ (≈ October 11)
Radiant	$\alpha = 84°$ $\delta = +44°$
$ZHR_{max} = 3$	$r = 3.0$ $V_\infty = 64$ km/s
Parent body	unknown

Orbital elements of the stream

Ω	ω	i	e	q	P
Kronk, 1988 (10 phot. + 24 radar meteor orbits)					
190.°9	227.°1	125.°9	0.859	0.720 au	3.068 yr
Drummond, 1982 (phot.)					
195.°5	228.°8	130.°7	0.965	0.826 au	

This is a working status shower in the IAU database, called 224 October δ-Aurigids (DAU). Previously, this shower was combined with the September Perseids. Its designation was mainly based on photographic data published by Drummond (1982). Visual data for the weeks preceding the observational period given by Drummond fitted the radiant drift and other parameters (e.g., the geocentric velocity) quite well. Therefore both showers were listed as one source being active continuously for about four weeks (Rendtel, 1989, 1992). Recent analyses of visual and orbital data (Dubietis & Arlt, 2002) as well as video data (Rendtel & Molau, 2010) indicate that the September ε–Perseids (see previous section) and the δ-Aurigids are two separate showers. A parent object is not yet known.

The radiant (Figure 2.20.1) is circumpolar for mid-northern locations and reaches high elevations above the horizon after about 22^h local time. Rates are close to the detection limit.

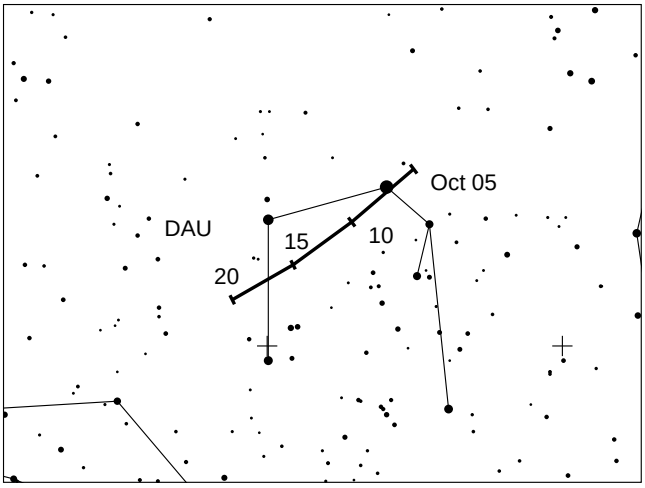


Figure 3.35: Radiant drift of the δ-Aurigids (AUR).

2.20.2 Research

recent analyses of video data especially from the period September and October revealed a number of various radiants (Rendtel & Molau, 2010). Seen the occurrence of AUR and SPE outbursts (see pages 38 and 40), it may well be possible that other showers with radiants in that region also show variable activity. The result would be a variable pattern from one year to another, caused by different minor showers. The fact that there are several photographic DAU meteors (i.e. bright meteors) observed in the 1960ies on which Drummond's (1982) analysis is based may be interpreted such that this (sub?-)shower DAU was more active in the past than it is currently. For further discussion of the showers in the Auriga region see the last paragraph in the description of the SPE at page 40.

References

Drummond J., 1982: A note on the Delta Aurigid meteor stream. *Icarus* **51,** 655–659.

Dubietis A., Arlt R., 2002: The current delta-Aurigid meteor shower. *WGN* **30,** 168–174.

Kronk G., 1988: Meteor Showers. A Descriptive Catalog. Enslow, Hillside, New Jersey.

Rendtel J., 1989: Radiants in the Per-Aur Region between August and October. In: *D. Heinlein, D. Koschny (eds.), Proceedings of the IMC Violau 1990*, Veitsbronn, 37–41.

Rendtel J., 1993: Radiants and orbits of δ-Aurigids and September Perseids. In: *D. Očenáš, P. Zimnikoval (eds.), Proceedings of the IMC Smolenice 1992*, Banská Bystrica, 67–73.

Rendtel J., Molau S., 2010: Meteor activity from the Perseus-Auriga region in September and October. *WGN* **38,** 161–166.

2.21 ε-Geminids (023 EGE)

2.21.1 Synopsis

Period	October 14 – 27
Maximum	$\lambda_\odot = 205°$ ($\approx$ October 18)
Radiant	$\alpha = 102°$ $\delta = +27°$
$ZHR_{max} = 3$	$r = 3.0$ $V_\infty = 70$ km/s
Parent body	possibly C/1964 N1 (Ikeya) or C/1987 B1 (Nishikawa-Takamizawa-Tago)

Orbital elements of the stream and the suspected parent comets

Ω	ω	i	e	q	a	P
Lindblad (1987); photographic						
206.°1	243.°9	173.°3	0.968	0.782 au	26 au	130 yr
Kashcheev & Lebedinets (1967); radar						
203°	223°	175°	0.75	0.88 au	3.6 au	7 yr
C/1964 N1						
269.°9	290.°8	171.°9	0.985	0.822 au	55 au	400 yr
C/1987 B1						
176.°1	200.°4	172.°2	0.996	0.870 au	200 au	(3000 yr)

The maximum is not distinct and occurs around October 18 (Figure 2.38). Meteors of this source will be noticed during many of the Orionid observations. In order to allow reliable shower association, the centre of the field of view should be chosen such that backward prolongations of the meteors do not line up with both radiants (Figure 2.21.1). Visual observers should plot all meteors possibly associated with the radiant and apply the procedures described in Chapter 3.

The ε-Geminids are in an orbit similar to the Orionids, the orbit of the ε-Geminids being 9° closer to the ecliptic. The ε-Geminids' ascending node and the argument of perihelion are reversed by about 180° (Southworth & Hawkins, 1963). Znojil (1968) showed that the ε-Geminids undergo larger planetary perturbations than the Orionids, and should therefore be younger. The association with a parent is not yet confirmed.

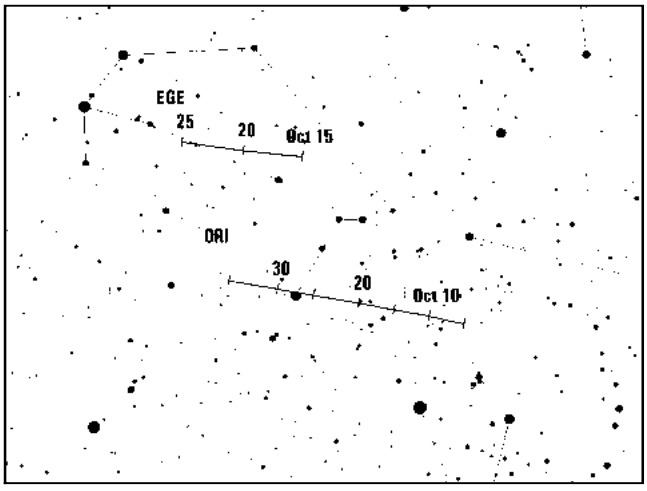


Figure 3.37: Radiant drift of the ε-Geminids shown together with the radiant of the Orionids.

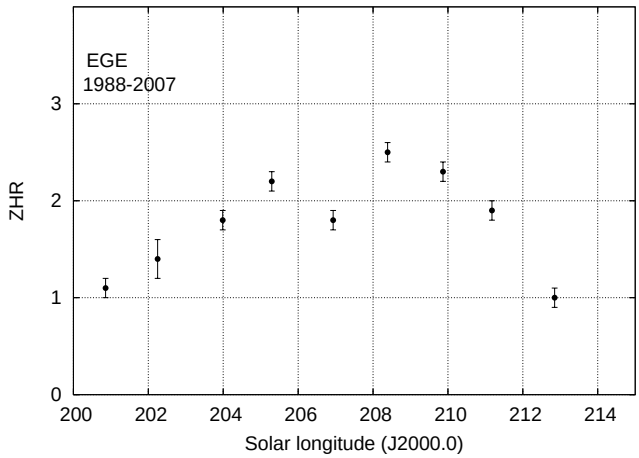


Figure 2.38: Activity of the ε-Geminids from visual observations stored in the VMDB covering the period 1988–2007 using a constant $r = 3.0$ over the activity period. The zenith correction included the standard sine term (no zenith coefficient $\gamma > 1.0$) and allowed only intervals with a radiant elevation of $\geq 20°$.

References

Kashcheyev B.L., Lebedinets V.N., 1967: Radar studies of meteors. *Smithson. Contr. Astrophys.* **11,** 183–199.

Lindblad B.A., 1987: Physics and orbits of meteoroids. In: *The Evolution of the Small Bodies of the Solar System*, Soc. Italiana di Fisica, Bologna.

Southworth R.B., Hawkins G.S., 1963: Statistics of meteor streams. *Smithson. Contr. Astrophys.* **7,** 261–285.

Znojil V., 1968: Frequency occurrence of small particles in meteor showers. II. Orionids, ε-Geminids. *BAC* **19,** 306–315.

2.22 Orionids (008 ORI)

2.22.1 Synopsis

Period	October 1 – November 10
Maximum	$\lambda_\odot = 208°$ ($\approx$ October 21)
Radiant	$\alpha = 95°$ $\delta = +16°$
$ZHR_{max} = 22$	$r = 2.9$ $V_\infty = 66$ km/s
Parent body	1P/Halley

Orbital elements of the stream and 1P/Halley

Ω	ω	i	e	q	a	P
Lindblad (1987); photographic						
28.°2	82.°7	164.°3	0.951	0.575 au	11.5 au	40 yr
Kashcheev & Lebedinets (1967); radar						
25°	86°	164°	0.83	0.57 au	4.8 au	10 yr
1P/Halley						
58.°8	111.°8	162.°2	0.967	0.582 au	18.2 au	77 yr

The earliest reports of Orionid activity come from Chinese observers (Zhuang, 1977; Imoto & Hasegawa, 1958). No European documents refer to the Orionids prior to 1864 when Herschel noticed them (Herschel, 1866; Denning, 1899, p. 246).

The Orionids are an annual shower which can be observed from both hemispheres from October 2 to November 7. The radiant (Figure 2.21.1) is well above the horizon already before local midnight. At maximum, an observer may expect about 20 Orionids per hour under perfect circumstances (Figure 2.39). The period of the broad maximum covers several days usually from October 20–24.

Since the late 1970s, observers have been mobilized to study the Orionids carefully because of the 1986 return of the parent comet. No unusual activity was reported in any year; rates were at the usual moderate level. In 1993, Dutch and German observers independently noted a remarkable ZHR of about 30 for 2 hours on the morning of October 18 (Rendtel & Betlem, 1993), a time when we would normally expect Orionid ZHRs to be closer to 10. The number of bright meteors was significantly higher during this period as well, a fact confirmed by photographic observations. This suggests that a filament of larger particles in the Orionid stream was encountered. For a long-term analysis, a number of data was transformed into the IMO's standard format. This gives information about the Orionid rates back to 1928 (Rendtel, 2008). Maximum ZHRs observed over the 20-year period 1981–2001 are shown in Figure 2.40 (Dubietis, 2003).

2.22.2 Research

Significantly enhanced rates have been observed in 2006 and 2007 (Figures 2.43 and 2.44). In both years, the Orionids showed ZHRs up to 60–80 over three days. In 2006, the high rates coincided with an unusually low population index r around 1.6 (Figure 2.41; Rendtel, 2007; Spurný & Shrbený, 2008). In 2007, we found a population index r to be slightly below 2.0 (Figure 2.42;

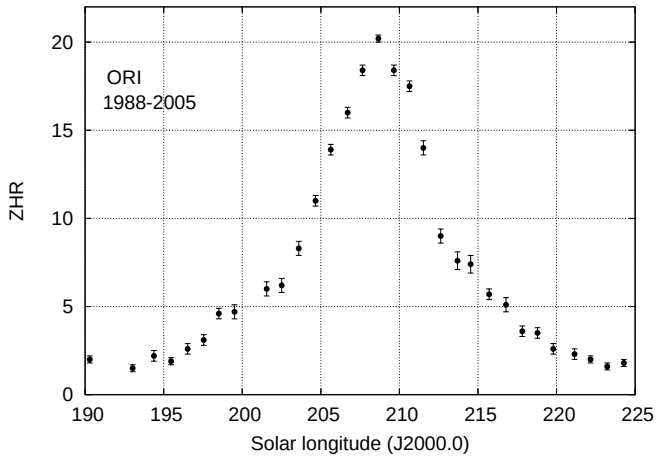


Figure 2.39: Activity of the Orionids from visual observations stored in the VMDB covering the period 1988-2005 using a constant $r = 2.5$ over the activity period. The zenith correction included the standard sine term (no zenith coefficient $\gamma > 1.0$) and allowed only intervals with a radiant elevation of $\geq 20°$. The returns of 2006 and 2007 are shown in Figures 2.43 and 2.44.

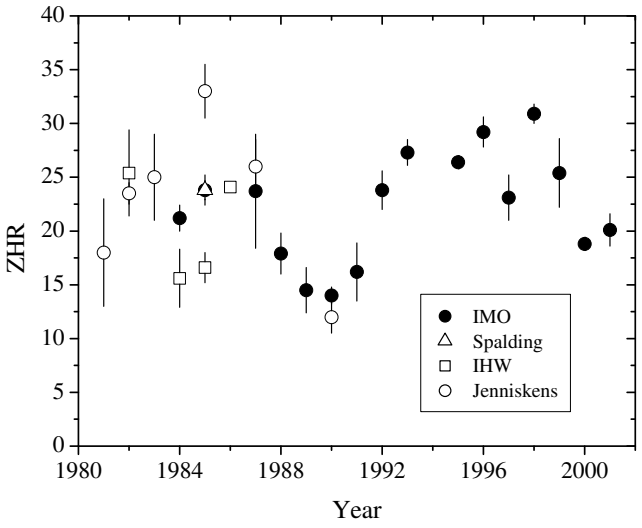


Figure 2.40: Evolution of the maximum ZHR of the Orionids from various sources of 1981 to 2001 (Dubietis 2003).

Arlt et al., 2008). The subsequent Orionid returns in 2008 and 2009 yielded still ZHRs of the order of 40–50, i.e. above the long-term average, but with no peculiar magnitude distribution as compared to the 2006b and 2007 returns.

The long-term average of the population index is between 2.3–2.9 (Rendtel, 2008). The meteoroids responsible for this activity are trapped in a 1:6 resonance with Jupiter (Sato & Watanabe, 2007; see also Rendtel, 2007). The parent comet, 1P/Halley, is not resonant with Jupiter. Hence, it may deliver meteoroids into all resonances over a long time. The quite large minimum distance between the orbits of the Comet and the Earth favours the 1:6 resonance because it has the greatest width of all discussed resonance zones (Emel'yanenko,

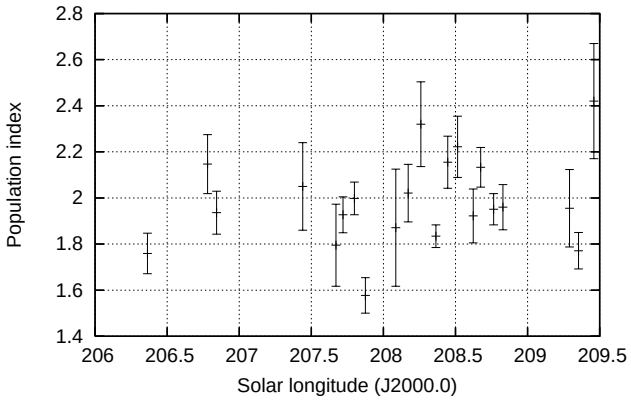


Figure 2.41: Population index r in the Orionid maximum period 2006 (Arlt et al., 2008). Note the very low values of r at several positions, showing the high portion of bright Orionids.

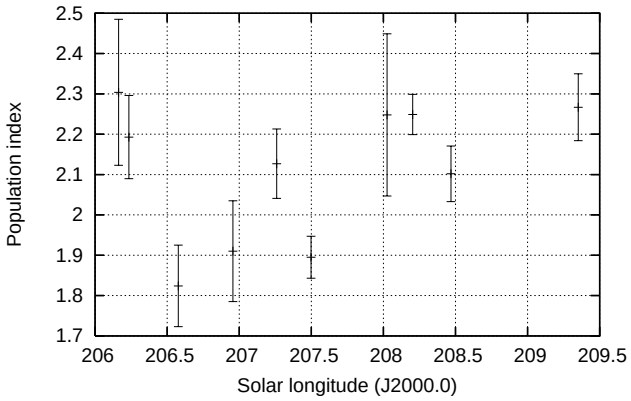


Figure 2.42: Population index r in the Orionid maximum period 2007 (Arlt et al., 2008). Although the r-values are not as low as in 2006 (Figure 2.41), they were significantly below the average of 2.5.

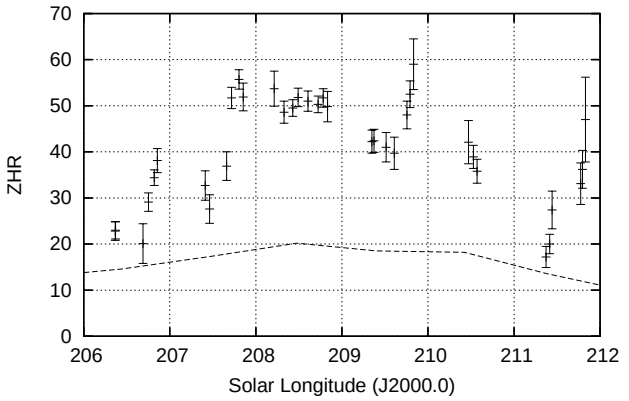


Figure 2.43: Orionid ZHR in the maximum period 2006 (Arlt et al., 2008) which is caused by meteoroids in resonant orbits. For comparison, the (smoothed) ZHR graph of the well-observed 1993 return is shown as a dashed line.

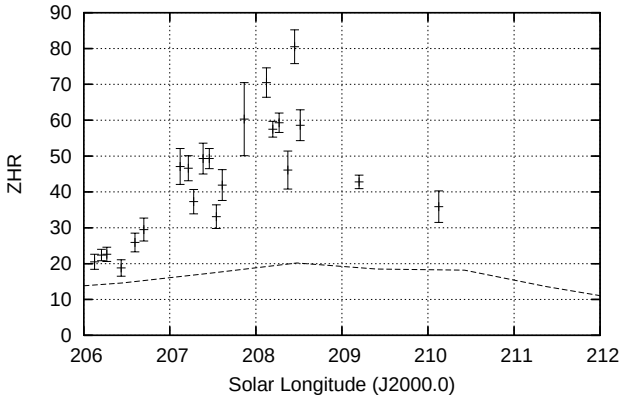


Figure 2.44: Orionid ZHR in the maximum period 2007 (Arlt et al., 2008), again caused by meteoroids moving near the 1:6 resonance with Jupiter. For comparison, the (smoothed) ZHR graph of the well-observed 1993 return is added (dashed line).

2001). Consequently, we could find Orionid rate enhancements that occurred six Jupiter revolutions earlier, i.e., about 72 years earlier than 2006. The strongest hint on Orionid rates exceeding the neighbouring years by a factor of about three is found in observations made by Loreta in Bologna in 1936 (Millman 1936). Similar hints can be found in Lovell (1954), although no calibration is possible and the original papers by Prentice (1936, 1939) do not allow further comparison.

References

Arlt R., Rendtel J., Bader P., 2008: The 2007 Orionids from visual observations. *WGN* **36,** 55–60.

Denning W.F., 1899: General catalogue of the radiant points of meteoric showers and of fireballs and shooting stars observed at more than one station. *Mem. Roy. Astron. Soc.* **53,** 202–292.

Dubietis A., 2003: Long-term activity of meteor showers from Comet 1P/Halley. *WGN* **31,** 43–48.

Emel'yanenko V.V., 2001: Resonance structure of meteoroid streams. In: *Proceedings of the Meteoroids 2001 Conference, Kiruna, 610 August 2001*, B. Warmbein (ed.). *(ESA SP-495)* Noordwijk, pp. 4345.

Herschel A.S., 1866: Radiant points of shooting stars. *MNRAS* **26,** 51–53.

Imoto S., Hasegawa, I., 1958: Historical records of meteor showers in China, Korea, and Japan. *Smithsonian Contr. Astrophys.* **2,** 131–144.

Kashcheyev B.L., Lebedinets V.N., 1967: Radar studies of meteors. *Smithson. Contr. Astrophys.* **11,** 183–199.

Lindblad B.A., 1987: Physics and orbits of meteoroids. In: *The Evolution of the Small Bodies of the Solar System*, Soc. Italiana di Fisica, Bologna.

Lovell A.C.B., 1954: Meteor Astronomy, Clarendon Press, Oxford.

Millman P.M., 1936: Observations of the Orionids in 1936. *J. R. astr. Soc. Canada* **30,** 416–418.

Olivier C.P., 1923: The Orionids 1922. *The Observatory* **46,** 17–18.

Prentice J.P.M., 1936: The radiants of the Orionid meteor shower. *JBAA* **46,** 329-336.

Prentice J.P.M., 1939: The radiants of the Orionid meteor shower. *JBAA* **49,** 148-153.
Rendtel J., 2007: Three days of enhanced Orionid activity in 2006 – Meteoroids from a Resonance Region?. *WGN* **35,** 41–45.
Rendtel J., 2008: The Orionid meteor shower observed over 70 years. *EMP* **102,** 103–110.
Rendtel J., Betlem H., 1993: Orionid meteor activity on Oct. 18, 1993. *WGN* **21,** 264–268.
Sato M, Watanabe J, 2007: Origin of the 2006 Orionid outburst.. *Publ. Astron. Soc. Japan* **59,** L1-L4.
Spurný P, Shrbený L, 2008: Exceptional fireball activity of Orionids 2006. *Earth, Moon, Planets* **102,** 141–150.
Zhuang T.-S., 1977: Ancient Chinese reports of meteor showers. *Chinese Astron.* **1,** 197–220.

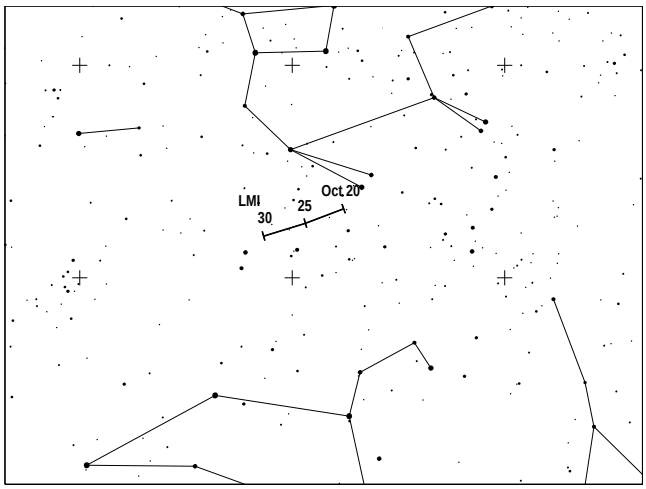


Figure 2.45: Radiant drift of the Leonis Minorids.

2.23 Leonis Minorids (022 LMI)

2.23.1 Synopsis

Period	October 17–27
Maximum	$\lambda_\odot = 211°$ (≈ October 24)
Radiant	$\alpha = 162°$ $\delta = +37°$
$ZHR_{max} = 2$	$r = 3.0$ $V_\infty = 62$ km/s
Parent body	C/1739 K1 (Zanotti)

Orbital elements of C/1739 K1 (Zanotti)

Ω	ω	i	e	q	a
C/1739 K1 (Zanotti)					
58.°8	111.°8	162.°2	0.967	0.582 au	18.2 au

This is a weak shower, but the ZHR near the detection threshold may be a result of neglecting the shower when other more prominent sources are active in late October. The radiant (Figure 2.45) can be seen from the northern hemisphere only and rises near local midnight.

The first mention of this shower dates back to McCrosky & Posen (1961) who found meteors with very similar orbits in their photographic survey. More recent compilations of photographic and video data by the Dutch Meteor Society confirmed this confined meteoroid stream (de Lignie & Betlem, 1999). Visual activity of the shower is weak; Jenniskens (1994) estimated the maximum ZHR to be 2 from a two-sided exponential fit. According to his graph, we set the activity period to October 19–27 use the solar longitude of 211° (approximately October 24) as it was listed in the very first IMO Working List as the maximum date. The average of ascending nodes of the photographic orbits given by de Lignie & Betlem (1999) is near $\lambda_\odot = 209°$, though, matching the peak time of the two-sided exponential fit by Jenniskens (1994). Their results for the geocentric velocity of the meteoroids was 61.9 km/s converting to an entry velocity of 63 km/s. The average radiant position for a solar longitude of 210° is $\alpha = 160.°2$, $\delta = 36.°8$. Recently, Borovička (2001) reported about a spectrum of a Leonis Minorid. The stream is also detected by the new search method by Welch (2001).

The data from the IMO video network also exhibit a weak but well confined radiant area very close to the photographic position of the Leonis Minorid radiant (Arlt & Rendtel, 2006).

References

Arlt R, Rendtel J, 2006: A new working list of meteor showers. *WGN* **34,** 71–84.
Borovička J, 2001: Video spectra of Leonids and other meteors, *Proceedings of the Meteoroids 2001 Conference, ESA SP-495*, 203–208.
deLignie M, Betlem H., 1999: A double-station video look on the October meteor showers. *WGN* **29,** 195–201.
Jenniskens P, 1994: Meteor stream activity. I. The annual streams. *Astron. Astrophys.* **287,** 990–1013.
McCrosky R.E., Posen A., 1961: Orbital elements of photographic meteors. *Smithson. Contr. Astrophys.* **4,** 15–84.
Welch P.G., 2001: A new search for streams in meteor data bases and its application. *MNRAS* **328,** 101–111.

2.24 Taurids (017 NTA, 002 STA)

2.24.1 Synopsis

The Taurids are embedded in the antihelion ecliptical activity and exhibit a northern and southern branch. The radiants are more confined than the ecliptical source in general, and they are part of a complex of minor bodies of the Solar System. These facts qualify them as an individual shower in the Working List.

017 Northern Taurids (NTA)

Period	October 20–December 10
Maximum	$\lambda_\odot = 230°$ ($\approx$ November 12)
Radiant	$\alpha = 58°$ $\delta = +22°$
$ZHR_{max} = 5$	$r = 2.3$ $V_\infty = 29$ km/s
Parent body	2P/Encke

Orbital elements of the NTA stream

Ω	ω	i	e	q	a	P
Lindblad (1987); photographic						
228.1	293.4	3.3	0.83	0.38 au	2.3 au	3.4 yr
Porubčan & Gavajdová (1994); photographic						
223.0	291.0	4.7	0.830	0.383 au	2.2 au	3.2 yr
Porubčan & Kornoš (2002); photographic						
226.2	294.9	3.1	0.832	0.350 au	2.1 au	3.1 yr
Ueda & Fujiwara (1994), video						
233.1	285.7	2.3	0.85	0.41 au	3.2 au	5.8 yr

Southern Taurids (002 STA)

Period	September 10–November 20
Maximum	$\lambda_\odot = 197°$ ($\approx$ October 10)
Radiant	$\alpha = 32°$ $\delta = +9°$
$ZHR_{max} = 5$	$r = 2.3$ $V_\infty = 27$ km/s
Parent body	2P/Encke

Orbital elements of the STA stream and 2P/Encke

Ω	ω	i	e	q	a	P
Lindblad (1987); photographic						
33.4	113.2	5.8	0.82	0.40 au	2.2 au	3.2 yr
Porubčan & Gavajdová (1994); photographic						
38.7	114.4	5.6	0.834	0.357 au	2.1 au	3.0 yr
Porubčan & Kornoš (2002); photographic						
37.3	115.4	5.4	0.825	0.352 au	2.1 au	3.0 yr
Ueda & Fujiwara (1994), video						
55.0	104.9	5.6	0.91	0.40 au	2.5 au	3.9 yr
Gartrell & Elford (1975); radar						
24°	129°	7.1	0.82	0.30 au	1.7 au	2.3 yr
2P/Encke						
334.6	186.5	11.8	0.847	0.339 au	2.2 au	3.3 yr

Because the radiants are close to the antihelion source (see Figure 2.46 and the details given below), the Taurid activity can be followed from both hemispheres and essentially during the entire night.

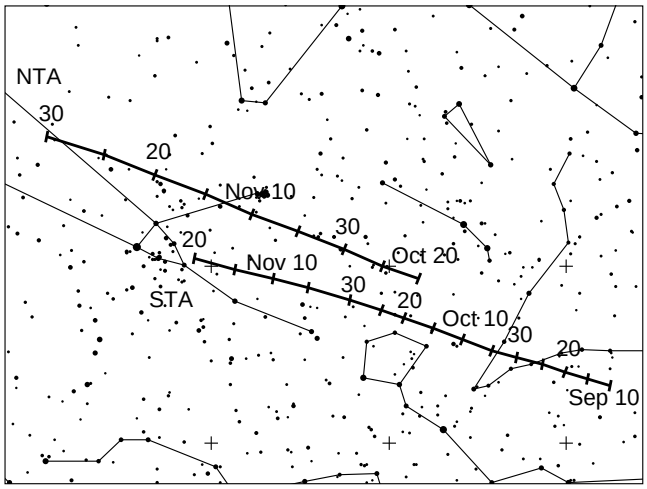


Figure 2.46: Radiant drift of the Northern and Southern Taurids.

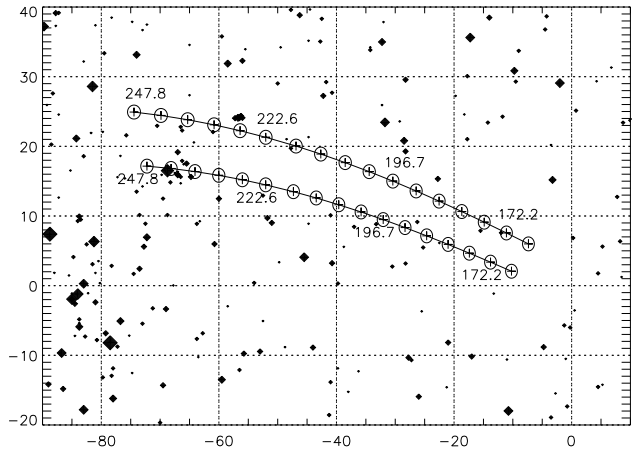


Figure 2.47: Radiant drift of the Northern and Southern Taurids derived by Triglav-Čekada & Arlt (2005).

The Taurids are a prominent source above the ecliptical background activity from end-September to early December. A radiant analysis of Triglav-Čekada & Arlt (2005) based on 57 778 video meteors shows that the ecliptical background starts to form a confined double-source in mid-September, but with variable strength in the northern and southern component. The average radiant motion of the two branches is shown in Figure 2.47. The prominence of the Taurids weakens in the end of November, the southern branch earlier on about November 20, and the northern branch about two weeks later. The ecliptical radiant structure in December returns to a very diffuse region as is typical for most of the ecliptical source throughout the year.

The orbital elements listed here are mean values. In fact, a detailed analysis allows the determination of trends in the elements over the two months while the Taurids are active (see Štohl & Porubčan, 1990; Porubčan & Očenáš, 1992; Porubčan & Kornoš, 2002).

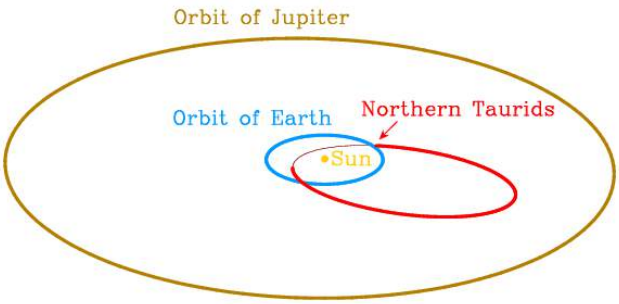


Figure 2.48: Taurids 'branch 1': the Northern Taurids. Comparison of the four diagrams (Figures 2.48 to 2.51) shows that if an orbit is twisted around in 3-dimensional space, it can be brought to Earth intersection in different ways (the orbit intersecting the Earth's orbit before or after perihelion, and coming from above or below the ecliptic). Under the gravitational influence of Jupiter and the other planets, a Taurid orbit can reach each of those configurations in turn, over a period of some millennia.

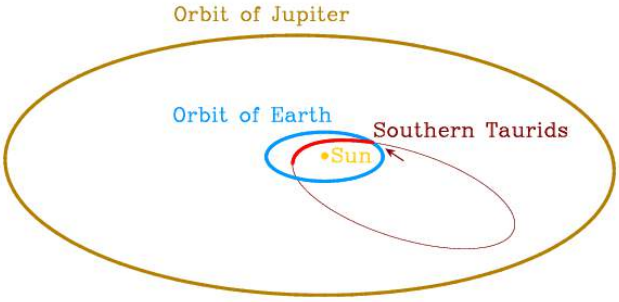


Figure 2.49: Taurids 'branch 2': the Southern Taurids.

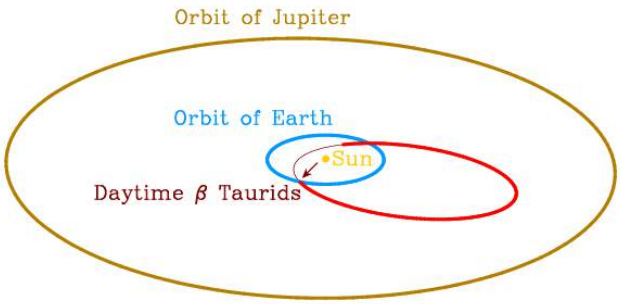


Figure 2.50: Taurids 'branch 3': the daytime β-Taurids.

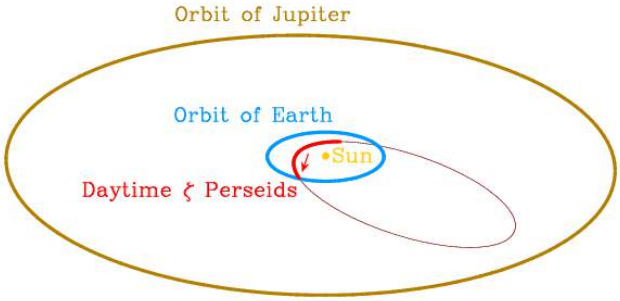


Figure 2.51: Taurids 'branch 4': the daytime ζ-Perseids.

2.24.2 Research

Whipple (1940) found indications for a possible association of the Taurids with Comet 2P/Encke. The Comet's orbit has a similar size and shape to the orbits of meteoroids in both NTA and STA streams, but is oriented differently in space (different argument of perihelion ω). In fact, the gravitational action of Jupiter allows any single orbit to precess through different ω over some millennia, and it is clear that NTA, STA and Encke all have the same origin. Moreover, other orientations allow the Earth's orbit to be intersected on the post-perihelion arc of the Taurid orbits, the resulting meteors hitting the daytime side of the Earth. Whipple (1940) postulated the existence of daytime showers. Radar observations in 1946 led to the discovery of the June Daytime β-Taurids (active from the end of June to early July; Figure 2.50) and the ζ-Perseids (present during the first half of June; Figure 2.51). As with the NTA and STA, there are northern (ζ-Perseid) and southern (β-Taurid) branches. Thus, what we observe on Earth are four cross sections of a continuous stream in space, orbits having dispersed to fill all 360° in ω (see, e.g., Babadzhanov, 2001).

Encke's short orbital period leads to a rapid evolution of the orbital elements and to a complex structure of the related meteoroid stream. The proximity of Encke and the Taurids (at their aphelion) to Jupiter's orbit, without being so close to Jupiter as to completely disrupt the stream, also causes the elements to evolve quite rapidly. (In contrast, e.g., (3200) Phaethon and the Geminids are much further from Jupiter's orbit and the orbital precession is much slower—see section 2.31.) The age of the Taurid stream should be estimated at about 10–20 thousand years in order to explain the observed spread in the longitude of perihelion (Babadzhanov & Obrubov, 1992; similarly estimated by Whipple & Hamid, 1952). There is no reason to believe that Taurid activity has been constant over this timescale. Fireball reports from the 11th century indicate remarkable Taurid activity then (Astapovich & Terentjeva, 1968). In more recent times, however, they have displayed only moderate activity.

The zodiacal cloud apparently requires a large cometary mass input in past few 10^4 years, and Encke or its progenitor has been suggested as a likely candidate (see Whipple, 1967, or Kresák, 1980). The breakup of a giant comet with several tens of kilometers diameter only about 20 000 to 30 000 years ago was proposed to produce the Taurid stream as well as numerous cometary nuclei (Clube & Napier, 1984) and this has prompted searches (e.g., Olsson-Steel, 1987; Asher et al., 1993; Babadzhanov et al. 2008) for Taurid complex members among the Apollo asteroid population (Table 2.7).

Taurid Complex objects often exist in mean-motion resonances with Jupiter (Steel, 1992) and undergo major orbital changes within rather short periods of time. A swarm moving in the 7:2 resonance with Jupiter was suggested to be part of the Taurid meteoroid stream. Studies by Asher (1994) and Asher & Izumi (1998) have

Table 2.7: Near-Earth Objects aligned with the Taurid Complex. The objects are listed in ascending order of D (Asher et al., 1993, 1994) which is used to test whether an orbit is 'Taurid-like'. In this list, D is calculated by D. Asher (August 2008, personal communication) using orbits in the IAU Minor Planet Center database. Asteroid 2004 TG_{10} is apparently related to the Taurids (Jenniskens, 2006; p. 470). Other than this, only larger asteroids (selected on the basis of absolute magnitude being 16.5 or brighter) are included. Among these larger asteroids having $D < 0.2$, a large proportion are aligned with the Taurid Complex (longitude of perihelion ϖ in the range 100° to 190°), although Jenniskens (2006; p. 464) has noted that many of these objects have taxonomic types *not* corresponding to extinct comet nuclei and perihelion distances a little higher than Taurid meteors. Diameter information is taken from `http://murison.alpheratz.net/calculators/OrbitalElements` for the asteroids and Fernández et al. (2000) for Encke.

Object	Orbital elements						Size
	a [au]	e	i	D	ϖ	Ω	[km]
2004 TG_{10}	2.24	0.86	4°	0.06	162°	212°	0.9
(6063) Jason	2.22	0.76	5°	0.07	146°	170°	5.1
(2201) Oljato	2.17	0.71	3°	0.12	173°	77°	1.8
(5143) Heracles	1.83	0.77	9°	0.13	177°	310°	8.7
(4197) 1982 TA	2.30	0.77	12°	0.14	129°	10°	6.8
(4341) Poseidon	1.84	0.68	12°	0.16	124°	108°	4.7
5025 P-L	2.52	0.75	4°	0.16	139°	346°	4.4
(17181) 1999 UM_3	2.38	0.67	11°	0.18	150°	114°	3.4
(8201) 1994 AH_2	2.53	0.71	10°	0.18	189°	164°	3.4
(5731) Zeus	2.26	0.65	11°	0.19	139°	282°	4.1
(4183) Cuno	1.98	0.64	7°	0.19	171°	296°	7.4
(106589) 2000 WN_{107}	2.15	0.61	14°	0.20	175°	163°	3.8
1990 HA	2.57	0.70	4°	0.20	133°	184°	3.3
Comet 2P/Encke	2.22	0.85	12°	0.05	161°	335°	4.8

indicated that enhanced Taurid fireball rates in specific years may result from such a 'swarm' of larger meteoroids within the Taurid Complex, rates increasing in years such as 1988 (Evans, 1993). The table of swarm encounters predicted by the model was published by Asher & Clube (1993). Meteoroids are concentrated within 60–70°in mean anomaly M (i.e. up to 30° or so from the 'resonance centre') with a gradual decrease over about 10°at each end. Encounters are listed in Table 2.8 for M within 40°of the centre. Calculations were based on the dates November 3 (pre-perihelion) and June 23 (post-perihelion); in fact, the swarm spans a week to each side of these dates (and the entire Taurid stream is even broader than the swarm). Negative ΔM means the swarm centre (resonance centre) is short of the Earth at the June or November date in question. Positive ΔM means the swarm centre is past the Earth.

The most recent suggested swarm encounters were due in 1995, 1998, and 2005. Indeed, the number of bright Taurids between late October and mid November 1995 was impressive. In 1998, the rates showed no significant increase, although a slightly enhanced portion of bright Taurids was recorded. The 2005 return yielded a large number of bright to brilliant Taurid fireballs as well as enhanced ZHRs of 10–15 (Dubietis & Arlt, 2007) from October 29 to November 10. Tests of this resonant swarm model require careful analyses covering years when the Earth does not encounter the swarm as well as years when it does (McBeath, 1999; Beech et al., 2004; Johannink & Miskotte, 2006). An analysis of plotted visual meteors suggested that the 1995 activity was stronger from south of the ecliptic (Triglav, 2000).

Table 2.8: Displacement in mean anomaly ΔM of the Earth from the swarm center. The reference dates are June 23 and November 3. This revision was made in April 2014 and follows the calculations published on p. 490 of Asher & Clube (1993) which ended with the line for 2008/2009.

Year (June)	ΔM	Year (Nov)	ΔM
1975	1°	1978	23°
1982	25°	1981	−18°
1985	−17°	1988	5°
1992	7°	1991	−36°
1995	−34°	1995	29°
1999	30°	1998	−13°
2002	−11°	2005	11°
2009	13°	2008	−30°
2012	−29°	2012	35°
2016	36°	2015	−7°
2019	−5°	2022	17°
2026	18°	2025	−25°
2029	−23°	2032	−1°
2036	1°	2039	23°

David Asher kindly provided us with the recent updates of the swarm encounters (as of May 2014). He pointed out, that if you want data for years beyond the end of Table 2.8, note that the numbers come close to

repeating every 61 years. This is because the swarm orbital period happens to be close to 61/18 years. So after the Earth goes around the Sun 61 times, and the swarm 18 times, the relative configuration of Earth and swarm repeats. Example: there was a good swarm encounter in 1954 (Asher & Izumi, 1998); so there should be one in 2015.

Computer simulations showed that over many thousands of years the swarm disperses across its orbit to have a crossing time at the Earth's orbit of 10 days or so, while the mechanism of the 7:2 resonance with Jupiter ensures that meteoroids remain concentrated within part of the orbit. More precisely, an 'equilibrium distribution' tends to be reached, in which meteoroids are concentrated, at a fairly uniform level, in the central ±30° in mean anomaly. Then, there is a decline over the next 10° or so at each end. Table 2.8 gives years in which the Earth moves through the Taurids at a time when the swarm arc is also intersecting the Earth's orbit.

References

Asher D., 1994: Meteoroid swarms and the Taurid complex. In *P. Roggemans (ed.): Proceedings of the IMC Puimichel 1993.* IMO, Mechelen, 88–91.

Asher D.J., Clube S.V.M., 1993: An extraterrestrial influence during the current glacial-interglacial. *Ql.J.R.A.S.* **34,** 481–511.

Asher D.J., Izumi K., 1998: Meteor observations in Japan: new implications for a Taurid meteoroid swarm. *MNRAS* **297,** 23–27.

Asher D.J., Clube S.V.M., Steel D.I., 1993: The Taurid complex asteroids. In *J. Štohl & I.P. Williams (eds.): Meteoroids and their parent bodies.* Slovak Acad. Sci., Bratislava, 93–96.

Asher D.J., Clube S.V.M., Napier W.M., Steel D.I., 1994: Coherent catastrophism. *Vistas Astron.* **38,** 1–27.

Astapovič I.S., Terenteva A.K., 1968: Fireball radiants of the 1st–15th centuries. In *L. Kresák & P.M. Millman (eds.): Physics and Dynamics of Meteors. IAU Symp. 33.* Reidel, Dordrecht, 308–319.

Babadzhanov P.B., 2001: Search for meteor showers associated with Near-Earth Asteroids. I. Taurid Complex. *Astron. Astrophys.* **373,** 329–335.

Babadzhanov P.B., Obrubov Yu.V., 1992: Evolution of short-period meteoroid streams. *Celestial Mechanics and Dynamical Astronomy* **54,** 111–127.

Babadzhanov P.B., Williams I.P., Kokhirova G.I., 2008: Near-Earth Objects in the Taurid complex. *MNRAS* **386,** 1436–1442.

Beech M., Hargrove M., Brown P., 2004: The running of the bulls: a review of Taurid fireball activity since 1962. *The Observatory* **124,** 277–284.

Clube S.V.M., Napier, W.M., 1984: The microstructure of terrestrial catastrophism. *MNRAS* **211,** 953–968.

Dubietis A., Arlt R., 2007: Taurid resonant-swarm encounters from two decades of visual observations. *MNRAS* **376,** 890–894.

Evans S.J., 1993: A comparison of the frequencies of photographic Taurid, Geminid and sporadic meteors during the period 1982–1991. *JBAA* **103,** 111–114.

Fernández Y.R. & 8 co-authors, 2000: Physical properties of the nucleus of Comet 2P/Encke. *Icarus* **147,** 145–160.

Gartrell G., Elford W.G., 1975: Southern hemisphere meteor stream determinations. *Austr. J. Phys.* **28,** 591–620.

Jenniskens P., 2006: *Meteor Showers and their Parent Comets.* Cambridge Univ. Press.

Johannink C., Miskotte K., 2006: Taurid activity 1988 – 2005. *WGN* **34,** 7–10.

Kresák L., 1980: Sources of interplanetary dust. In: *I. Halliday & B.A. McIntosh (eds.): Solid particles in the solar system. IAU Symposium 90.* Reidel, Dordrecht, 211–222.

Lindblad B.A., 1987: Physics and orbits of meteoroids. In *M. Fulchignoni & L. Kresák (eds.): The evolution of the small bodies of the Solar System.* Soc. Italiana di Fisica, Bologna, 229–251.

McBeath A., 1999: On the occurrence of bright Taurids. *WGN* **27,** 53-56.

Olsson-Steel D., 1987: Asteroid 5025 P-L, comet 1967 II Rudnicki, and the Taurid meteoroid complex. *The Observatory* **107,** 157–160.

Porubčan V., Gavajdová M., 1994: A search for fireball streams among photographic meteors. *Planet. Space Sci.* **42,** 151–155.

Porubčan V., Kornoš L., 2002: The Taurid meteor shower. In *B. Warmbein (ed.): Proceedings of Asteroids, Comets, Meteors 2002 (ESA SP-500).* ESA, Noordwijk, 177–180.

Porubčan V., Očenáš D., 1992: The Taurid meteor complex. In: *J. Rendtel & R. Arlt (eds.): Proceedings of the IMC Potsdam 1991.* IMO, Potsdam, 7–13.

Steel D., 1992: The importance of the Taurids. *WGN* **20,** 17–20.

Štohl J., Porubčan V., 1990: Structure of the Taurid meteor complex. In *C.-I. Lagerkvist et al. (eds.): Asteroids Comets Meteors III.* Uppsala Univ., 571–574

Triglav M., 2000: The analysis of two Taurid radiants from 10 years of plotted meteors. In *R. Arlt (ed.): Proceedings of the IMC Frasso Sabino 1999.* IMO, Potsdam, 101–111.

Triglav-Čekada M., Arlt R., 2005: Radiant ephemeris of the Taurid meteor complex. *WGN* **33,** 41-58.

Ueda M., Fujiwara Y., 1994: Television meteor radiant mapping. *'Meteoroids' conference 1994, Bratislava*

Whipple F.L., 1940: Photographic meteor studies. III. The Taurid shower. *Proc. Amer. Phil. Soc.* **83,** 711–745.

Whipple F.L., 1967: On maintaining the meteoritic complex. In: *J.L. Weinberg (ed.): The Zodiacal Light and the Interplanetary Medium (NASA SP-150).* NASA, Washington, D.C., 409–426.

Whipple F.L., Hamid S.E., 1952: On the origin of the Taurid meteor streams. *Helwan Obs. Bull., No. 41* **,** 224–252.

2.25 Leonids (013 LEO)

2.25.1 Synopsis

Period	November 6–30
Maximum	$\lambda_\odot = 235\,^\circ\!.27$ ($\approx$ November 17)
Radiant	$\alpha = 152^\circ$ $\delta = +22^\circ$
$\mathrm{ZHR_{max}} = var.$	$r = 2.5$ $V_\infty = 71$ km/s
Parent body	55P/Tempel-Tuttle

Orbital elements of the stream and comet 55P/Tempel-Tuttle

Ω	ω	i	e	q	a	P
Lindblad (1987); photographic						
$234\,^\circ\!.5$	$173\,^\circ\!.1$	$162\,^\circ\!.3$	0.931	0.984 au	15 au	54 yr
Lindblad et al. (1993); photographic						
$234\,^\circ\!.8$	$172\,^\circ\!.4$	$162\,^\circ\!.5$	0.935	0.984 au	15 au	60 yr
55P/Tempel-Tuttle						
$235\,^\circ\!.5$	$172\,^\circ\!.6$	$162\,^\circ\!.4$	0.907	0.964 au	10.3 au	33 yr

The Leonids are beyond doubt the most spectacular meteor stream observed in the past 200 years. They contributed enormously to the understanding of meteoroid streams over this entire period. The shower is a periodic shower of which the Earth crosses the main body every 33 years and causes very large meteor rates at a few occasions. A sequence of such events was observed in 1998–2002. Table 2.9 summarizes the observed positions and peak rates as well as the predicted values.

The radiant (Figure 2.52) rises only after local midnight as it is not far from the apex. Therefore the Leonid meteors enter the Earth's atmosphere with $V_\infty = 71$ km/s which is close to the maximum possible collision velocity for Solar System objects.

2.25.2 Research

55P/Tempel-Tuttle was first observed by Wilhelm Tempel in Marseilles, France, on 1865 December 19. It was subsequently, independently, discovered by Horace P. Tuttle on 1866 January 6 from Harvard Observatory in the USA (due to the slow trans-Atlantic communication then, this was readily possible). By the end of 1866, von Oppolzer had computed the Comet's orbit, and le Verrier had published his calculated orbit for the 'November meteors'. At the same time, but independently, Peters (Germany), Schiaparelli (Italy) and von Oppolzer (Austria) recognised the connection between the Leonids and 55P/Tempel-Tuttle (cf. Littmann 1998).

A large number of observations of the period 1799–1997 was compiled by Brown (1999). The storms of 1799, 1833, 1866, 1901, and 1966 all occurred at solar longitudes considerably later than the passage of the Earth at the comet's node in the particular year.

The Leonid meteor shower has contributed a lot to the progress of meteor science in the 20th century. While the 1966 Leonid storm was observed by surprise, the epoch near the end of the century was accompanied by advanced theoretical modelling of the meteoroid stream. An early prediction of the 1998/1999 Leonid storms came from Yeomans et al. (1996). The times when the Earth passes through the orbital plane of the Comet were considered the most probable moments of high activity. These were 1998 Nov 17, $19^\mathrm{h}43^\mathrm{m}$ UT and 1999 Nov 18, $1^\mathrm{h}48^\mathrm{m}$ UT.

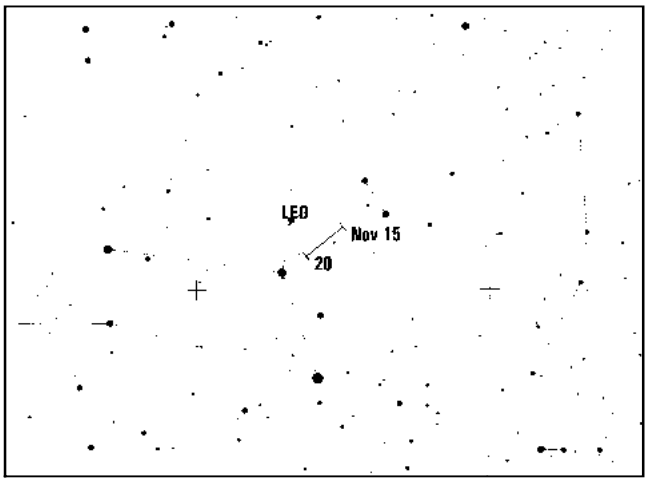


Figure 2.52: Radiant drift of the Leonids.

A model accounting for the orbital perturbations to meteoroids was introduced by Kondrat'eva & Reznikov (1985). Particles did not have the meaning of individual meteoroids, but were used as tick marks on a trail of dust. Only a few test particles have to be integrated over time and the arc running through them is evaluated with respect to its minimum distance from the Earth. The method is called 'dust-trail method' and has become a powerful tool for predicting meteor storms since. Leonid activity peaks of 1999–2006 have been successfully predicted by this method by McNaught & Asher (1999).

The modelling of a full stream where number densities of particles in space are direct indications for the meteoroid influx is computationally demanding. As many as 3 million particles were ingrated by Brown & Jones (1996) to explain the Leonid showers of 1902 and 1965. The model also predicted the heightenend activity in 1997–2001 or 2002 with highest rates in 1998–2000 at $\lambda_\odot = 235\,^\circ\!.6$. Table 2.9 summarizes the predictions and observational data of the dust trail encounters in the period 1998–2008.

The 1998 Leonids clearly demonstrate the effect of the population index r on the shape of the ZHR (Figure 2.53) and flux profiles. The highest ZHRs are caused mainly by larger meteoroids (Figure 2.55), while the lower peak close to the 2-revolution trail at $235\,^\circ\!.3$ is mainly due to smaller meteoroids (Figures 2.54). The 2001 data clearly show a higher population index r (Figure 2.57) at the positions of the rate peaks (Figure 2.58).

Uchiyama (2002) was able to separate the two 4- and 9-revolution dust trails by assuming different population indices.

Rendtel et al. (2000) detected short periodic variations of the order of 3 minutes duration in the ZHR (oscillations) in the 1999 Leonid data. These hint at structures of about 3000 km size. There is also a number deficiency at faint magnitudes.

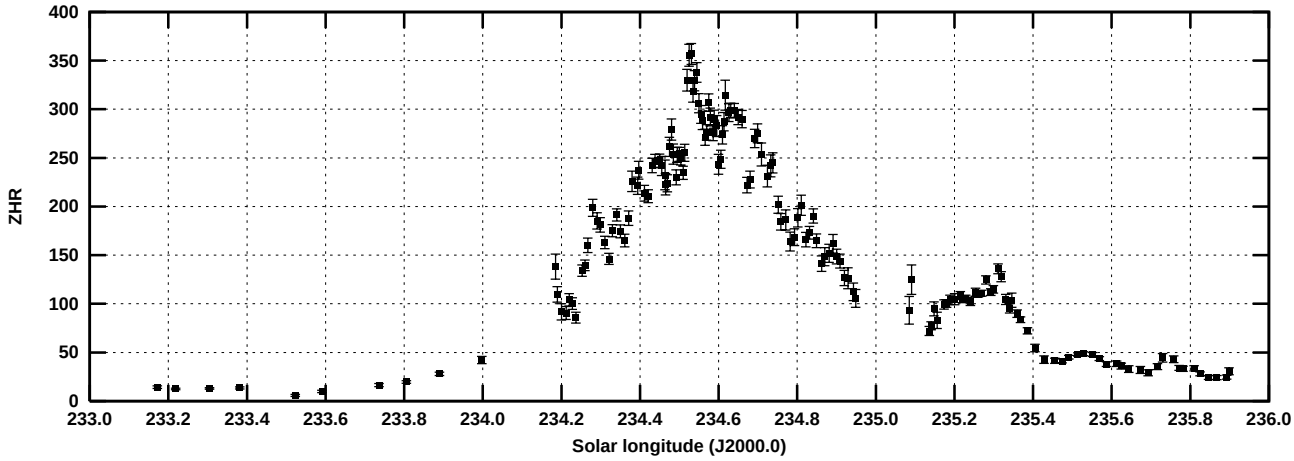


Figure 2.53: Activity profile of the 1998 Leonids with the broad fireball maximum (see also the cover photo) and the additional peak due to the 2-revolution dust trail.

Table 2.9: Predicted and observed encounters with Leonid dust trails between 1998 and 2008. 'Trail' denotes the age since the particle ejection (in comet revolutions). 'Time' lists the day (of November) and UT of the peaks.

Year	Trail (rev.)	Predicted time	Observed time	Pred. $\lambda_\odot$	Observed $\lambda_\odot$	Predicted ZHR	Observed ZHR	Figure
1998	2	17, 19^h30^m	17, 20^h33^m	$235\overset{\circ}{.}27$	$235\overset{\circ}{.}311\pm0\overset{\circ}{.}007$	–	$136\pm\ 5$	2.53
	20	17, 02^h	17, 01^h55^m	$234\overset{\circ}{.}55$	$234\overset{\circ}{.}528\pm0\overset{\circ}{.}006$	–	$357\pm\ 11$	
1999	3	17, 02^h08^m	17, 02^h02^m	$235\overset{\circ}{.}29$	$235\overset{\circ}{.}285\pm0\overset{\circ}{.}001$	1500	3700 ± 100	2.56
2000	2	17, 07^h52^m	17, 08^h07^m	$235\overset{\circ}{.}27$	$235\overset{\circ}{.}28\ \pm0\overset{\circ}{.}01$	215	$130\pm\ 20$	
	4	18, 07^h52^m	18, 07^h12^m	$236\overset{\circ}{.}28$	$236\overset{\circ}{.}25\ \pm0\overset{\circ}{.}01$	700	$480\pm\ 20$	
2001	4	18, 18^h20^m(1)	18, 18^h16^m	$236\overset{\circ}{.}44$	$236\overset{\circ}{.}458\pm0\overset{\circ}{.}003$	6100	$3430\pm\ 90$	2.58
	7	18, 10^h28^m(2)	18, 10^h39^m	$236\overset{\circ}{.}11$	$236\overset{\circ}{.}137\pm0\overset{\circ}{.}003$	2000	$1620\pm\ 40$	
	9	18, 18^h03^m(3)	18, 18^h02^m	$236\overset{\circ}{.}41$	$236\overset{\circ}{.}448\pm0\overset{\circ}{.}003$	1500–2000	$2830\pm\ 70$	
2002	7	19, 03^h53^m	19, 04^h10^m	$236\overset{\circ}{.}60$	$236\overset{\circ}{.}616\pm0\overset{\circ}{.}001$	2600 ± 200	$2510\pm\ 60$	
	4	19, 10^h29^m	19, 10^h47^m	$236\overset{\circ}{.}88$	$236\overset{\circ}{.}894\pm0\overset{\circ}{.}001$	3200 ± 200	2940 ± 210	
2003	15	13, 17^h17^m	13, 18^h	$236\overset{\circ}{.}89$	$230\overset{\circ}{.}9\ \ \pm0\overset{\circ}{.}3$	120	$25\pm\ 8$	
	8	19, 16^h50^m(4)	19, 15^h	$236\overset{\circ}{.}89$	$236\overset{\circ}{.}8\ \ \pm0\overset{\circ}{.}2$	70	$63\pm\ 4$	
2004	20	19, 01^h30^m(5)	17, 21^h	$237\overset{\circ}{.}00$	$235\overset{\circ}{.}8\ \ \pm0\overset{\circ}{.}1$	10	$37\pm\ 4$	
	8	19, 21^h49^m(6)	20, 00^h10^m	$237\overset{\circ}{.}85$	$237\overset{\circ}{.}95\ \pm0\overset{\circ}{.}03$	30	$26\pm\ 3$	
2005		21, 01^h10^m	–	$238\overset{\circ}{.}74$	–	< 50	–	
2006	2	19, 04^h45^m	19, 04^h46^m	$236\overset{\circ}{.}61$	$236\overset{\circ}{.}613\pm0\overset{\circ}{.}004$	150, 600	$75\pm\ 8$	
2007	8	20, 01^h15^m	18, 23^h50^m	$237\overset{\circ}{.}22$	$236\overset{\circ}{.}15\ \pm0\overset{\circ}{.}07$	10	$35\pm\ 5$	
2008	2	18, 21^h38^m	–	$236\overset{\circ}{.}80$	–	10–100	–	
	16	17, 01^h32^m	17, 02^h04^m	$234\overset{\circ}{.}95$	$234\overset{\circ}{.}97\ \pm0\overset{\circ}{.}02$	100	$98\pm\ 14$	

(1) 17^h55^m–18^h20^m– see Gural et al., 2004.

(2) 09^h55^m–10^h28^m– see Gural et al., 2004.

(3) 17^h08^m–18^h03^m– see Gural et al., 2004.

(4) erratum by Lyytinen to Vaubaillon et al., 2003.

(5) pred. by Lyytinen; Vaubaillon: 06^h42^m; McNaught & Asher: 06^h40^m.

(6) pred. by Vaubaillon; Lyytinen: 19^h00^m; 21^h49^m; McNaught & Asher: 21^h20^m.

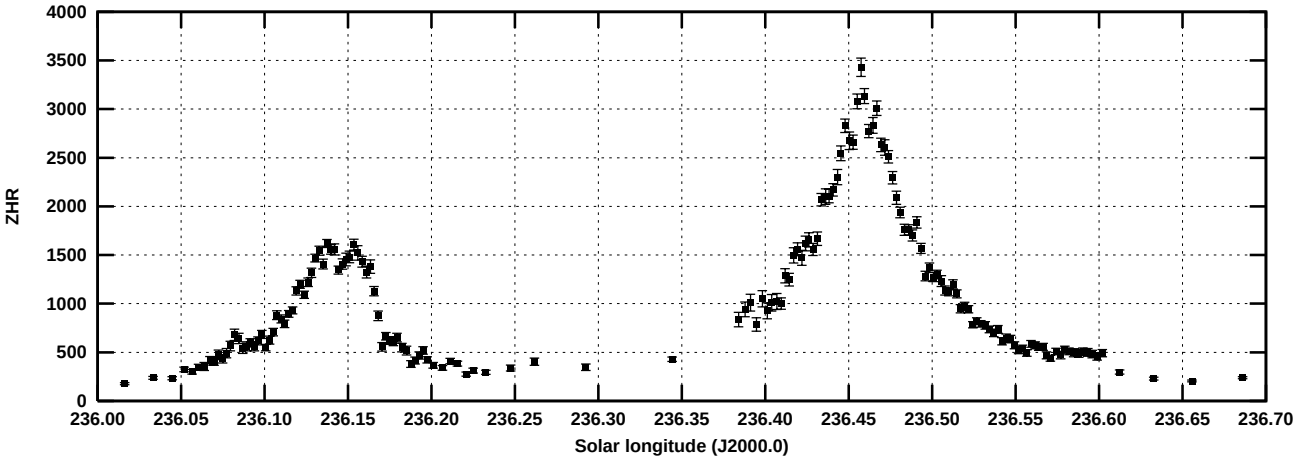


Figure 2.58: Activity profile of the 2001 Leonids with their two encounters of young dust trails – both composed of a high fraction of small meteoroids as indicated by their higher r (Figure 2.57).

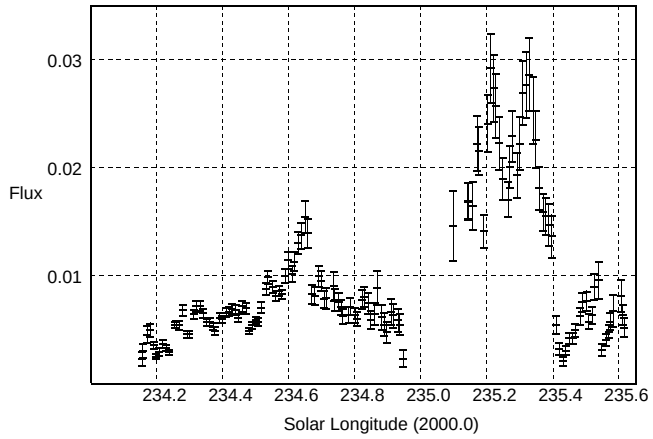


Figure 2.54: Flux density profile of the 1998 Leonids for particles causing meteors of up to magnitude +6.5.

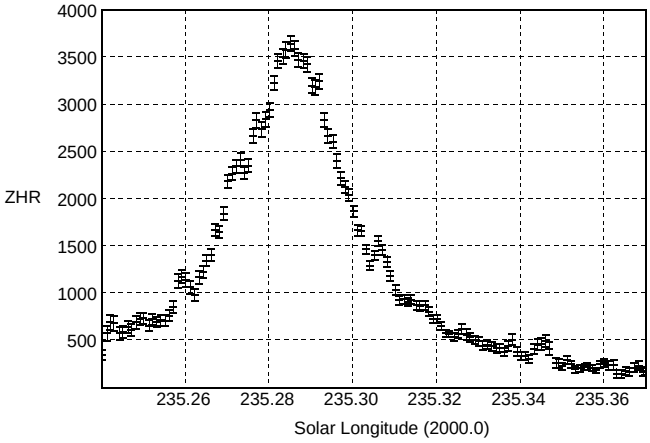


Figure 2.56: Activity profile of the 1999 Leonids near the encounter with the 3-revolution dust trail.

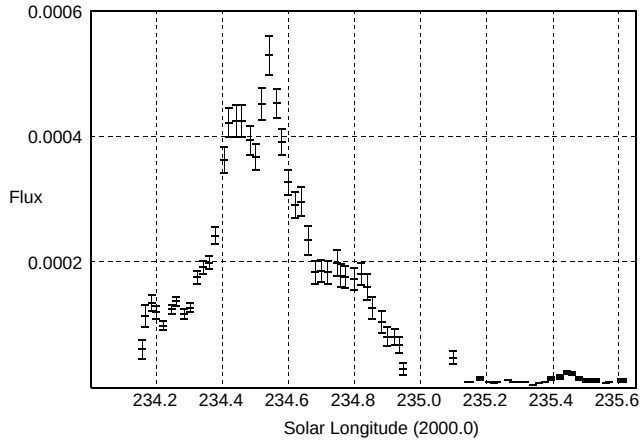


Figure 2.55: Flux density profile of the 1998 Leonids for particles larger than 1 g, coinciding with the first ZHR peak in Figure 2.53.

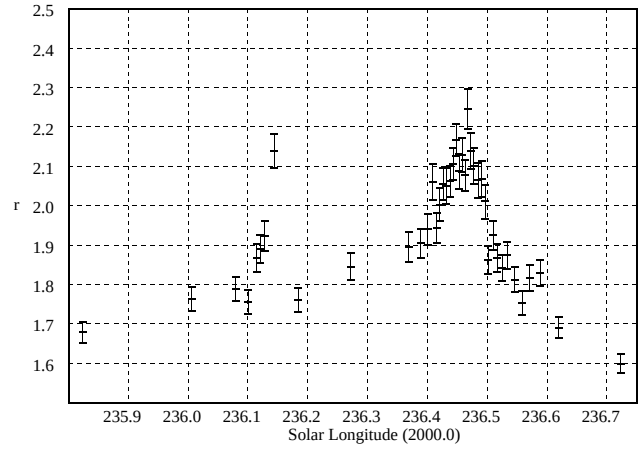


Figure 2.57: Population index profile of the 2001 Leonids with their two encounters of young dust trails.

Measurements of Suzuki et al. (2003) show that the begin height h_b of the luminous trail decreases with the absolute magnitude. Their TV data covered the range from +2 ($h_b \approx 145$ km) to +9 ($h_b \approx 105$ km). The end heights were found to be constant near 91 km.

References

Arlt R., 1998: Bulletin 13 of the International Leonid Watch: The 1998 Leonid meteor shower. *WGN* **26,** 239–248.

Arlt R., Bellot Rubio L., Brown P., Gyssens M., 1999:

Bulletin 15 of the International Leonid Watch: First global analysis of the 1999 Leonid storm. *WGN* **27,** 286–295.

Arlt R., Brown P., 1999: Bulletin 14 of the International Leonid Watch: Visual results and modelling of the 1998 Leonids. *WGN* **27,** 267–285.

Arlt R., Gyssens M., 2000: Bulletin 16 of the International Leonid Watch: Results of the 2000 Leonid meteor shower. *WGN* **28,** 195–208.

Arlt R., Kac J., Krumov V., Buchmann A., Verbert J., 2001: Bulletin 17 of the International Leonid Watch: First global analysis of the 2001 Leonid storms. *WGN* **29,** 187–194.

Arlt R., Krumov V., Buchmann A., Verbert J., 2002: Bulletin 18 of the International Leonid Watch: Preliminary analysis of the 2002 Leonid meteor shower. *WGN* **30,** 205–212.

Asher D.J., McNaught R.H., 2000: Expectations for the 2000 Leonids. *WGN* **28,** 138–143.

Betlem H., Jenniskens P., Spurný P., et al., 2000: Precise trajectories and orbits of meteoroids from the 1999 Leonid meteor storm. *Earth, Moon and Planets* **82–83,** 277–284.

Brown P., 1999: The Leonid Meteor Shower: Historical Visual Observations. *Icarus* **138,** 287.

Brown P., Jones J., 1996: Dynamics of the Leonid Meteoroid Stream: a Numerical Approach. In: B.A.S. Gustafson, M.S. Hanner (eds.): Physics, Chemistry, and Dynamics of Interplanetary Dust. ASP Conf. Series 104, 113.

Gural P.S., Jenniskens P., Koop M., Jones M., Houston-Jones J., Holman D., Richardson J., 2004: The relative activity of the 2001 Leonid storm peaks and implications for the 2002 return. *Adv. Space Res.* **33,** 1501–1506.

Kondrat'eva E.D., Reznikov E.A., 1985. *Sol. Syst. Res.* **31,** 489.

Littmann M., 1998: The heavens on fire. Cambridge University Press, Cambridge.

Lyytinen E., Nissinen M., Van Flandern T., 2001: Improved 2001 Leonid storm predictions from a refined model. *WGN* **29,** 110–118.

McNaught R.H., Asher D.J., 1999: Leonid dust trails and meteor storms. *WGN* **27,** 85–102.

McNaught R.H., Asher D.J., 2002: Leonid dust trail structure and predictions for 2002. *WGN* **30,** 132–143.

Molau S., Gural P.S., Okamura O., 2002: Comparison of the "American" and the "Asian" 2001 Leonid meteor storm. *WGN* **30,** 3–21.

Rendtel J., Molau S., Koschny D., Evans S., Okamura O., 2000: Video observtions of the 1999 Leonid meteor storm recorded at different locations. *WGN* **28,** 150–165.

Suzuki S., Akebo T., Suzuki K., Yoshida T., 2003: Multi-station TV observations of the 2001 Leonids. *WGN* **31,** 183–188.

Uchiyama S., 2002: Estimated ZHR profiles of the 4-revolution and 9-revolution dust trails during the 2001 Leonid meteor storm. *WGN* **30,** 47–55.

Vaubaillon J., 2002: Activity level prediction for the 2002 Leonids. *WGN* **30,** 144–148.

Vaubaillon J., Colas F., Jorda L., 2005: A new method to predict meteor showers. III Application to the Leonids. *A & A* **439,** 761–770.

Vaubaillon J., Lyytinen E., Nissinen M., Asher D.J., 2003: The 2003 Leonid shower from different approaches. *WGN* **31,** 131–134.

Yeomans D.K., Yau K.K., Weissmann P.R., 1996: The impending appearance of Comet Tempel-Tuttle and the Leonid meteors. *Icarus* **124,** 407–413.

2.26 α-Monocerotids (246 AMO)

2.26.1 Synopsis

Period	November 15–25
Maximum	$\lambda_\odot = 239\,^\circ\!.3$ ($\approx$ November 21)
Radiant	$\alpha = 118^\circ$ $\delta = +1^\circ$
$\mathrm{ZHR_{max}} = 3$; variable	$r = 2.4$ $V_\infty = 65$ km/s
Parent body	unknown

Orbital elements of the stream
(Jenniskens, 2006, photographic, DMS

Ω	ω	i	q	a
$59\,^\circ\!.322$	$90\,^\circ\!.66$	$134\,^\circ\!.13$	0.488 au	(500 au)

This shower is active from November 15 to 25 with a weak maximum occurring on November 21 and a radiant position which allows useful observations from almost all latitudes (Figure 2.59). Sometimes the shower is listed as 'November Monocerotids' (Lindblad, 1987) in order to distinguish it from the better known Monocerotids in December. The maximum activity of the α-Monocerotids is variable with ZHRs usually close to the visual detection limit (Figure 2.60. As described below, occasional ZHRs over 100 have been recorded within short time intervals. The typical duration of the observed outbursts was of the order of 15 minutes only.

The shower has been recognised the first time on 20/21 November 1925, when the American observer Bradley recorded 37 meteors in 13 minutes between $23^\mathrm{h}02^\mathrm{m}$–$23^\mathrm{h}15^\mathrm{m}$ (Eastern Standard Time, not mentioned; EST = UT $- 5^\mathrm{h}$) in Crozet, Virginia (Olivier, 1926). However, the shower was over after this burst, and when Bradley got out his charts after $23^\mathrm{h}25^\mathrm{m}$ local time no further shower meteors appeared. Bradley was not able to determine a radiant, but some other observations led to a (uncertain) position at $\alpha = 97\,^\circ\!.5$, $\delta = +8\,^\circ\!.5$ (Olivier, 1926).

Since the 1925 event, the α-Monocerotids have produced two further fine displays in 1935, as seen by Khan in India (Olivier, 1936) and in 1985 by Baker and Ducoty (1986) in the USA.

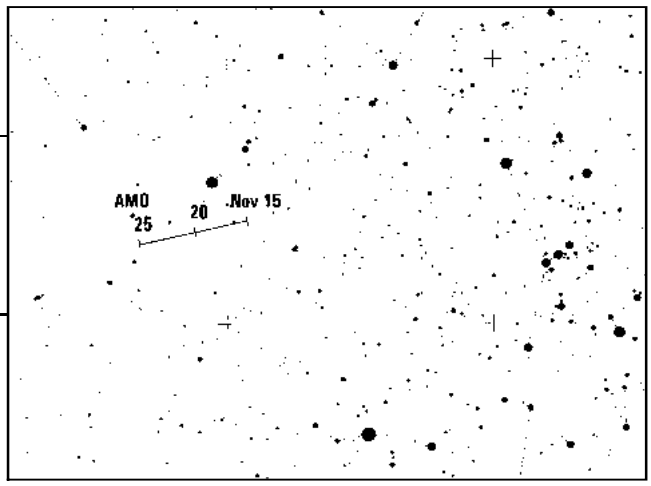


Figure 2.59: Radiant drift of the α-Monocerotids.

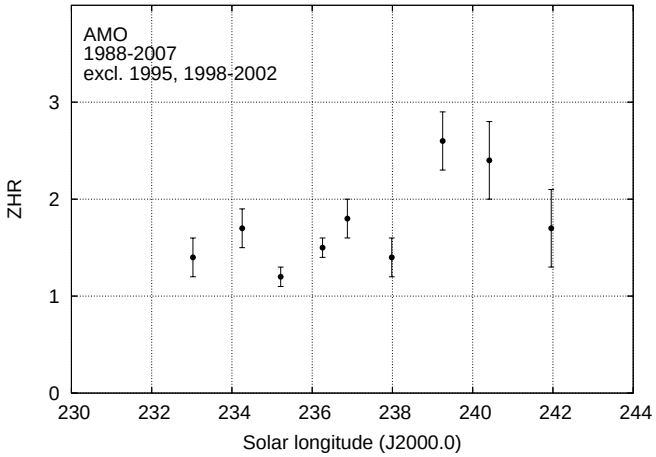


Figure 2.60: Activity of the α-Monocerotids from visual observations stored in the VMDB covering the period 1988-2007 using a constant $r = 2.4$ over the activity period. The zenith correction included the standard sine term (no zenith coefficient $\gamma > 1.0$) and allowed only intervals with a radiant elevation of $\geq 20^\circ$. The 1995 return (outburst) is excluded here. Further, the 1998–2002 returns interfering with the strong Leonid peaks are excluded from the data set to avoid effects due to the high activity and probable disregard of minor sources.

2.26.2 Research

In 1995 another outburst was predicted (Jenniskens, 1995) and successfully observed with different methods. The peak ZHR reached 450 (Figures 2.61 and 2.62) and lasted for about 40 minutes (Rendtel et al., 1996; Jenniskens et al., 1997).

The observers had the impression that the shower was poor in bright meteors. Indeed, a cut-off at -1 mag was found, and the shower was indeed dominated by 'large' meteoroids. Further, there was a lack of sodium found in the spectra (Borovička et al., 2005) thus making a significant difference in the appearance of the meteors.

Long-period comets may produce coherent dust trails—a compilation is given by Jenniskens (2006; 193–200) and Lyytinen & Jenniskens (2003). These trails wave around, reflecting the motion of the main planets around the Sun (Jenniskens, 2006; pp. 179ff)

A small chance for another outburst is calculated for 2019 November 22, $04^\mathrm{h}52^\mathrm{m}$ UT. However, the minimum distance to the dust trail is not very favourable (Lyytinen & Jenniskens, 2003: minimum distance to the trail -0.00036 au). Further in the future, there will be a close encounter on 2043 November 22, $10^\mathrm{h}58^\mathrm{m}$ UT, with a minimum distance of -0.00008 AU. The expected radiant is at $\alpha = 117^\circ$, $\delta = +1^\circ$ in both cases (Lyytinen & Jenniskens, 2003).

References

Baker K., Ducoty R., 1986: Unusual display of Nov. 20/21, 1985 *Meteor News*, Nr. 73, 6.

Borovička J., Koten P., Spurný P., Boček J., Štork R.,

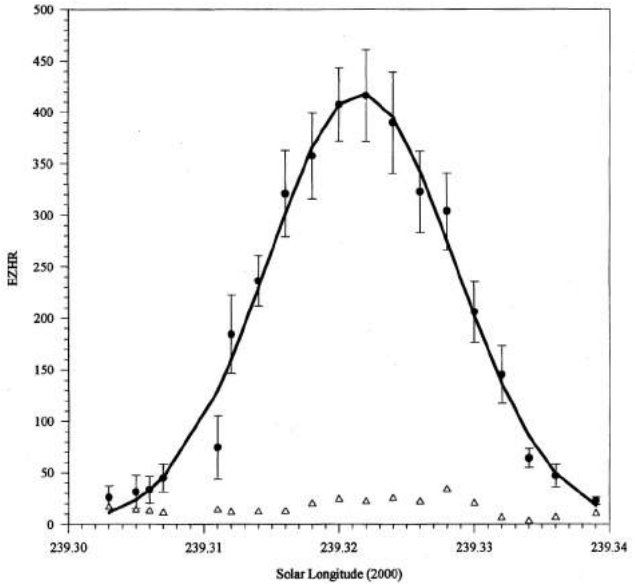


Figure 2.61: ZHR peak of the outburst of the α-Monocerotids on 1995 November 22 from the analysis of Rendtel et al. (1996). The length of the averaging interval was 0.°004 with the intervals shifted by 0.°002, or 3 min. The peak occurred at $\lambda_\odot = 239.°320 \pm 0.°002$, or November 22, 01^h28^mUT. The solid line shows a Gaussian fit of the profile, the triangles mark the sporadic rate.

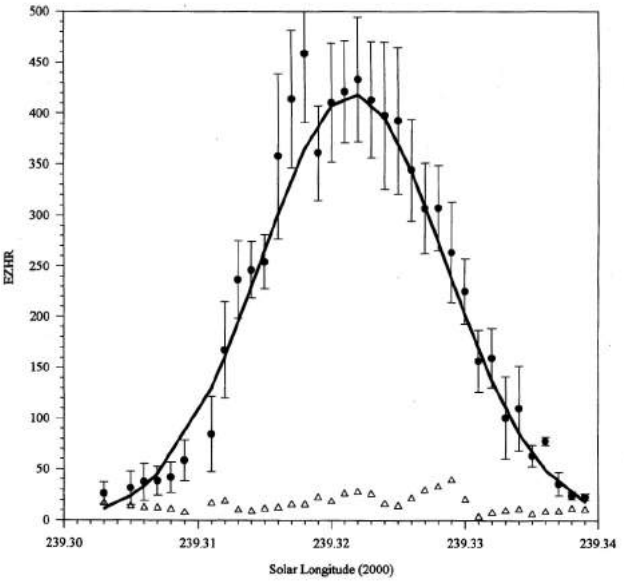


Figure 2.62: Peak of the 1995 α-Monocerotids with a higher time resolution of 1.5 min. The structures in the profile—if real—would correspond to spatial extents of about 3000 km (Rendtel et al., 1996).

2005: A survey of meteor spectra and orbits: evidence for three populations of Na-free meteoroids. *Icarus* **174,** 15-30.

Jenniskens P., 2006: Meteor showers and their parent comets. Cambridge Univ. Press.

Jenniskens P., 1995: Good prospects for α-Monocerotid outburst in 1995. *WGN* **23,** 84–86.

Jenniskens P., Betlem H., deLignie M.C., Langbroek M., 1997: The dtection of a dust trail in the orbit of an Earth-threatening long-period comet. *Astron. J.* **479,** 441–447.

Lindblad B.A., 1987: Comet 1944I and the Nov Monocerotids. *WGN* **15,** 154.

Lyytinen E., Jenniskens P., 2003: Meteor outbursts from long period comet dust trails. *Icarus* **162,** 443–452.

Olivier C.P., 1926: Report of the American Meteor Society for 1925. *Popular Astr.* **34,** 165–169.

Olivier C.P., 1936: Meteor Notes, Oct.-Nov. 1935. *Popular Astr.* **44,** 88-91.

Rendtel J., Brown P., Molau S., 1996: The 1995 outburst and the possible origin of the α-Monocerotid meteoroid stream. *MNRAS* **279,** L31–L36.

2.27 Phoenicids (254 PHO)

2.27.1 Synopsis

Period	November 28–December 9
Maximum	$\lambda_\odot = 254\,^\circ\!.25$ ($\approx$ December 6)
Radiant	$\alpha = 18^\circ$ $\delta = -53^\circ$
ZHR_{max} = variable	$r = 2.8$ $V_\infty = 18$ km/s
Parent bodies	D/1819 W1 (Blanpain) and 2003 WY_{25}

Orbital elements of the stream and the parent objects

Ω	ω	i	e	q	a	P
Jenniskens & Lyytinen, 2005 (obs. 1956)						
$74\,^\circ\!.14$	$358\,^\circ\!.15$	$15\,^\circ\!.93$		0.985 au	(3.05 au)	
D/1819 W1 (Jenniskens & Lyytinen, 2005: obs. 1956)						
$75\,^\circ\!.20$	$359\,^\circ\!.72$	$9\,^\circ\!.56$		0.9966 au	3.03 au	
2003 WY_{25} (Jenniskens & Lyytinen, 2005: orbit (a))						
$74\,^\circ\!.18$	$360\,^\circ\!.59$	$9\,^\circ\!.64$		0.9967 au	3.03 au	

This shower is only visible from the southern hemisphere (Figure 2.63). Meteors can be seen from November 28 to December 9. There is a gradual rise to a maximum on December 6, and although the maximum ZHR is usually below 3, on odd occasions much greater rates have been recorded. Jenniskens (1995) lists four such events of which three are based on single reports only.

2.27.2 History

On the evening of 1956 December 5, visual observers from South Africa, New Zealand, Australia, and from some ships, counted up to a hundred meteors per hour (Ridley, 1962). However, only a few of the listed reports can be used to derive a rate (Rendtel, 1996). The observations cover the period between 10^h10^m to 22^h45^m UT, but they do not allow an estimation of the time of the maximum. Ridley finally adopts 1956 December 5, 19^h UT.

Furthermore, the radiants given by the individual observers differ considerably from each other. Considering only reports based on more than 10 possible shower meteors, one gets radiants between $\alpha = 10 - 70^\circ$ and $\delta = -45 - -58^\circ$ (Table I of Ridley, 1962). The adopted radiant at $\alpha = 15^\circ$, $\delta = -45^\circ$ refers to meteor plots from one observer (Venter of South Africa).

Weiss (1958) conducted Adelaide (Australia) radar observations of this event. He derived a radiant at $\alpha = 15^\circ$, $\delta = -55^\circ$. The radar count rates reached only 30, which has been explained by Weiss in terms of the time of the observation (11^h00^m to 12^h30^m UT) and the low ionizing efficiency of slow meteors. However, *no velocity was measured* either visually nor by radar.

2.27.3 Research

Jenniskens (1995) lists three other occurrences of the Phoenicids in 1887, 1938 and 1972, but gives no references. The events are based only on one report each and should be regarded as uncertain. No further activity of this shower has been reported in the subsequent years after 1956. Visual observers of Australia noted low ZHRs of the Phoenicids during their regular campaigns in the 1980s (NAPOMS Bulletins 55, 132, 173, and 280), with an activity already below the detection limit in 1988 (anon., 1988). The data stored in the VMDB also reveal rates at the detection limit and hence cannot yield a rate profile.

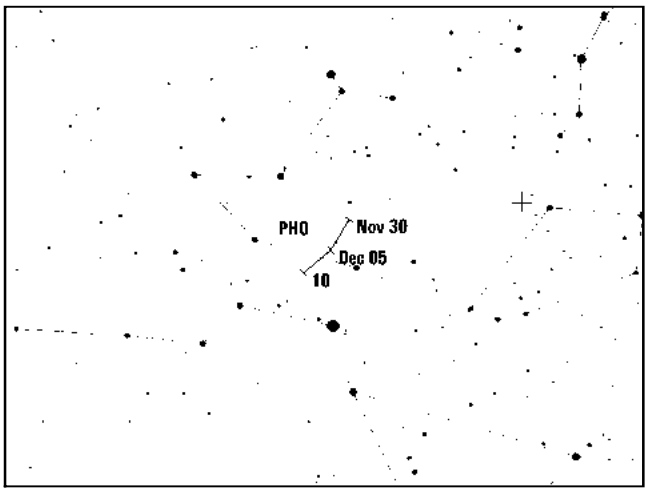


Figure 2.63: Radiant drift of the Phoenicids.

The Minor Planet 2003 WY_{25} is among the meteoroids causing the Phoenicid shower and may be a remnant of comet D/1819 W1 (Blanpain). Backward integration of 2003 WY_{25} to 1819 shows agreement in angular elements to 0.2 day accuracy. This proves the association, with no better agreement expected because of the poorly determined orbit of D/Blanpain (Jenniskens & Lyytinen, 2005). 2003 WY_{25} is suggested to be a fragment of ~ 400 m in diameter, broken up shortly before or during the 1819 return. New observations strongly support the identification of 2003 WY_{25} with the lost comet D/1819 W1 (Blanpain) made on the basis of dynamical similarity. It also shows that 2003 WY_{25} is a continuing but weak source of particles for the Phoenicid meteoroid stream (Jewitt, 2006).

Forward integration of the perturbations on the dust trail that would be generated in such a breakup shows that this dust accounts for the 1956 outburst of Phoenicids and establishes the link between the meteoroids and the Comet (Jenniskens & Lyytinen, 2005; Watanabe et al., 2005). This new result adds further evidence to a new paradigm: that most of our short-period meteor showers are due to the breakup of comets. These showers as well as the remaining fragments include at least the Geminids (3200 Phaethon), the Quadrantids (2003 EH_1), the Daytime Arietids (Marsden group of sunskirters), the Andromedids (fragments of 3D/Biela), and now also the Phoenicids (2003 WY_{25}).

Nevertheless, it seems that this shower currently does not show any observable activity. As in the case of other periodic or occasionally active showers, the observers should include the period in their observing efforts. Since the 1956 event lasted longer than other out-

bursts, a good coverage of the period may help in collecting reliable data on the current status of the shower. Since it will be at the detection limits, plotting of meteors is advised.

References

Jenniskens P., 1995: Meteor stream activity. II. Meteor outbursts. *A&A* **295,** 206–235.

Jenniskens P., Lyytinen E., 2005: meteor showers from the debris of broken comets: D/1819 W1 (Blanpain), 2003 WY25, and the Phoenicids. *Astron. J.* **130,** 1286–1290.

Jewitt D., 2006: Comet D/1819 W1 (Blanpain): not dead yet. *Astron. J.* **131,** 2327–2331.

Rendtel J., 1996: Meteors, literature—what to believe? In *P.Roggemans (ed.): Proceedings IMC 1995, Brandenburg.* IMO, Mechelen, 72–75.

Ridley H.B., 1962: The Phoenicid meteor shower of 1956 December 5. *JBAA* **72,** 266–272.

Watanabe J.-I., Sato M., Kasuga T., 2005: Phoenicids in 1956 Revisited. *Publ. Astron. Soc. Japan* **57,** L45–L49.

Weiss A.A., 1958: The 1956 Phoenicid meteor shower. *Austr. J. Phys.* **11,** 113–117.

—, 1988: The 1988 Phoenicid meteor stream. *NAPOMS Bull.* 280.

2.28 Puppid-Velids (301 PUP)

2.28.1 Synopsis

Period	December 1–15	
Maximum	$\lambda_\odot = 255°$	($\approx$ December 6)
Radiant	$\alpha = 123°$	$\delta = -45°$
$ZHR_{max} = 10$	$r = 2.9$	$V_\infty = 38$ km/s
Parent body	unknown	

Orbital elements of the stream

Ω	ω	i	e	q	a	P
Gartrell & Elford (1975), radar						
83°	360°	70°	0.2	0.98 au	1.3 au	1.5 yr
Nilsson (1964), radar						
78°	345°	70°	0.5	0.98 au	2 au	2.8 yr

There are indications of a number of radiants active in the Puppis-Vela region (several numbers assigned in the IAU data base) from late October through February. The radiant listed in the synopsis table represents to some extent the "average" position and coincides with the parameters given as 301 PUP (see below). Activity from this region was noticed by Hoffmeister (1948) during his observations in Southwest Africa and may extend beyond the dates given here. Generally, the Puppids-Velids (Figure 2.64) produce about 2 meteors per hour over most of this time, but they are more obvious during the first half of December, when rates can exceed 5 meteors per hour (Figure 2.65).

Obviously there are several sub-centres active. Gartrell & Elford (1975) found different radiant positions for the consecutive dates December 6, 7, and 8. Outside the period listed here, not only the rates are lower, but also the radiants appear more dispersed, except perhaps for the Centaurids in January–February. Hence a radiant diameter of 20° should be used for shower association. Plotting is strongly recommended for visual observations, which in combination with other optical and radar techniques may help to answer some of the open questions about this shower complex. It is impossible to distinguish between the various sub-radiants from only counting meteors.

Since the Puppid-Velids are now a collection of what was regarded as a larger number of sub-radiants before, the amount of consistent data is still low. From 1992 onwards, there are 139 reports of meteors associated with that complex. Unfortunately, the period of the major activity around $\lambda_\odot = 255°$ is not yet sufficiently covered with data. Close to this longitude, the IAU database includes:

305 SPU σ-Puppids: $\alpha = 102°$, $\delta = -45°$
300 ZPU ζ-Puppids: $\alpha = 123°$, $\delta = -43°$
301 PUP γ-Puppids: $\alpha = 123°$, $\delta = -45°$
302 PVE b-Puppids: $\alpha = 128°$, $\delta = -45°$
303 LVL λ-Velids: $\alpha = 133°$, $\delta = -46°$
all with velocities between 33 and 39 km/s.

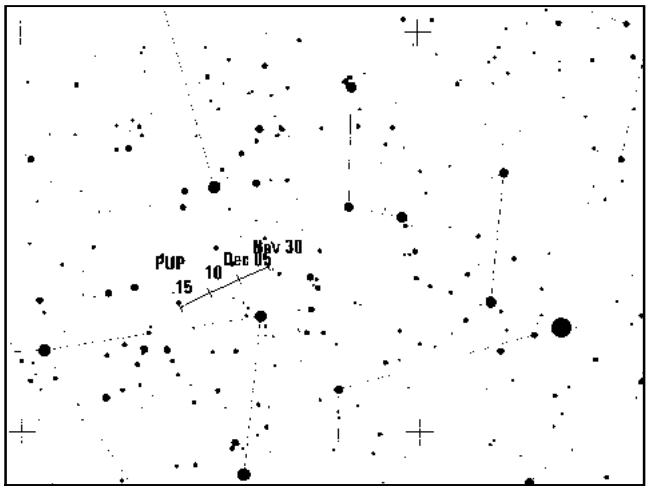


Figure 2.64: Radiant drift of the Puppid-Velids.

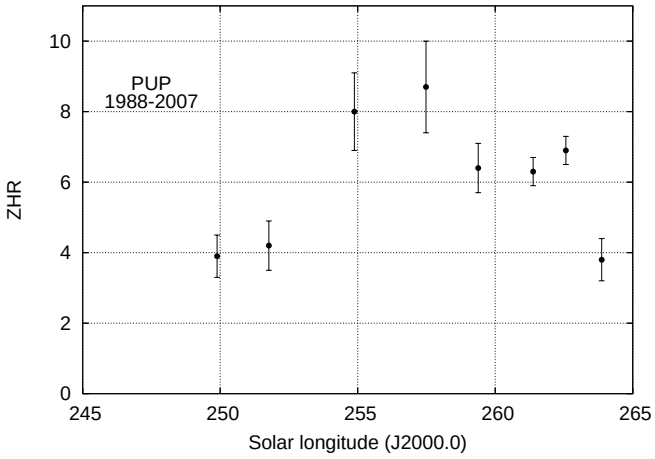


Figure 2.65: Activity of the Puppids-Velids from visual observations stored in the VMDB covering the period 1988–2007 using a constant $r = 2.9$ over the activity period. The zenith correction included the standard sine term (no zenith coefficient $\gamma > 1.0$) and allowed only intervals with a radiant elevation of $\geq 20°$.

2.28.2 Research

The Apollo asteroid (2102) Tantalus, discovered in 1975, has been associated with the Puppid-Velid complex (Drummond, 1982; Olsson-Steel, 1987; Hasegawa et al., 1992). However, the theoretical radiant position ($\alpha = 134°$, $\delta = -45°$ for December 26), the node and the semimajor axis of the stream (which is larger than that of (2101) Tantalus) do not fit the observed values very well (Hasegawa et al., 1992).

Recent southern hemisphere radar data (Janches et al., 2013) yield two radiants representing the average Puppid radiant position and activity period and show two radiants in the vicinity, supporting the above assumption of a longer activity period. The radar data show the ζ-Puppids (300 ZPU) between $\lambda_\odot = 234°$ and 240° (earlier than in the Table) and the γ-Puppids (301 PUP) coinciding with the data listed here. The other two radiants are given as η-Carinids (313 ECR) between $\lambda_\odot = 280°$ and 291° in early January and slightly south near $\delta = -51°$ and b-Puppids (302 PVE) in a short interval (274°–276°).

References

Drummond J.D., 1982: Theoretical meteor radiants of Apollo, Amor, and Aten asteroids. *Icarus* **49,** 143–153.

Gartrell G., Elford W.G., 1975: Southern hemisphere meteor stream determinations. *Aust. J. Phys.* **28,** 591–620.

Hasegawa I., Ueyama Y., Ohtsuka K., 1992: Predictions of the meteor radiant point associated with an Earth-approaching minor planet. *Publ. Astron. Soc. Japan* **44,** 45–54.

Heis E., Neumayer G., 1867: On the meteors in the southern hemisphere. Schneider, Mannheim.

Hoffmeister C., 1948: Die Meteorströme. J.A.Barth, Leipzig.

Janches D., Hormaechea J.L., Brunini C., Wocking W., Fritts D.C., 2013: An initial meteoroid stream survey in the southern hemipshere using the Southern Argentina Agile Meteor Radar (SAAMER). *Icarus* **223,** 677–683.

McIntosh B.A., 1935: An index to southern meteor showers. *MNRAS* **95,** 709–718.

Nilsson C.S., 1964: A southern hemisphere radio survey of meteor streams. *Austr. J. Phys.* **17,** 205–256.

Olsson-Steel D., 1987: Theoretical meteor radiants of Earth-approaching asteroids and comets. *Austr. J. Astron.* **2,** 21–35.

2.29 Monocerotids (019 MON)

2.29.1 Synopsis

Period	November 27–December 17	
Maximum	$\lambda_\odot = 257°$	($\approx$ December 8)
Radiant	$\alpha = 100°$	$\delta = 8°$
$ZHR_{max} = 2$	$r = 3.0$	$V_\infty = 42$ km/s
Parent body	C/1917 F1	(Mellish)

Orbital elements of the stream and C/1917 F1 (Mellish)

Ω	ω	i	e	q	a	P
Sekanina (1973), radar						
68.°0	141.°2	24.°7		0.119 au	7.11 au	
Jenniskens (2006)						
80.°2	128.°1	35.°2		0.193 au	50.7 au	
C/1917 F1 (Mellish)						
88.°67	121.°32	32.°68	0.993	0.190 au	28 au	145 yr

The December Monocerotid radiant (IAU number 019) is quite close to the radiants of the Geminids and the σ-Hydrids (Figure 2.68). Hence the shower association from visual observations may become difficult, particularly because the velocities of the Geminids and the Monocerotids are similar. A careful selection of the observing direction helps if the radiants do not line up. Hints given in Chapter 3 need to be applied (see also the example of shower association just dealing with this period of the year).

So far, most Monocerotid observational data have been obtained during the Geminid activity. As a consequence, the first 10 days of the Monocerotid activity have remained almost unexplored and thus we are left with a rather incomplete picture of the stream activity (Figure 2.66). Analyses have generally yielded very low rates, often just 1 to 2 Monocerotids per hour, and there is no obvious maximum. Some reports indicating a maximum at the same time as the Geminids should be treated with care. Our analysis (Figure 2.66) shows that there is no obvious effect of Geminid meteors 'polluting' the Monocerotid sample near their peak (around $\lambda_\odot = 262.°2$).

This shower had not been reported until Whipple (1954) determined two meteor orbits from photographic surveys, with a radiant at $\alpha = 103°$, $\delta = +8°$. In addition to these two shower meteors, McCrosky & Posen (1961) found further photographic Monocerotids. Ohtsuka (1989) lists 15 respective orbits, and he argues that also those listed by Kresáková (1974) belong to this shower. Radar data of Gartrell & Elford (1975) yielded a slightly different radiant ($\alpha = 106°$, $\delta = +6°$). A summary of radiant position determinations and orbits obtained by radio methods is given by Lindblad & Olsson-Steel (1990).

2.29.2 Research

The orbit of the photographic Monocerotids indicates a link with Comet D/1917 F1 (former designation P/Mellish) as shown in Figure 2.67. The long period

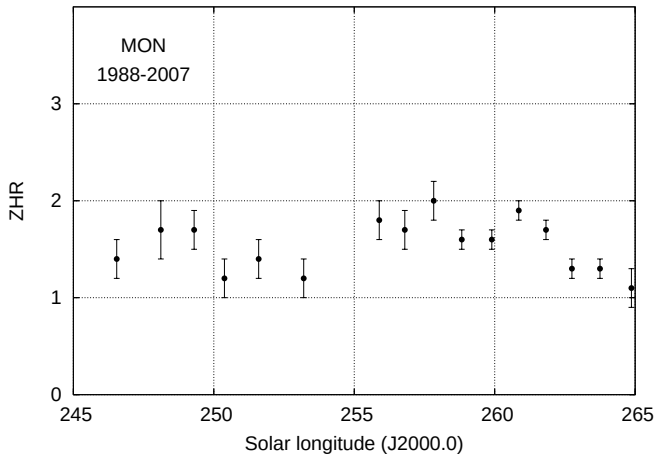


Figure 2.66: Activity of the Monocerotids from visual observations stored in the VMDB covering the period 1988–2007 using a constant $r = 3.0$ over the activity period. The zenith correction included the standard sine terms (no zenith coefficient $\gamma > 1.0$) and allowed only intervals with a radiant elevation of $\geq 20°$.

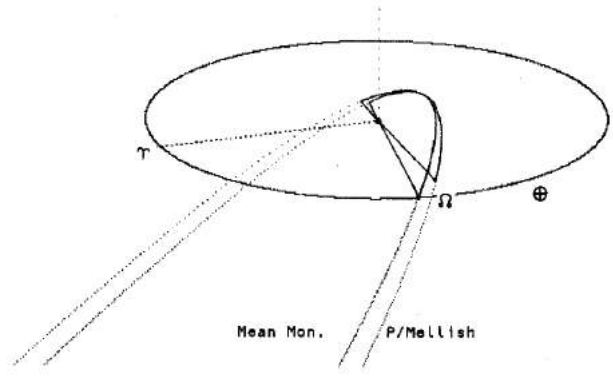


Figure 2.67: Orbit of comet D/1917 F1 (P/Mellish) and the Monocerotids (Ohtsuka, 1989).

and very small perihelion distance of the Monocerotid stream is unusual. The probability of a chance association of the orbits of the Monocerotids and the comet is small (Lindblad & Olsson-Steel, 1990).

Furthermore, the Monocerotids may be responsible for a number of ancient fireballs (Astapovich & Terentjeva, 1968). Investigations of the orbital evolution indicates that the fireballs are possibly related to the Monocerotids rather than the Geminids (Fox & Williams, 1985). Both the orbits of D/1917 F1 and the meteor shower are very stable.

Considering this, it is rather surprising that there are only weak hints of earlier visual observations. Hoffmeister (1948) lists a radiant at $\alpha = 92°$, $\delta = +9°$ (1950) based on two separate notes: $\alpha = 91°$, $\delta = +11°$ from one of his southern hemisphere expeditions, and $\alpha = 92°$, $\delta = +7°$ from observations in Germany.

References and bibliography

Astapovich I.S., Terent'eva A.K., 1968: Fireball radiants of the 1st–15th centuries. In *L.Kresák &*

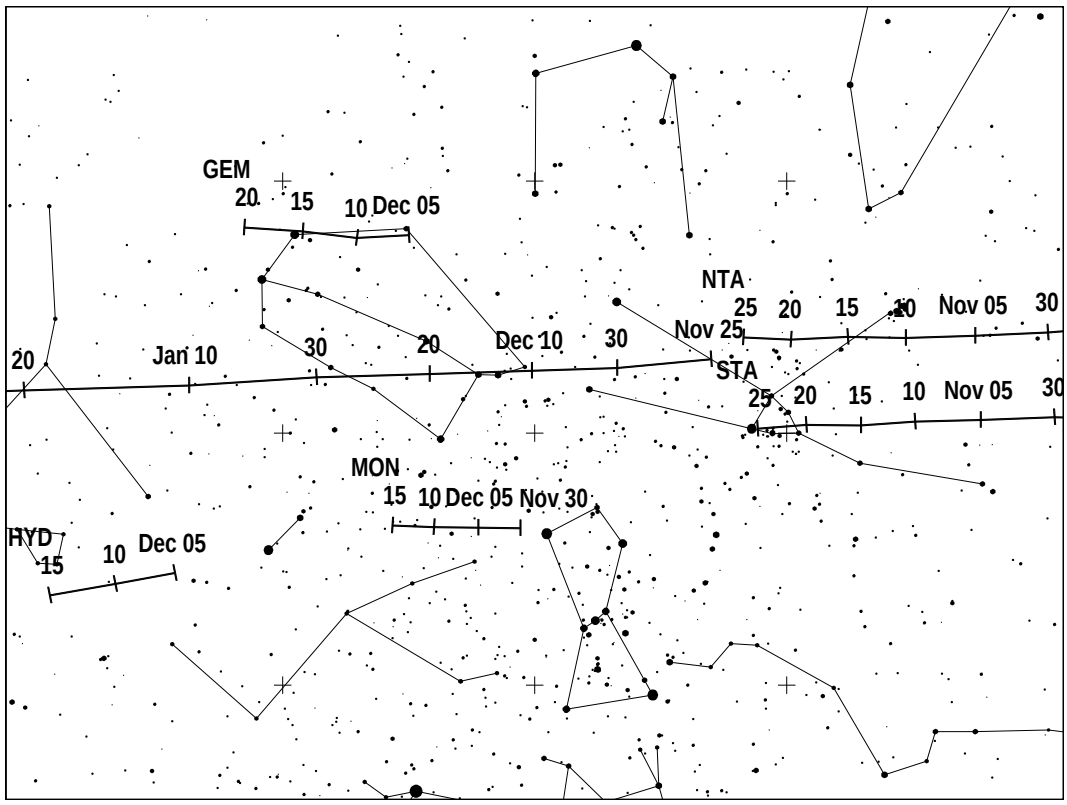


Figure 2.68: Radiant drift of the Geminids (GEM), the Monocerotids (MON), the σ-Hydrids (HYD) and the Antihelion Source. Shower association requires careful consideration of the direction, apparent trail length and angular velocity as described in the example in Chapter 3 of the techniccal description part of the Handbook.

P.Millman (eds.): Physics and dynamics of meteors. Reidel, Dordrecht. 308–319.

Fox K., Williams I.P., 1985: A possible origin for some ancient December fireballs. *MNRAS* **217,** 407–411.

Gartrell G., Elford W.G., 1975: Southern hemisphere meteor stream determinations. *Aust. J. Phys.* **28,** 591–620.

Hoffmeister C., 1948: Die Meteorströme. J.A.Barth, Leipzig.

Jenniskens P., 2006: Meteor showers and their parent comets. Cambridge Univ. Press.

Kresáková M., 1974: Meteors of periodic comet Mellish and the Geminids. *BAC* **25,** 20–33.

Lindblad B.A., Olsson-Steel, 1990: The Monocerotid meteor stream and comet Mellish. *BAC* **41,** 193–200.

McCrosky R.E., Posen A., 1961: Orbital elements of photographic meteors. *Smithson. Contr. Astrophys.* **4,** 15–84.

Ohtsuka K., 1989: The December Monocerotids and P/Mellish. *WGN* **17,** 93–95.

Sekanina Z., 1973: Statistical model of meteor streams. III Stream search among 19303 radio meteors. *Icarus* **18,** 253–284.

Whipple F.L., 1954: Photographic meteor orbits and their distribution in space. *AJ* **59,** 201–217.

2.30 σ-Hydrids (016 HYD)

2.30.1 Synopsis

Period	December 3–15	
Maximum	$\lambda_\odot = 260°$	(≈ December 11)
Radiant	$\alpha = 127°$	$\delta = +2°$
$ZHR_{max} = 3$	$r = 3.0$	$V_\infty = 58$ km/s
Parent body	unknown	

Orbital elements of the stream

Ω	ω	i	e	q	a	P
Lindblad (1987), photographic)						
77.°8	120.°8	127.°4	0.978	0.249 au	11 au	37 yr
Porubčan & Gavajdová (1994), photographic						
73.°2	114.°4	132.°5	0.991	0.294 au	37 au	220 yr
Ueda & Fujiwara (1994), video						
80.°4	118.°2	134.°1	0.99	0.26 au	46 au	320 yr
Jenniskens (2006)						
84.°4	124.°0	124.°9		0.224 au	12.3 au	

Very little is known about this shower which is listed in many shower compilations, but no systematic investigation of it has yet taken place. With an activity period which almost entirely coincides with that of the Geminids and a radiant close to the celestial equator (Figure 2.69), this shower offers excellent possibilities for all observers. The radiant rises over the course of the night. Only observations after midnight will yield useful σ-Hydrid data. This may be an additional reason for the low number of σ-Hydrids in the data samples. Our analysis of data collected over 20 years (Figure 2.70) yields ZHRs below 3, although at a few occasions higher ZHRs have been found. The Hydrid maximum occurs before the Geminid peak, and the analysis shows no increase of the Hydrid rates at the Geminid peak position. This indicates that there is little or no pollution from the major shower.

There are no reliable reports of this shower in the distant past. Some radiants mentioned in 19th century lists may refer to this shower, and Hoffmeister (1948; appendix I) lists five 'convergences' found during his observations in Southwest Africa in 1937. However, the first clear indication came only when McCrosky & Posen (1961) published orbital elements from photographic surveys. The shower is present in photographic orbital data (Lindblad, 1971), and it can also be found from fireball data (Porubčan & Gavajdová, 1994) as well as in investigations using video systems (Ueda & Fujiwara, 1995; Molau, 2007).

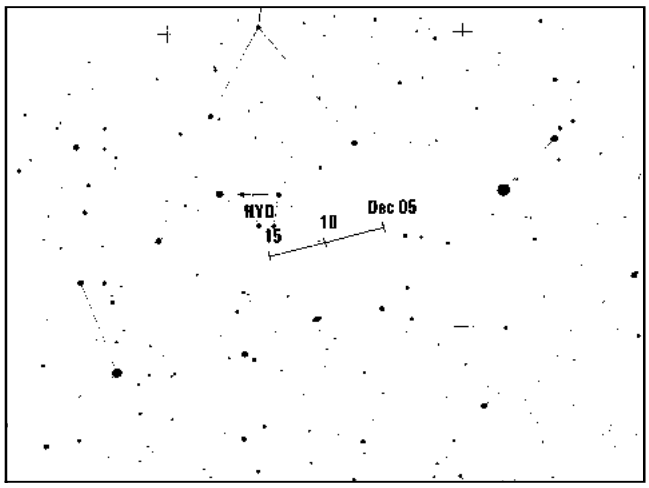


Figure 2.69: Radiant drift of the σ-Hydrids. The higher velocity helps to distinguish the σ-Hydrids from the slower Geminid and the Monocerotid meteors (see Figure 2.68).

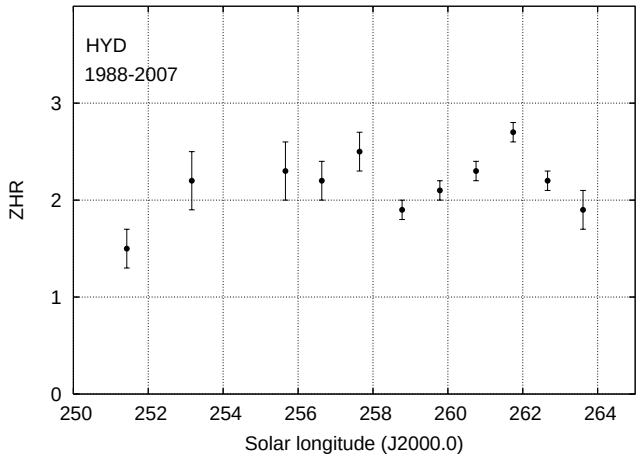


Figure 2.70: Activity of the σ-Hydrids from visual observations stored in the VMDB covering the period 1988-2007 using a constant $r = 3.0$ over the activity period. The zenith correction included the standard sine term (no zenith coefficient $\gamma > 1.0$) and allowed only intervals with a radiant elevation of $\geq 20°$.

References

Hoffmeister C., 1948: Die Meteorströme. J.A.Barth, Leipzig.

Jenniskens P., 2006: Meteor showers and their parent comets. Cambridge Univ. Press.

Lindblad B.A., 1971a: A stream search mong 865 precise photographic meteor orbits. *Smithson. Contr. Astrophys.*, No. 12, 1–13.

Lindblad B.A., 1971b: A computerized stream search among 2401 photographic orbits. *Smithson. Contr. Astrophys.*, No. 12, 14–24.

McCrosky R.E., Posen A., 1961: Orbital elements of photographic meteors. *Smithson. Contr. Astrophys.* **4,** 15–84.

Molau S., 2007: How good is the IMO working list of meteor showers? A complete analysis of the IMO video meteor database. In: *F.Bettonvil and J.Kac (eds.): Proc. IMC 2006, Roden,* IMO, pp.38–54

Porubčan V., Gavajdová M., 1994: A search for fireball streams among photographic meteors. *Planet. Space Sci.* **42,** 151–155.

Ueda M., Fujiwara Y., 1995: Television meteor radiant mapping. *EMP* **68,** 585–603.

2.31 Geminids (004 GEM)

2.31.1 Synopsis

Period	December 7–17
Maximum	$\lambda_\odot = 262\,^\circ\!.2$ ($\approx$ December 13)
Radiant	$\alpha = 112^\circ$ $\delta = 33^\circ$
$\mathrm{ZHR_{max}} = 120$	$r = 2.6$ $V_\infty = 34.6$ km/s
Parent body	(3200) Phaethon

Orbital elements of the stream and (3200) Phaethon

Ω	ω	i	e	q	a	P
Jenniskens 2006; DMS, photographic						
$261\,^\circ\!.49$	$324\,^\circ\!.42$	$24\,^\circ\!.02$		0.141 au	1.372 au	
Jenniskens 2006; radar						
$259\,^\circ\!.2$	$324\,^\circ\!.9$	$23\,^\circ\!.9$		0.141 au	1.376 au	
(3200) Phaethon						
$265\,^\circ\!.394$		$22\,^\circ\!.19$	0.890	0.140 au	1.271 au	

The position of the radiant (Figure 2.68) allows observations essentially during the entire night in mid-northern latitudes with low elevations only in the early evening. The high hourly rates, the shower's richness in bright meteors and the fact that this major shower is still poorly observed should motivate visual observers and photographers to defy the cold December nights.

For most major showers, there are detailed reports of rich appearances which occurred many centuries ago. Yet the Geminids were not noticed before the 19th century. The first indications of the Geminid meteor shower were published by Quételet (1841, 1861), who mentioned high meteor activity on 1830 December 12–13 at Heiligenstadt (Germany), from where 40 fireballs were reported. No details such as radiant positions, hourly rates, etc., are available from these early observations, and in fact, only the dates suggest that these are early observations of Geminid activity at all. Most authors cite Greg (1872) as the 'discoverer' of the Geminids in 1862. From 1862 onwards, Denning mentions the Geminid radiant in successive years. Rates were not very high, but the radiant was easily detectable.

The first observer to watch the Geminids carefully was Dole from Massachusetts, USA, in 1901, 1908 and 1910. Dole (1911) wrote: *Next to the Perseid shower in August, the Geminids seem to be the most consistent meteor shower.* The main reason for the lack of reports on the shower's *intensity* is that all the leading meteor workers of the period were interested in visual radiant studies only.

2.31.2 Research

Recent activity

Visual observations collected over 60 years (1944–2003) show that the rate profiles and values of the population index r near the activity peak are rather constant over the entire period (Figure 2.71). The peak activity is characterized by a plateau in the profile with a ZHR between 120 and 130 lasting for about 12 hours between

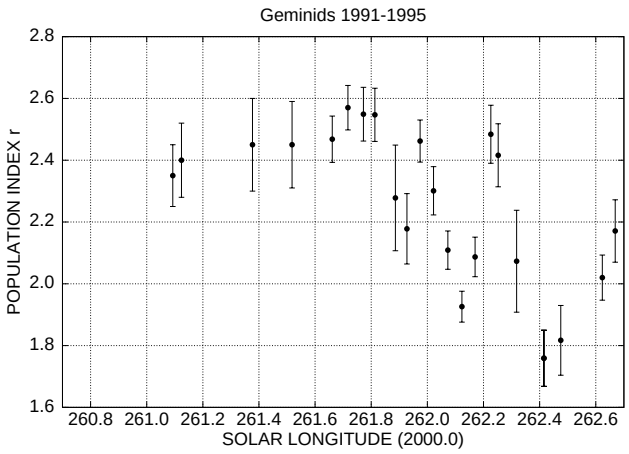


Figure 2.71: Average r-profile from the moonless Geminid returns 1991–2001 (Rendtel, 2005).

$\lambda_\odot = 261\,^\circ\!.5 \pm 0\,^\circ\!.15$ and $262\,^\circ\!.4 \pm 0\,^\circ\!.05$ (Rendtel, 2005). A double peak as seen in Figures 2.72 and 2.73 is expected from Jones' work (1982) as well as from Ryabova (2001). The ZHR profiles of 1991 and 1993 show some fine structure. Similar variations of about 10% of the ZHR can be found in other profiles (Rendtel, 2005). Because of the Geminid's short periodic orbit, no low-order resonances are to be expected. Possible reasons for such structures can be planetary perturbations or remains of particle ejections at different revolutions of the parent. More probably, different ejection trails are subsequently disturbed by the planets and cause the Earth to cross the structures at different positions.

Modelling the Geminids is very hard to model (Vaubaillon, 2013: `http://www.imcce.fr/en/ephemerides/phenomenes/meteor/predictions.php`). Considering the past orbit of 3200 Phaethon the main activity does not appear but an activity extending well behind the maximum period. Hence observers should carefully consider also the post-maximum period for systematic observations. Analyses of visual data concerning the late part of the peak profile show some interesting features, too (Rendtel, 2005). Observers are asked for observations covering the entire activity period to collect suitable data to check with the models.

Peculiarities of the stream

The orbit of the Geminids is unusual among the known major showers with its very small perihelion distance ($q = 0.14$ au), its high eccentricity of $e = 0.89$ and its short orbital period $P = 1.43$ yr which have caused problems for the classification of the shower.

The general appearance and behaviour of the Geminid meteors is peculiar: unlike meteors of other showers, their beginning heights do not increase with the meteoroid mass (Koten et al., 2004). The average luminous end heights of Geminid meteors are well below 80 km (e.g., Betlem et al., 1994b). The bulk density is about $3\,\mathrm{g\,cm^{-3}}$ (Ceplecha & McCrosky, 1992; Babadzhanov, 2002). The Geminid meteoroids are severely depleted in Na and also in other volatiles (Borovička, 2006). At

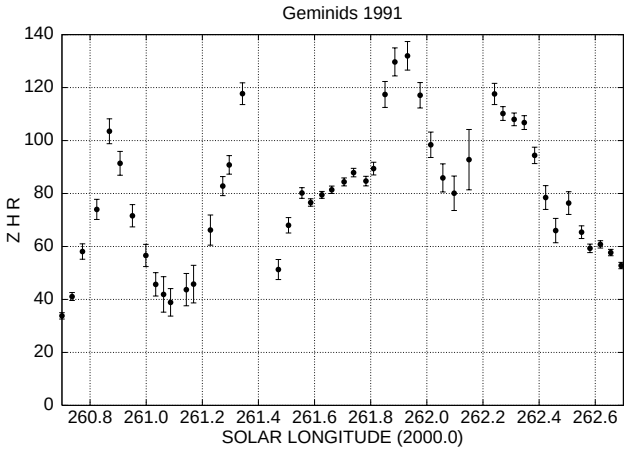


Figure 2.72: ZHR profile of the 1991 Geminids (Rendtel, 2005).

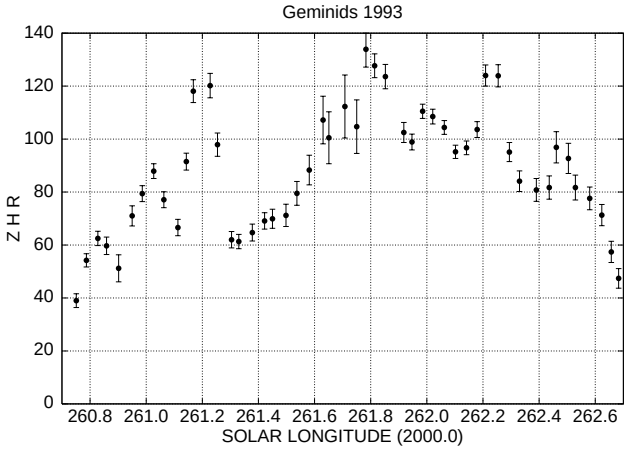


Figure 2.73: ZHR profile of the 1993 Geminids (Rendtel, 2005).

the low perihelion distance of 0.14 au, the meteoroids are heated by solar radiation to about 700 K. Borovička et al. (2005) found that all small meteoroids with perihelia of less than 0.2 au are completely depleted in Na and compacted. Elsewhere in the stream, the Na depletion is not complete and varies from one meteoroid to another (Borovička, 2006). This suggests that the meteoroids are of various ages or originate from various depths inside Phaethon. Borovička argues in the same paper that the high strength is not an evidence of their asteroidal origin. The Fe/Mg ratio is similar to Halley type cometary material and suggests cometary origin of the Geminids, Phaethon and other members of this complex. The material strength of the meteoroids is also obvious from a bright Geminid which probably dropped a meteorite (reported by Borovička during the *Meteoroids 2013*).

Parent object

Little is known about the asteroid (3200) Phaethon. Although it moves on an orbit with an aphelion slightly outside the Earth's orbit, there are long periods during which the asteroid hardly gets brighter than magnitude +18. Phaethon could be the degassed nucleus of a comet. This is supported by observations of another Apollo asteroid, 1999 YC, reported recently (Kasuga & Jewitt, 2008). 1999 YC perhaps shares a dynamical association with the *Phaethon-Geminid stream complex* (Ohtsuka et al., 2006) which also includes 155140 (2005 UD). Kasuga and Jewitt found that the total mass loss of 1999 YC is very low (of the order of 10^7 kg), while the assumed Geminid stream mass is about $10^{12} - 10^{13}$ kg. Therefore, Kasuga and Jewitt suggest that the stream may be the product of a catastrophic rather than a steady breakup of the parent object. Ohtsuka et al. (2006) argue that 155140 (2005 UD) may be a split nucleus of Phaethon. The (Daytime) Sextantid shower seems to be more closely associated with 155140 (2005 UD) than 3200 (Phaethon).

Modelling of the stream

Ryabova (2001) showed from mathematical modelling of the stream evolution that particles ejected before and after perihelion passage of the parent body form two branches of evolution. The meteoroids form two sheets in space crossing each other like sissors. Such an evolution may explain the double peak structure of the activity curves of the Geminids. Ryabova (2001) compiled radar and visual peak timing covering meteoroid masses from less than 10^{-5} g to almost 0.1 g. The splitting between acivity maxima is as large as 6° in solar longitude for the smallest particles and diminishes to 0.°3 for the largest meteoroids.

The model by Ryabova (2004) provides flux density profiles and mass index profiles at various cross-sections through the stream. Visual and radar observations may give the necessary calibration of the model in order to give it predictive power. The theoretical stream structure is shown in Figure 2.74.

Another attempt was published by Ryabova (2007). Several authors have summarized that "modelling the Geminids is very hard". A conclusive report was given by Ryabova (2014). Model calculations of Vaubaillon (see IMCCE website) are based on the past orbit of (3200) Phaethon. Obviously this does not reproduce the observed main activity but a possible later peak. Analyses of the Geminid profile over decades also indicate peculiarities at the end of the high activity plateau (Rendtel, 2005). Both may be weak indications for activity extending behind the maximum period. Hence we want to encourage observers to continue observations over this late section of the Geminids. With a suitable data set we may be able to check the models.

References

Babadzhanov P.B., 2002: Fragmentation and densities of meteoroids. *A & A* **384,** 317–321.

Betlem H., ter Kuile C., van't Leven J., van Vliet M., 1994a: Geminiden 1990: Fotografische resultaten (1) Baanelementen. *Radiant* **16,** 33–38.

Betlem H., ter Kuile C., van't Leven J., van Vliet M., 1994b: Geminiden 1990: Fotografische resultaten (2) Trajekten en radiantposities. *Radiant* **16,** 57–62.

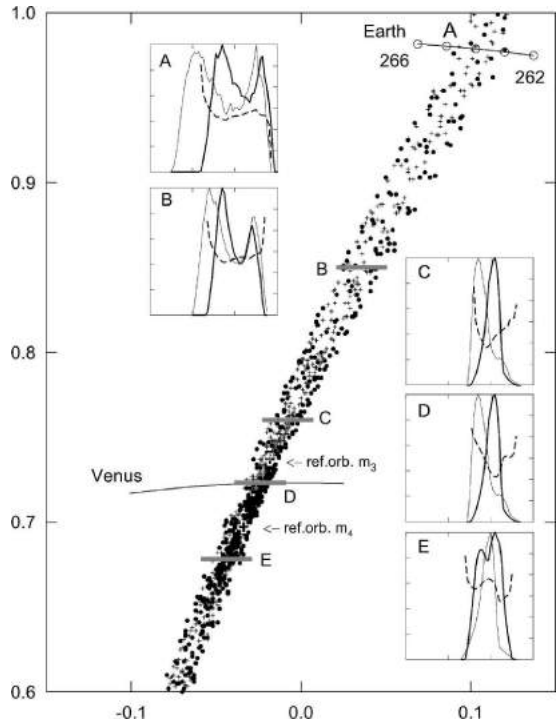


Figure 2.74: Possible cross-sections through the Geminid meteoroid stream according to a model by Ryabova (2004).

Borovička J., 2006: Properties of meteoroids from different classes of parent bodies. In *A. Milani, G.B. Valsecchi, D. Vokrouhlický (eds.): Near Earth Objects, our Celestial Neighbors: Opportunity and risk,* A survey of meteor spectra and orbits: evidence for three populations of Na-free meteoroids. IAU Symp. No. 236, IAU. 107–120

Borovička J., Koten P., Spurný P., Boček J., Štork R., 2005: A survey of meteor spectra and orbits: evidence for three populations of Na-free meteoroids. *Icarus* **174,** 15-30.

Ceplecha Z., McCrosky R.E., 1992: Gross-fragmentation of meteoroids and bulk density of Geminids from photographic fireball records. In: *A.W. Harris, E. Bowell (eds.): Asteroids, Comets, Meteors 1991,* Houston, LPI, 109.

Dole R.M., 1911: The Geminids Dec. 12, 1910. *Popular Astron.* **19,** 119.

Greg R.P., 1872: A general comparative table of radiant positions and duration of meteor showers. *MNRAS* **32,** 345–355.

Jenniskens P., 2006: Meteor showers and their parent comets. Cambridge Univ. Press.

Jones J., 1982: The annual variation in the activity of the Geminid shower and the theory of the dispersal of meteoroid clusters. *MNRAS* **198,** 23–32.

Kashcheyev B.L., Lebedinets V.N., 1967: Radar studies of meteors. *Simthson. Contr. Astrophys.* **11,** 183–199.

Kasuga T., Jewitt D., 2008: Observation of 1999 YC and the breakup of the Geminid stream parent. *Astron. J.* **arXiv:0805.2636v1,** astro-ph 17 May 2008.

Koten P., Borovička J., Spurný P., Betlem H., Evans S., 2004: Atmospheric trajectories and light curves of shower meteors. *A & A* **428,** 683–690.

Ohtsuka K., Sekiguchi T., Kinoshita D., Watanabe J.-I., Ito T., Arakida H., Kasuga T., 2006: Apollo asteroid 2005 UD: split nucleus of (3200) Phaethon?. *A & A* **450,** L25–L28.

Quételet A., 1841: Nouveau catalogue des principales apparitions d'étoiles filantes. Acad. Royale de Bruxelles.

Quételet A., 1861: Sur la physique du globe, des étoiles filantes, aperçu historique. Chap. IV, Sur la physique di globe. 266–322.

Rendtel J., 2005: Evolution of the Geminids observed over 60 years. *EMP* **95,** 27–32.

Ryabova, G.O., 2001: Mathematical model of the Geminid meteor stream formation. In: Proc. Meteoroids 2001 Conf., ESA SP-495, 77–81.

Ryabova, G.O., 2004: The Geminid meteoroid stream: a new model. In: *M. Triglav-Čekada, C. Trayner (eds.), Proc. Int. Meteor Conf. 2003,* IMO, 131–135.

Ryabova, G.O., 2007: Mathematical modelling of the Geminid meteoroid stream. *MNRAS* **375,** 1371–1380.

Ryabova, G.O., 2014: The Geminid stream modelling: lessons of history, in: P. Roggemans (ed.), Proc. Int. Meteor Conf. 2013, IMO, submitted.

2.32 December Leonis Minorids (032 DLM)

2.32.1 Synopsis

Period	December 5 – February 4	
Maximum	$\lambda_\odot = 268°$	($\approx$ December 20)
Radiant	$\alpha = 161°$	$\delta = 30°$
$ZHR_{max} = 5$	$r = 3.0$	$V_\infty = 64$ km/s
Parent body	unknown	

Meteor shower compilations listed the Comae Berenicids as a minor source in December. Observational data showed that there is another radiant producing slightly higher rates over a longer period.

2.32.2 Research

A recent analysis (Molau & Rendtel, 2009) yielded the December Leonis Minorids (DLM) as the shower responsible for this activity (Figure 2.32.2), although the rates of this high-inclination shower are also very low. However, due to the generally low rates especially in January, activity from the DLM radiant can be detected until early-February. A parent object is not known.

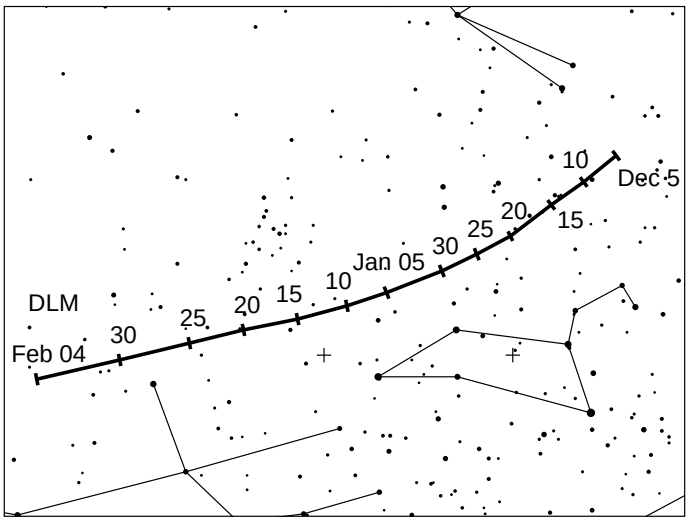


Figure 3.75: Radiant drift of the December Leonis Minorids as determined from video data.

References

Molau S., Rendtel J., 2009: A comprehensive list of meteor showers obtained from 10 years of observations with the IMO Video Meteor Network. *WGN* **37,** 98–121.

2.33 Comae Berenicids (020 COM)

2.33.1 Synopsis

Period	December 12–December 23
Maximum	$\lambda_\odot = 264°$ ($\approx$ December 16)
Radiant	$\alpha = 175°$ $\delta = 18°$
$ZHR_{max} = 5$	$r = 3.0$ $V_\infty = 64$ km/s
Parent body	unknown

Orbital elements of the stream

Ω	ω	i	e	q	a	P
Lindblad 1987, photographic						
283.°1	262.°2	136.°0	0.961	0.560 au	14.6 au	55 yr

Rates are very low and inferior to the December Leonis Minorids (DLM) described above, usually 1 or 2 per hour, and some care must also be taken in order to not associate fast sporadic meteors from the Apex Source as Comae Berenicids with their radiant east of the DLM (Figure 2.76. The drift and position shown here are derived from video data (Molau & Rendtel, 2009).

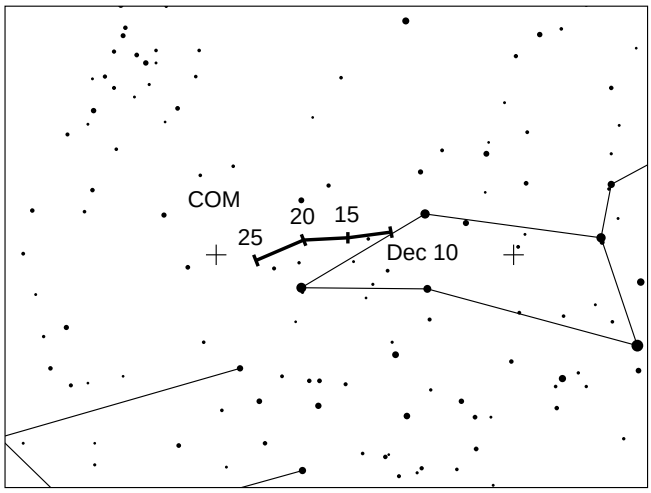


Figure 2.76: Radiant drift of the Comae Berenicids as determined from video data.

2.33.2 Research

This shower has not been associated successfully with a parent object. Whipple (1954) found a coincidence between a meteoroid orbit (meteor 1918 photographed on 1950 January 20) and the Comet Lowe (1913 I). Although there were some attempts to calculate an orbit of the Comet (Viljev, 1913a, 1913b), this must be regarded as a mere speculation. The Comet was seen by B. Lowe of Laura, Australia, on 1912 December 31, and four further days until 1913 January 9. He did not announce his discovery and observations until January 7, and a search at Adelaide on January 8 as well as further searches failed to locate the Comet. The positions reported by Lowe were so rough that the path of it could not be determined with any certainty (Dodwell, 1913).

Despite this, Whipple (1954) still hoped that 'if future meteor observations confirm the association, we may learn more about the orbit of Comet Lowe by meteor studies than we can glean from direct observations'. The comet is not included in the catalogue of cometary orbits (Marsden & Williams, 1995 and subsequent editions).

References

Dodwell G.J., 1913: Komet 1912d (Lowe). *Astron. Nachr.* **194,** 29–32.

Lindblad B.A., 1987: Physics and orbits of meteoroids. In *The evolution of the small bodies of the Solar System.* Soc. Italiana di Fisica, Bologna.

Marsden B.G., Williams G.V., 1995: Catalogue of cometary orbits (10th ed.) Minor Planet Center. Cambridge, Massachusetts.

Molau S., Rendtel J., 2009: A comprehensive list of meteor showers obtained from 10 years of observations with the IMO Video Meteor Network. *WGN* **37,** 98–121.

Viljev M., 1913a: Comet notes. *The Observatory* **36,** 313.

Viljev M., 1913b: Comet notes. *The Observatory* **36,** 347–348.

Whipple F.L., 1954: Photographic meteor orbits and their distribution in space. *AJ* **59,** 201–217.

2.34 Ursids (015 URS)

2.34.1 Synopsis

Period	December 17–26	
Maximum	$\lambda_\odot = 270\,\overset{\circ}{.}7$ ($\approx$ December 22)	
Radiant	$\alpha = 217°$	$\delta = +76°$
$ZHR_{max} = 10$	$r = 3.0$	$V_\infty = 33$ km/s
Parent body	8P/Tuttle	

Orbital elements of the stream and 8P/Tuttle

Ω	ω	i	e	q	a	P
Lindblad 1987, photographic						
$270\,\overset{\circ}{.}66$	$207\,\overset{\circ}{.}5$	$52\,\overset{\circ}{.}6$	0.836	0.958 au	5.8 au	14 yr
8P/Tuttle						
$270\,\overset{\circ}{.}5$	$206\,\overset{\circ}{.}7$	$54\,\overset{\circ}{.}7$	0.824	0.998 au	5.6 au	13.5 yr

This radiant (Figure 2.77) is circumpolar for observers at mid-northern latitudes. While the Ursids can be observed all night, their radiant reaches somewhat higher altitudes after midnight. On average, an observer may expect about 10 Ursids per hour close to the maximum. The Ursids have produced short bursts of higher activity at several occasions and will continue to do so (Table 2.10). Most outbursts occurred when the Comet was away from its perihelion.

In 1945, on December 22 at 16^h30^m UT, Slovakian observers at the Skalnaté Pleso observatory reported unexpected meteor activity. Bečvář (1948) computed a ZHR of 170 and a radiant at $\alpha = 233° \pm 1°$, $\delta = 82\,\overset{\circ}{.}6 \pm 0\,\overset{\circ}{.}9$.

This surprisingly high ZHR has been quoted in most reports for this event, but Ceplecha (1951) recomputed the rates and found a ZHR of the order of 50. Slovak observers watched for the Ursids again in 1946 when rates were at a very minor level, with the radiant at $\alpha = 217° \pm 0\,\overset{\circ}{.}8$, $\delta = 76\,\overset{\circ}{.}7 \pm 1\,\overset{\circ}{.}0$. In the next few years, maximum rates were observed to be inferior to 15.

The 1981 return of the Ursids also gave higher ZHRs than ususal (see Table 2.10). The maximum occurred on 1981 December 22 at $\lambda_\odot = 270\,\overset{\circ}{.}82$ (Ohtsuka, 1995). Another unusual peak in Ursid rates occurred around 20^h UT on 1986 December 22 (Roggemans, 1987). The ZHRs exceeded 50, but unfavourable observing conditions may have led to overestimating rates. Some details of this event are discussed by Jenniskens (1995). As in the case of the 1945 Ursid activity outburst, 8P/Tuttle was much closer to its *aphelion* than to the perihelion position. This outburst happened exactly three revolutions after the 1945 event.

Another observation of enhanced rates has been reported for the 1994 return (Ohtsuka et al., 1995). The highest ZHRs occurred around 1994 December 22, 18^h10^m UT ($\lambda_\odot = 270\,\overset{\circ}{.}75$). Rates well above the average have also been reported in 2000 (ZHR = 90) on December 22, 08^h06^mUT $\pm 7^m$(Jenniskens & Lyytinen, 2001; Jenniskens, 2001), in 2004 (ZHR = 48) and in 2007 (ZHR = 34) on December 22, 21^h16^mUT (IMO web page). The 2007 event was badly affected by moonlight. Video data do not show a great difference between the 2006 and 2007 numbers (Molau, 2008).

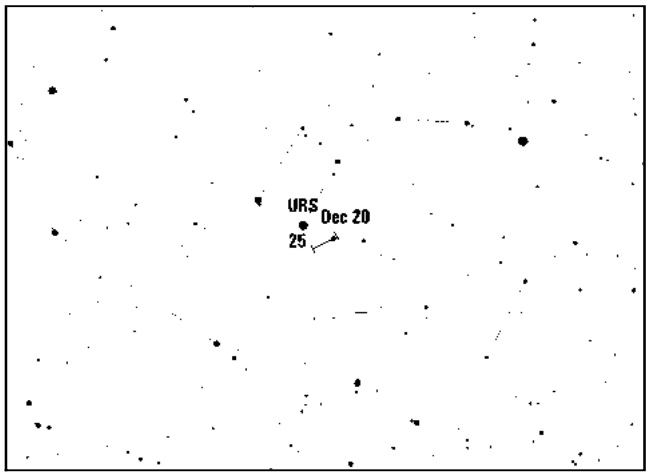


Figure 2.77: Radiant drift of the Ursids.

The 1945 outburst was caused by a dust trail from 1392, and the 1986 outburst is an encounter with the 1378 dust trail (Jenniskens et al., 2002). Encounters with dust trails of 1405 and 1392 caused the well-observed outburst in 2000.

2.34.2 Research

Comet 8P/Tuttle has a 13.6-year orbit, passing just outside the Earth's orbit. Meteoroids may become trapped in the 6:7 mean motion resonance with Jupiter, while the Comet librates around the 13:15 resonance which yields a slightly shorter period (Jenniskens et al., 2002). Over about six centuries, the perihelia of the meteoroid orbits decrease until they intersect the Earth's orbit. In the same time the meteoroids separate in mean anomaly by 6 years from the Comet (Jenniskens et al., 2007). Hence, the outbursts occur about 6 years after the Comet's perihelion passage.

Other activity enhancements also occurred when the comet was close to its perihelion. This was observed in 1980 as well as 1993 and 1994 (Jenniskens, 2006). The reason for these near-comet outbursts is not yet clear (Jenniskens et al., 2007).

Modelling of the stream evolution by Lyytinen (1999 model) and by Vaubaillon (2005 model) yield slightly different results (for details, refer to Jenniskens et al., 2007). Table 2.10 summarizes the information given in that paper. Observations of the 2008 and future returns may not only provide further insight in the stream, but also in the conditions of dust ejection of the parent comet 8P/Tuttle.

References

Bečvář A., 1948: Activity of great meteoric swarms 1946-1947. *BAC* **1,** 34–36.

Ceplecha Z., 1951: Ursids – Bečvář's meteor stream. *BAC* **2,** 156–160.

Jenniskens P., 2001: 2000 Ursid outburst confirmed. *WGN* **29,** 41–45.

Jenniskens P., Lyytinen E., 2001: Dynamical models of meteoroid streams in relation to recent and upcom-

Table 2.10: Calculated circumstances for the encounter with dust trails of 8P/Tuttle ejected AD 307–788 with minimum distances < 0.0015au to the Earth's orbit (model by Lyytinen) and AD 700–900 dust trails with minimum distances < 0.002au (model by Vaubaillon) published by Jenniskens et al. (2007).

	Lyytinen model					Vaubaillon model				
Year AD	$\lambda_\odot$ (J2000)	Day Dec.	Time (UT)	ZHR 413–788	ZHR 307–788	$\lambda_\odot$ (J2000)	Day Dec.	Time (UT)	ZHR calc.	ZHR obs.
1980	270.°90	22	07^h40^m	111	156	270.°80	22	05^h24^m	25	–
1981	270.°90	22	13^h53^m	17	39	270.°80	22	11^h36^m	23	55 ± 25
1982	270.°90	22	20^h00^m	26	23	270.°94	22	20^h54^m	58	> 35
1983	270.°95	23	03^h24^m	8	32	270.°77	22	23^h14^m	14	–
1993	270.°96	22	17^h03^m	78	95	270.°91	22	15^h52^m	40	100 ± 10
1994	270.°75	22	18^h21^m	67	62	270.°56	22	13^h48^m	70	50 ± 6
1995	270.°60	22	21^h01^m	31	20	270.°62	22	21^h28^m	14	–
1996	270.°70	22	05^h29^m	153	92	270.°54	22	01^h44^m	22	25 ± 5
1997	270.°60	22	09^h26^m	18	35	270.°48	22	06^h33^m	13	16 ± 4
1998	270.°65	22	16^h44^m	1	18	270.°79	22	19^h54^m	14	13 ± 3
1999						270.°44	22	17^h54^m	14	–
2004	270.°90	22	11^h24^m	40	18					48 ± 6
2005	270.°63	22	11^h16^m	3	1					21 ± 6
2006	270.°70	22	10^h03^m	12	15					15 ± 5
2007	270.°57	22	22^h08^m	63	40					34 ± 5 (1)
2008	270.°60	22	05^h07^m	23	30	270.°48	22	02^h18^m	20	
2009						270.°43	22	07^h14^m	14	
2010						270.°42	22	13^h02^m	23	
2011						270.°29	22	16^h11^m	12	
2012						270.°49	22	03^h01^m	15	

(1) 21^h16^m – preliminary result

ing Leonid and Ursid showers. *Bull. Amer. Astron. Soc.* **33,** 1188.

Jenniskens P., Lyytinen E., deLignie M.C., Johannink C., Jobse K., Schievink R., Langbroek M., Koop M., Gural P., Wilson M.A., Yrjölä I., Suzuki K., Ogawa H., deGroote P., 2002: Dust trails of 8P/Tuttle and the unusual outbursts of the Ursid shower. *Icarus* **159,** 197–209.

Jenniskens P., Lyytinen E., Nissinen M., Yrjölä I., Vaubaillon J., 2007: Strong Ursid shower predicted for 2007 December 22. *WGN* **35,** 125–133.

Jenniskens P., 1995: Meteor stream activity. II.Meteor outbursts. *A & A* **295,** 206–235.

Lindblad B.A., 1987: Physics and orbits of meteoroids. In *The evolution of the small bodies of the Solar System.* Soc. Italiana di Fisica, Bologna.

Molau S., 2008: personal communication

Ohtsuka K., Shioi H., Hidaka E., 1995: Enhanced activity of the 1994 Ursids from Japan. *WGN* **23,** 69–72.

Roggemans P., 1987: Again on the Ursids. *WGN* **15,** 25–26.

Chapter 3

Daytime showers

3.1 Observing possibilities

Meteoroids can collide with the Earth potentially from all directions, and the shower radiants are widely distributed over the sky. The majority of the known radiants described in the previous Chapter are best visible after local midnight. Further, there are a few evening showers such as the π-Puppids, the Draconids and the Puppid-Velids. Studies of radar and radio data show also radiants close to the Sun's position. Among these are the Helion Source of the sporadic meteor background (see Section 1.4 in the *Handbook for Meteor Observers*) as well as a number of showers which orbit the Sun in a way that their radiant is above the horizon only during daytime. Hence meteors of these showers are not observable by optical means from the Earth's surface. The radiants remain very low in the sky even in twilight so that systematic data can only be collected by radio and radar techniques. Our current knowledge of the daytime showers is not as detailed as for most of the nighttime showers described in the Chapter 2. Recent research provided data on the mass index s of some radar showers as well (Blaauw et al., 2011).

Some daytime showers are closely related to known (nighttime) showers:
One example are the ζ-Perseids (172 ZPE) and the β-Taurids (173 BTA) which both belong to the **Taurid complex** described in detail on page 51 and illustrated in Figures 2.48–2.51.
Further, the Sextantids (221 DSX) are part of the **Phaethon-Geminid complex** (Ohtsuka et al., 2006)
Another complex is formed by the comet **96P/Machholz 1** and the minor planet **(196 256) 2003 EH**$_1$. The related shower complex includes four well-known meteor showers (Daytime Arietids (171 ARI), Southern δ-Aquariids (005 SDA), Quadrantids (010 QUA), and the Northern δ-Aquariids (026 NDA). The stream filaments corresponding to the 171 ARI and two Aquariids (005 SDA, 026 NDA) constitute the ecliptical component, and those corresponding to the 010 QUA and their southern counterpart constitute the toroidal component of the complex (Neslušan, Kaňuchová & Tomko, 2013; Neslušan, Hajduková & Jakubík, 2013). This is also discussed in the Quadrantid section on page 14.
Modelled meteor showers of a group of six near-Earth asteroids with related orbits were found to be identical. They could be recognized as two nighttime showers in the antihelion radiant area (χ- and δ-Scorpiids) and two daytime showers (β- and σ-Librids). Babadzhanov, Williams & Kokhirova (2013) assume that this complex is a result of the fragmentation of an unknown comet several millennia ago. A similar complex of Earth crossing minor planets (2008 BO$_{16}$, 2011 EC$_{41}$ and 2013 CT$_{36}$) and four theoretical showers has been analysed by Babadzhanov et al. (2014). The four radiants – two nighttime and two daytime – should be in Capricornus (among them the Sagittariids/Capricornids, 115 DSC). Two further objects (2101) Adonis and 1995 CS are assumed to be related with the (nighttime) Capricornids. The authors suggest that all five objects may be fragments of a former large comet.

Daytime shower activity has been observed regularly, but most of the recorded data still await detailed analysis to obtain comparable results to the optical range with rate, flux and population index profiles. McBeath (1998) developed a largely non-mathematical and certainly limited model for radio forward scatter data analyses, from which a part of the estimates of activity period and level are derived. Sugimoto developed an analysing method originally for the now defunct Japanese International Project for Radio Meteor Observation (IPRMO) project. It was applied to meteor shower data between 2001 and the Quadrantids 2004, particularly for the Leonids (Ogawa et al., 2002). The idea was continued for a later Quadrantid data analysis by Brower (2006), and a method to determine shower activity was further updated by Steyaert et al. (2006).

Nevertheless there is a need not only for monitoring of **daytime showers** but a stronger need to regularly analyse the data to determine their activity level, activity period and moment of maximal activity. This is a pity because forward scatter detects substantially more meteors than visual or video observations. If only overdense reflections are taken into consideration then the recorded numbers tend to resemble those obtained by visual and video observers.

But as in the case of the nighttime showers, monitoring is useful to detect peculiarities in the streams and to follow the evolution of the streams, particularly as forward scatter radio observations cover a meteoroid mass range which is close to the optical (visual) region while the majority of meteors recorded by backscatter radars are much smaller and thus deviate in several aspects (mass index, flux).

The most active (northern summer) daytime shower

interval, May to early July, is also part of that in which observers often struggle because of interference, especially Sporadic-E (Es; the worst of the Es "season" commonly runs from May to September). The two may be connected, given the ion sheets forming Es must originate somewhere, and Es sheets generally form in the lower meteor-ablation zone. Changing radio frequencies, or recording from more than one frequency, can sometimes help overcome this, but of course this is heavily dependent on suitable broadcast signals being available to observers in different geographic regions.

As there seems no statistical peak in especially bright fireball occurrence during daylight, or in the near-dusk and near-dawn periods, during the strongest daytime showers in June and late September–early October, this could be taken, in conjunction with the nature of the showers as recorded by radio **(not radar)**, to imply a fairly typical "shower" magnitude/particle size distribution in the ARI, ZPE and DSX showers. We have also previously alerted observers via the Shower Calendar to possible northern summer daytime fireballs during the potential Taurid "swarm" returns, though it seems there were no records of such made. Perhaps a simple analysis of one of the larger fireball databases, that of the AMS maybe, might be worth conducting at some stage to provide evidence in support of (the lack of?) such daylight/crepuscular fireballs.

3.2 List of daytime showers

In addition to the list provided in Table 3.1, we add information based on recent radio meteor observations and recommendations for observers. The short descriptions summarize the avilable information and add some specific hints. Although it is clear that radar and (forward scatter) radio systems look at different meteoroid populations, we use both information. The orbital data are based on the CMOR radar analysis paper, considering the mean values in Table 6 of (Brown et al., 2008).

In the second half of May and throughout June, most of the annual meteor action appears from the daylight sky. Occasional meteors from the **ω-Cetids (293 DCE)** and the **Arietids (171 ARI)** have been claimed as seen from tropical and southern hemisphere sites visually. However, such data do not allow us to derive parameters such as ZHR or flux. Further, the general information is scarce particularly regarding the radiant positions.

After the peak period in June daylight sources include the visually-impossible **γ-Leonids (203 GLE**; Sekanina, 1976). Later there is a tricky visual shower, the **Sextantids (221 DSX)**. Optical observers may hope to catch some Sextantids in the pre-dawn of late September, though radiant-rise is less than an hour before sunrise in either hemisphere. So the majority of observational data is expected from radio and radar equipment.

It is quite obvious that a lot of information is missing. All observers can contribute to our knowledge about this rather invisible portion of meteor showers.

Table 3.1: Working List of Daytime Radio Meteor Showers. The showers' designations are listed here omitting 'Daytime'. The 'Best Observed' columns give the approximate local mean times between which Steyaert's Observability Function (Steyaert et al., 2006) for a 4 element Yagi antenna at an elevation of 45 degrees and pointed towards the azimuth of a 30 kW transmitter with isotropical gain 1000 km away reaches 85% or more of its daily maximum for that stream. Note that this is often heavily dependent on the compass direction in which the antenna is pointing, however, and applies only to dates near the shower's maximum. More details of the observation and the Observability Function including consequences for the data analysis are discussed in Chapter 6 of the IMO's *Handbook for Meteor Observers.*

Shower	Activity	Max Date	$\lambda_\odot$ 2000	Radiant α	Radiant δ	Best observed 50° N	Best observed 35° S	Rate
Sgr/Capricornids (115 DSC)	Jan 13–Feb 04	Feb 01	312.5	299°	−15°	11^h–14^h	09^h–14^h	Medium
χ-Capricornids (114 DXC)	Jan 29–Feb 28	Feb 13	324.7	315°	−24°	10^h–13^h	08^h–15^h	Low
April Piscids (144 APS)	Apr 20–Apr 26	Apr 22	32.5	9°	+11°	07^h–14^h	08^h–13^h	Low
ε-Arietids (154 DEA)	Apr 24–May 27	May 09	48.7	44°	+21°	08^h–15^h	10^h–14^h	Low
May Arietids (294 DMA)	May 04–Jun 06	May 16	55.5	37°	+18°	08^h–15^h	09^h–13^h	Low
S. May Arietids (156 SMA)	Apr 20–May 22	May 08	47.5	29°	+10°	08^h–15^h	09^h–13^h	Low
o-Cetids (293 DCE)	May 05–Jun 02	May 20	59.3	28°	−04°	07^h–13^h	07^h–13^h	Low
N. ω-Cetids (152 NOC)	Apr 20–May 20	May 08	47.5	9°	+19°	07^h–13^h	07^h–13^h	Low
S. ω-Cetids (153 OCE)	Apr 24–May 20	May 10	49.5	23°	−03°	07^h–13^h	07^h–13^h	Low
Arietids (171 ARI)	May 14–Jun 24	Jun 07	76.5	42°	+25°	06^h–14^h	08^h–12^h	High
ζ-Perseids (172 ZPE)	May 07–Jun 26	Jun 14	83.5	65°	+28°	07^h–15^h	09^h–13^h	Low
β-Taurids (173 BTA)	Jun 12–Jul 04	Jun 28	96.5	85°	+23°	08^h–15^h	09^h–13^h	Low
γ-Leonids (203 GLE)	Aug 14–Sep 12	Aug 25	152.2	155°	+20°	08^h–16^h	10^h–14^h	Low
κ-Leonids (212 KLE)	Sep 06–Oct 03	Sep 21	178.5	159°	+18°	07^h–15^h	09^h–13^h	Low
Sextantids (221 DSX)	Sep 23–Oct 07	Sep 30	187.5	154°	00°	06^h–12^h	06^h–13^h	Medium

3.3 Daytime Sagittariids/ Capricornids (115 DSC)

Period	January 13–February 04
Maximum	$\lambda_\odot = 312\,\overset{\circ}{.}5$ ($\approx$ February 01)
Radiant	$\alpha = 299^\circ \quad \delta = -15^\circ$
Velocity	28 km/s

In February, there are two showers with radiants being 10–15° west of the Sun at maximum. Hence these cannot be regarded as targets for optical observations from both hemispheres. The Sagittariids/Capricornids (115 DSC) have been listed by several authors in the 1970s (Sekanina 1973; Gartrell & Elford 1975; Sekanina 1976). Recent radio results have implied that the DSC maximum may fall variably between February 1 and 4. The radiant positions given in the referenced papers differ from each other and indicate some uncertainty here.

3.4 Daytime χ-Capricornids (114 DXC)

Period	January 29–February 28
Maximum	$\lambda_\odot = 324\,\overset{\circ}{.}7$ ($\approx$ February 13)
Radiant	$\alpha = 315^\circ \quad \delta = -24^\circ$
Velocity	18.5 km/s

Little is known about this shower. The only reference given in the MDC database to the χ-Capricornids (114 DXC) is Sekanina (1973). The shower does not appear in the recent CMOR study. Janches et al. (2013). find it earlier between January 11 and 21, then with a radiant west of the given position (300°, −32°). The activity level is low.

3.5 Daytime April Piscids (144 APS)

Period	April 08–29
Maximum	$\lambda_\odot = 30\,\overset{\circ}{.}3$ ($\approx$ April 20)
Radiant	$\alpha = 7^\circ \quad \delta = +7^\circ$
Velocity	29 km/s

Orbital elements of the stream

Ω	ω	i	e	q	a
$32\,\overset{\circ}{.}3$	$216\,\overset{\circ}{.}9$	$79\,\overset{\circ}{.}2$	0.865	0.912 au	6.8 au

At end-April the April Piscids (144 APS) are noted with a low activity. The only reference given in the MDC database is Kashcheyev & Lebedinets (1967), but the shower is also found recently by the CMOR (Brown et al., 2008) and activity has been reported by radio observers as well.

3.6 Daytime ε-Arietids (154 DEA)

Period	April 24–May 27
Maximum	$\lambda_\odot = 48\,\overset{\circ}{.}7$ ($\approx$ May 09)
Radiant	$\alpha = 44^\circ \quad \delta = +21^\circ$
Velocity	21 km/s

The situation is not much different for the ε-Arietids (154 DEA) with radiant positions differing in right ascension by about 15° between the only two references, Nilsson (1964) and Sekanina (1976). Like for the previous daytime showers, the activity level is low.

3.7 Daytime May Arietids (294 DMA)

Period	May 04–June 06
Maximum	$\lambda_\odot = 55\,\overset{\circ}{.}5$ ($\approx$ May 16)
Radiant	$\alpha = 37^\circ \quad \delta = +18^\circ$
Velocity	22 km/s

No precise data for radiant and activity period is given for the entry May Arietids (294 DMA) in the MDC list, where it is designated as "Daytime May Arietid Complex". The shower which is listed in the CMOR data (Brown et al., 2008) deviates in its radiant position and activity period and is called "Southern Daytime May Arietds" (see next section). The activity level is reported to be low.

3.8 Southern Daytime May Arietids (156 SMA)

Period	Apr 20–May 22
Maximum	$\lambda_\odot = 47\,\overset{\circ}{.}5$ ($\approx$ May 08)
Radiant	$\alpha = 29^\circ \quad \delta = +10^\circ$
Velocity	28 km/s

Orbital elements of the stream

Ω	ω	i	e	q	a
$227\,\overset{\circ}{.}1$	$232\,\overset{\circ}{.}3$	$4\,\overset{\circ}{.}4$	0.779	0.297 au	1.3 au

This shower is considered as an "established shower" in the MDC list. It is detected in the CMOR data (Brown et al., 2008), but is another shower with a low activity level.

The shower's designation indicates that there might be a northern branch as well, but this is not detected in the CMOR data. The references to the Northern Daytime May Arietids (155 NMA; MDC working status) go back to Nilsson (1964) and Sekanina (1976).

3.9 Daytime ω-Cetids (152 NOC, 153 OCE)

	Northern ω-Cetids (152 NOC)
Period	April 20–May 20
Maximum	$\lambda_\odot = 47\overset{\circ}{.}5$ ($\approx$ May 08)
Radiant	$\alpha = 9^\circ \quad \delta = +19^\circ$
Velocity	37 km/s
	Southern ω-Cetids (153 OCE)
Period	April 24–May 20
Maximum	$\lambda_\odot = 49\overset{\circ}{.}5$ ($\approx$ May 10)
Radiant	$\alpha = 23^\circ \quad \delta = -3^\circ$
Velocity	37 km/s
	***o*-Cetids (293 DCE)**
Period	May 05–June 02
Maximum	$\lambda_\odot = 59\overset{\circ}{.}3$ ($\approx$ May 20)
Radiant	$\alpha = 28^\circ \quad \delta = -4^\circ$
Velocity	37 km/s

Orbital elements of the streams

Ω	ω	i	e	q	a
152 NOC					
$45\overset{\circ}{.}1$	$33\overset{\circ}{.}4$	$29\overset{\circ}{.}9$	0.902	0.131 au	1.3 au
153 OCE					
$225\overset{\circ}{.}2$	$216\overset{\circ}{.}8$	$31\overset{\circ}{.}4$	0.897	0.150 au	1.5 au

For example, we refer to the 293 DCE listed in the IAU MDC database as "Daytime ω Cetid complex" (some compilations list *o*-Cetids here). Data is needed to clarify the uncertain radiant and activity as there is no reference given for the entry 293 of the MDC database. Radio observers, however, reported "medium" activity from the *o*-Cetids in the past. Recent observations for all the activity which can be associated with either of the Cetid sources show a "low" activity level only.

CMOR data (Brown et al., 2008) yield the two radiants designated as Northern ω-Cetids (152 NOC) and Southern ω-Cetids (153 OCE). The table of radiants detected by the southern SAAMER system (Janches et al., 2013) includes only the Southern ω-Cetids (153 OCE) between $\lambda_\odot = 40^\circ$ and 57°(May 1–18), fitting the radiant derived from the CMOR data.

3.10 Daytime Arietids (171 ARI)

Period	May 22–July 02
Maximum	$\lambda_\odot = 76\overset{\circ}{.}7$ ($\approx$ June 07)
Radiant	$\alpha = 44^\circ \quad \delta = +24^\circ$
Velocity	38 km/s

Orbital elements of the stream

Ω	ω	i	e	q	a
$75\overset{\circ}{.}0$	$30\overset{\circ}{.}0$	$3\overset{\circ}{.}3$	0.943	0.096 au	1.7 au

The Arietids are one of the showers listed with a high activity level. The original data go back to Clegg, Hughes & Lovell (1947), Lovell (1954) and Sekanina (1976). Almond (1951) published orbits of the streams. The CMOR data (Brown et al., 2008) indicates its strength as the stream is defined by more than 2100 orbits (typical numbers for other streams are of order a few hundred). The shower is also well detected by the southern SAAMER radar (Janches et al, 2013).

The same authors are quoted by the MDC for the showers ζ-Perseids (172 ZPE) and β-Taurids (173 BTA), which are prominent in recent analyses (Brown et al., 2008) as well. The Arietid and ζ-Perseid maxima tend to blend into one another, producing a strong radio signature for several days in early to mid June. There are indications these two June shower maxima currently each occur up to a day later than indicated in our Table.

The radiant is about 30° west of the Sun. For observers roughly between the tropics there is a chance to observe a few shower meteors in early June close to dawn, albeit with low radiant position. Some data of such optical (video) observations have been reported by Fujiwara et al. (2004) and Jenniskens et al. (2012). The radiant is also detected from EDMOND video data (Rudawska et al., 2014). While the radiant and orbital data are well established, there are only estimates of the activity or flux. Campbell-Brown (2004) gives a ZHR of about 200 and compares the shower with the Quadrantids, assuming $r = 2.75$ ($s = 2.1$).

Based on meteoroid orbital data Jenniskens et al. (2012) suggest an association of the Arietids with the Marsden group comet C/1999 J6 (= 2004 V9 = 2010 H3) and argue that it seems possible that the meteoroids are debris from a breakup which created the Marsden group comets or are connected with an earlier fragmentation that left comet 96P/Machholz,

3.11 Daytime ζ-Perseids (172 ZPE)

Period	May 20–July 05
Maximum	$\lambda_\odot = 78\overset{\circ}{.}6$ ($\approx$ June 09)
Radiant	$\alpha = 62^\circ \quad \delta = +23^\circ$
Velocity	26 km/s

Orbital elements of the stream

Ω	ω	i	e	q	a
$75\overset{\circ}{.}0$	$58\overset{\circ}{.}9$	$3\overset{\circ}{.}7$	0.763	0.349 au	1.5 au

As mentioned, the shower is listed in Lovell (1954) and Sekanina (1976) and was recorded by radio observers with a rather high activity. The numbers found from the CMOR analysis (Brown et al., 2008) hint at a lower activity level. From the available data it is difficult to judge whether this difference is due to the fact that the radar sees much smaller meteoroids as compared to the forward scatter systems. Further, the ac-

tivity period and the radiant position differ between the two populations: May 20–July 05, maximum June 09, $\alpha = 62°$, $\delta = +23°$ (radio); May 07–June 26, maximum June 14, $\alpha = 65°$, $\delta = +28°$ (radar)

3.12 Daytime β-Taurids (173 BTA)

Period	June 05–July 17
Maximum	$\lambda_\odot = 96\overset{\circ}{.}7$ ($\approx$ June 28)
Radiant	$\alpha = 86°$ $\delta = +19°$
Velocity	27 km/s

Orbital elements of the stream

Ω	ω	i	e	q	a
$274\overset{\circ}{.}1$	$244\overset{\circ}{.}7$	$3\overset{\circ}{.}5$	0.787	0.377 au	1.8 au

The situation regarding the data is similar to the two entries above. In this case, the radio observers list it as a medium active shower, while the radar data hint at a low activity level only. The activity period, the expected maximum and the radiant position are in good agreement between the few referenced sources. There are almost continuous annual observations reported in publications from Jodrell Bank between 1947–1958 inclusive, with published southern hemisphere results from 1953 and 1961, before Sekanina between 1961–65 and 1968–69, but no more recent data.

3.13 Daytime γ-Leonids (203 GLE), Daytime κ-Leonids (212 KLE)

	γ-Leonids (203 GLE)
Period	August 14–September 12
Maximum	$\lambda_\odot = 152\overset{\circ}{.}2$ ($\approx$ August 25)
Radiant	$\alpha = 155°$ $\delta = +20°$
Velocity	20 km/s
	κ-Leonids (212 KLE)
Period	September 06–October 03
Maximum	$\lambda_\odot = 178\overset{\circ}{.}5$ ($\approx$ September 21)
Radiant	$\alpha = 159°$ $\delta = +18°$
Velocity	42 km/s

Orbital elements of the stream: 212 KLE

Ω	ω	i	e	q	a
$182\overset{\circ}{.}6$	$33\overset{\circ}{.}9$	$22\overset{\circ}{.}7$	0.970	0.099 au	3.3 au

After the peak period in June daylight sources include the visually-impossible γ-Leonids (203 GLE; Sekanina, 1976). The peak should be on August 25, albeit not found in recent radio results. Another shower, not listed in the compilations from forward scatter radio data is the κ-Leonids (212 KLE) found in radar data between September 6 and October 3 with a maximum on September 21 (Brown et al., 2008). The data strongly suggest that these are different streams because of the very different velocities. For both the expected activity level is low.

3.14 Daytime Sextantids (221 DSX)

Period	September 09–October 09
Maximum	$\lambda_\odot = 184\overset{\circ}{.}3$ ($\approx$ September 27)
Radiant	$\alpha = 152°$ $\delta = 0°$
Velocity	32 km/s

Orbital elements of the stream

Ω	ω	i	e	q	a
$6\overset{\circ}{.}5$	$213\overset{\circ}{.}7$	$20\overset{\circ}{.}4$	0.8336	0.168 au	1.0 au

For this shower with 'medium' activity we find more than just one recent reference, indicating that it is regularly found in various radar data (Galligan & Baggaley, 2002; Brown et al., 2008). The 'medium' activity level comes from Weiss (1960), giving a numerical level like the Jodrell Bank ones for the o-Cetids and β-Taurids. Forward-scatter data could even suggest 'high' activity, at least occasionally.

The DSX-maximum is expected around September 27 ($\lambda_\odot = 184\overset{\circ}{.}3$). In 1999 a strong return was detected at $\lambda_\odot \sim 186°$, while in 2002, the September 27 peak was not found, but one around September 29–30 was. The CMOR radar data confirm rather the late maximum at $\lambda_\odot = 187\overset{\circ}{.}5$. Janches et al. (2013) detect activity with their radar between $\lambda_\odot = 179°$ and 184°. Several minor maxima in early October may also be due to this radio shower.

Optical observers may hope to catch some Sextantids in the pre-dawn of late September, though radiant-rise is less than an hour before sunrise in either hemisphere. For example, at 25° northern latitude, the radiant reaches about 15° elevation at 5^h local time. The radiant is found from video data (Rudawska et al., 2014). Activity analyses are still missing.

3.14.1 Concluding remarks

Radar and radio (forward scatter) data will be the major source regarding daytime meteor showers. The shower identification (radiant and orbits) found from different observational data sets is consistent. Physical parameters, such as the population/mass index and rate/flux, need to be determined. In the case of two showers, the Arietids (171 ARI) and Sextantids (221 DSX), a limited amount of optical data may be used for calibration purposes.

References

Almond M., 1951: The summer daytime meteor streams of 1949 and 1950. III. Computation of the orbits. *MNRAS* **111,** 37–44.

Babadzhanov P.B., Kokhirova G.I., Khamroev U.Kh., 2014: The Capricornids asteroid-meteoroid complex, in: T.J. Jopek, F.J.M. Rietmeijer, J. Watanabe, I.P. Williams (eds.), Meteoroids 2013, Proc. Int. Conf. Poznań, Poland, 199–204

Babadzhanov P.B., Williams I.P., Kokhirova G.I., 2013: Near-Earth asteroids among the Scorpiids meteoroid complex. *A & A* **556,** A25, 5pp..

Blaauw R.C., Campbell-Brown M.D., Weryk R.J., 2011: A meteoroid stream survey using the Canadian Meteor Orbit Radar – III. Mass distribution indices of six major meteor showers. *MNRAS* **414,** 3322–3329.

Brown P., Weryk R.J., Wong D.K., Jones J., 2008: A meteoroid stream survey using the Canadian Meteor Orbit radar I. Methodology and radiant catalogue. *Icarus* **195,** 317–339.

Brower J., 2006: Global forward scatter observations of the 2006 Quadrantid maxima. *WGN* **34,** 25–29.

Campbell-Brown M.D., 2004: Radar observations of the Arietids. *MNRAS* **352,** 1421–1425.

Clegg J.A., Hughes V.A., Lovell A.C.B., 1947: The daylight meteor streams of 1947 May-August. *MNRAS* **107,** 369–378.

Fujiwara Y., Ueda M., Sugimoto M., Sagayama T., Abe S., 2004: TV observation of the daytime meteor shower; the Arietids. *EMP* **95,** 595–600.

Galligan D.P., Baggaley W.J., 2002: Wavelet enhancement for detecting shower structure in radar meteoroid data II. Application to the AMOR data, in: S.F. Green, I.P. Williams, J.A.M. McDonnell and N. McBride (eds.), Dust in the Solar System and Other Planetary Systems, Proceedings of IAU Coll. 181, Kent, UK, April 2000, Oxford, Pergamon (COSPAR colloquia series, Vol. 15), p.48

Gartrell G., Elford W.G., 1975: Southern hemisphere meteor stream determinations. *Australian Journal of Physics* **28,** 591–620.

Janches D., Hormaechea J.L., Brunini C., Wocking W., Fritts D.C., 2013: An initial meteoroid stream survey in the southern hemipshere using the Southern Argentina Agile Meteor Radar (SAAMER). *Icarus* **223,** 677–683.

Jenniskens P., Duckworth H., Grigsby B., 2012: Daytime Arietids and Marsden sunskirters (ARI, IAU #171). *WGN* **40,** 98–100.

Kashcheyev B. L., Lebedinets V. N., 1967: Radar studies of meteors. *Smithsonian Contr. Astrophysics* **11,** 183–199.

Lovell B., 1954: Meteor astronomy. Oxford, Clarendon Press.

McBeath A., 1998: The forward scatter meteor year, in: A. Knöfel & A. McBeath (eds.), Proc. IMC Petnica 1997, 39–54

Neslušan L., Kaňuchová Z., Tomko D., 2013: The meteor-shower complex of 96P/Machholz revisited. *Astron. Astrophys.* **551,** A87, 14 pp. (DOI: 10.1051/0004-6361/201220299.

Neslušan L., Hajduková, jr. M., Jakubík M., 2013: Meteor-shower complex of asteroid 2003 EH1 compared with that of comet 96P/Machholz. *Astron. Astrophys.* **560,** A47, 10 pp. (DOI: 10.1051/0004-6361/201322228).

Nilsson C.S., 1964: A southern hemisphere radio survey of meteor streams. *Australian Journal of Physics* **17,** 205–256.

Ogawa H., Toyomasu S., Ohnishi K., Amikura S., Maegawa K., Jenniskens P., 2002: The 2002 Leonids as monitored by the International Project for Radio Meteor Observations. *WGN* **30,** 225–231.

Ohtsuka K., Sekiguchi T., Kinoshita D., Watanabe J.-I., Ito T., Arakida H., Kasuga T., 2006: Apollo asteroid 2005 UD: split nucleus of (3200) Phaethon?. *Astron. Astrophys.* **450,** L25–L28.

Rudawska R., Matlovič P., Tóth J., Kornoš L., 2014: Independent identification of meteor showers in EDMOND database, *to be published in Astron. Astrophys.*, eprint arXiv:1406.6598

Sekanina Z., 1973: Statistical model of meteor streams. III. stream search among 19303 radio meteors. *Icarus* **18,** 253–284.

Sekanina Z., 1976: Statistical model of meteor streams. IV a study of radio streams from the synoptic year. *Icarus* **27,** 265–321.

Steyaert C., Brower J., Verbelen F., 2006: A numerical method to aid in the combined determination of stream activity and observability function. *WGN* **34,** 87–93.

Weiss A., 1960: Radio-echo observations of southern hemisphere meteor shower activity from 1956 December to 1958 August. *MNRAS* **120,** 387–403.

Chapter 4

Appendix

4.1 List of extreme events documented over the past ≈ 50 years

Table 4.1: Highest visible activity (ZHR/EZHR)

Shower (trail)	Year	ZHR	Reference
Highest ZHR			
Leonids (1 revolution)	1966	$\approx 120\,000$	Jenniskens, 2006
Leonids (3 revolution)	1999	3700±100	Table at page 55
Leonids (4 revolution)	2001	3430± 90	Table at page 55
Leonids (4 revolution)	2002	2940±210	Table at page 55
Leonids (9 revolution)	2001	2830± 70	Table at page 55
Leonids (7 revolution)	2002	2510± 60	Table at page 55
Leonids (7 revolution)	2001	1620± 40	Table at page 55
Draconids	1998	720± 90	Arlt, 1998a
Leonids (4 revolution)	2000	480± 20	Table at page 55
Draconids	2011	400±100	Borovička et al., 2012
Leonids (20 revolution)	1998	357± 11	Table at page 55
Perseids	1991	284± 63	Brown & Rendtel, 1996
Perseids	1993	264± 17	Brown & Rendtel, 1996
Perseids	1994	238± 17	Brown & Rendtel, 1996
Highest EZHR			
α-Monocerotids	1995	450± 30	Rendtel et al., 1996
Aurigids	2007	132± 26	Rendtel, 2007

Table 4.2: Extreme particle population – lowest population index r

Shower	Year	r	Reference
Leonids (20 revolution)	1998	1.19 ± 0.02	Arlt, 1998b
September ε–Perseids	2013	1.45 ± 0.15	Rendtel et al., 2014
Orionids	2006	1.58 ± 0.08	Rendtel, 2007a
Leonids (background component)	2001	1.60 ± 0.05	Arlt et al., 2001
Geminids (end of peak plateau)	2004	1.73 ± 0.04	Arlt & Rendtel, 2006
Aurigids	2007	1.74 ± 0.08	Rendtel, 2007b
Perseids	1993	1.75 ± 0.05	Rendtel, 1993

Table 4.3: Longest peak duration (FWHM) of active showers (minor showers with no pronounced peak may have wider FWHM) and most narrow peaks.

Longest peak duration			
Orionids	2006	5 days, ZHR ≈ 55	Arlt et al., 2008
Orionids	2007	2 days, ZHR ≈ 75	Arlt et al., 2008
Geminids	regular maximum	1 day, ZHR 100–120	Rendtel, 2005
Leonids	1998	12 hours, ZHR ≈ 350	Arlt, 1998b
June Bootids	1998	$\geq$ 12 hours, ZHR 50–100	Arlt et al., 1999
Most narrow peaks			
α-Monocerotids	1995	20 min	Rendtel et al., 1996
Aurigids	2007	30 min	Rendtel, 2007

References

Arlt R., 1998a: Summary of 1998 Draconid outburst observations. *WGN* **26,** 256–259.

Arlt R., 1998b: Bulletin 13 of the International Leonid Watch: the 1998 Leonid meteor shower. *WGN* **26,** 239–248.

Arlt R., Kac J., Krumov V., Buchmann A., Verbert J., 2001: Bulletin 17 of the International Leonid Watch; first global analysis of the 2001 Leonid storms. *WGN* **29,** 187–194.

Arlt R., Rendtel J., 2006: The activity of the 2004 Geminid meteor shower from global visual observations. *MNRAS* **367,** 1721–1726.

Arlt R., Rendtel J., Bader P., 2008: The 2007 Orionids from visual observations. *WGN* **36,** 55–60.

Arlt R., Rendtel J., Brown P., Velkov V., Hocking W.K., Jones J., 1999: The 1998 Outburst and History of the June Bootid Meteor Shower. *MNRAS* **308,** 887–896.

Borovička J., Koten P., Shrbený L., Štork R., Hornoch K., 2012: Radiants, orbits, spectra and deceleration of slected 2011 Draconids. In: M. Gyssens & P. Roggemans (eds.) Proc. of the IMC 2012, IMO, 2013, pp. 65–69.

Brown P., Rendtel J., 1996: The Perseid meteoroid stream: characterization of recent activity from visual observations. *Icarus* **124,** 414–428.

Jenniskens P., 2006: Meteor showers and their parent comets. Cambridge Univ. Press.

Rendtel J., 1993: Perseids 1993: a first analysis of global data. *WGN* **21,** 235–239.

Rendtel J., 2005: Evolution of the Geminids observed over 60 years. *EMP* **95,** 27–32.

Rendtel J., 2007a: Three days of enhanced Orionid activity in 2006 – meteoroids from a resonance region?. *WGN* **35,** 41–45.

Rendtel J., 2007b: Visual observations of the Aurigid peak on 2007 September 1. *WGN* **35,** 108–112.

Rendtel J., Brown P., Molau S., 1996: The 1995 outburst and the possible origin of the α-Monocerotid meteoroid stream. *MNRAS* **279,** L31–L36.

Rendtel J., Lyytinen E., Molau S., Barentsen G., 2014: Peculiar activity of the September ε-Perseids on 2013 September 9. *WGN* **42,** 40–47.

4.2 Glossary

a: → semimajor axis of an orbit.

ablation: removal of material by attrition, e.g., by passage through the atmosphere.

absolute magnitude: the stellar magnitude any meteor would have if placed in the observer's zenith at a height of 100 km.

altiude: the angular distance of a celestial body above or below the horizon, measured along the great circle passing through the body and the zenith. Altitude is 90° minus zenith distance.

Amor asteroids: asteroids having perihelion distance $1.017\text{au} < q \leq 1.3\text{au}$.

aphelion distance: Q, distance of greatest heliocentric separation for a body in an eccentric orbit; $Q = a(1 + e)$.

Apollo asteroids: asteroids having semimajor axis $a \geq 1.0$au, and perihelion distance $q \leq 1.017$au.

ascending node: → nodes.

asteroid: one of a number of objects ranging in size from sub-km to about 1000 km, most of which lie between the orbits of Mars and Jupiter; also called 'minor planet'. Their designations are supplied by the Minor Planet Center.

The preliminary designations consist of the year of discovery, an upper case letter to indicate the half-month in that year (A = Jan. 1–15, B = Jan. 16–31, ... Y = Dec. 16–31, I being omitted), a second upper case letter in sequence, and when this sequence of 25 (I again being omitted) has been completed it is repeated and followed by a sequential number (written as a subscript, if possible). Before 1925 the system consisted simply of a sequential pair of letters (and initially only a single letter), and the subsequent interpolation of additional objects was troublesome. The modern system is therefore now also used for unnumbered pre-1925 objects, except that the initial 1 in the year is replaced by A.

The permanent designation consists of numbers and names, beginning with 1 Ceres, given to asteroids for which orbits are accurately determined. Asteroid 4000 was numbered in February 1989. The numbers are supplied by the Minor Planet Center after orbits have been fitted to observations at several different oppositions. Names are proposed by discoverers to the Committee on Small Body Nomenclature of IAU Commission 20 and cannot be adopted until the least two months after an asteroid is numbered. If the discoverer is deceased there is a waiting period of six months, and names are usually proposed by the orbit identifier or by the discoverer's former colleagues.

Aten asteroids: asteroids having semimajor axis $a < 1.0$ au, and aphelion distance $Q > 0.983$ au.

au: astronomical unit. The mean distance of the Earth from the Sun, equal to 1.496×10^{11} m.

azimuth: the angular distance measured clockwise along the horizon from a specified reference point (usually north) to the intersection with the great circle drawn from the zenith through a body on the celestial sphere.

bolide: → fireball.

Brownlee particles: interplanetary dust particle (IDP), also known as a micrometeoroid or, after entry into the Earth's atmosphere, a → micrometeorite. Sometimes called Brownlee particle.

comet: an object composed of solid particles and volatile ices (such as H_2O, CO, CO_2, NH_3). When a comet moves close enough to the Sun, the higher temperature causes ices near the surface to sublimate. As the gases expand, they drag → meteoroids with them, away from the comet's solid nucleus. Meteoroids escaping the nucleus move on to orbits independent of (though initially similar to) the comet. Gas molecules liberated from the nucleus are subsequently photodissociated (producing OH, CN, C_2 etc.) or ionized by solar radiation.

Icy bodies too far from the Sun to show activity (escaping gas and dust) are classified observationally and in databases with → asteroids. An active comet shows a coma (expanding cloud of escaping matter), and sometimes a dust tail and an ion tail, around perihelion. Comets become extinct if enough volatiles are lost. Active lifetimes are typically hundreds of perihelion passages.

Most active comets have highly elliptical orbits (or even parabolic to within observed accuracy), nearly always dynamically unstable. Orbits can reach a few times 10^4 au from the Sun. Long-period (> 200 year) orbits comprise a substantial majority of the discovered population. Known, active comets tend to have a nuclear diameter between a kilometer and a few tens of km.

comets, nomenclature (old): when a newly discovered comet is confirmed, the IAU Central Bureau for Astronomical Telegrams assigns a provisional designation consisting of the year of discovery followed by a lowercase letter in order of discovery for that year. The discoverer's name is attached to the designation. If a reliable orbit is later established, the comet is given a permanent designation consisting of the year of perihelion passage followed by a Roman numeral in order of perihelion passage. Comets with orbital periods > 200 years are called 'long-period'; those with periods < 200 years are indicated by P/ preceding the name of the comet and are called 'short period' comets.

comets, nomenclature (new): the principal designations used for comets consist of the year and an upper-case letter to indicate the halfmonth of discovery in that year (A = Jan. 1–15, B = Jan. 16–31, C = Feb. 1–15, ..., Y = Dec. 16–31, I being omitted), followed by a numeral showing the order of announcement of discovery in that halfmonth. The halfmonths are as used for discoveries of minor planets, the difference being that minor-planet designations have a second letter (in addition to possible numerals) to indicate the order of discovery announcement. 'Discovery' refers to the time when the discovery observation is actually made. The new cometary designations are prefixed, generally by P/ or C/, according as to whether it is a short-period orbit or not. The symbol D/ is used for 'defunct' comets, or periodic comets which either are known no longer to exist, or for which the (current) orbit is poorly known. The prefix A/ would be used to denote an object given a cometary designation but deemed to be a minor planet. X/ is used for comets for which it is not possible to compute orbits – and that in some cases may never in fact have existed. Permanent numbers are given to periodic comets when they are confirmed as returning to perihelion more than once; the permanent number is written before the P, e.g. 1P/Halley.

declination: angular distance north or south of the celestial equator.

descending node: → nodes.

direct motion: → prograde motion.

dust: particles originating or existing in space with sizes smaller than 100μm.

e: eccentricity of an elliptical orbit. The amount by which the orbit deviates from circularity: $e = c/a$, where c is the distance from the center to a → focus and a is the → semimajor axis.

ecliptic: plane of the Earth's orbit.

epoch: an arbitrary fixed instant of time or date used as a chronological reference datum for calendars, celestial reference systems, star catalogs, or orbital motions.

escape velocity: the velocity required to escape entirely from the gravitational field of an astronomical body; equlas the minimum impact velocity for any body arriving from a very great distance.

fall: a meteorite that was seen to fall. Such meteorites are usually recovered soon after the fall and are relatively free of terrestrial contamination and weathering effects.

find: a meteorite that was not seen to fall but was found and recognized subsequently.

fireball: a bright meteor, also called bolide. Several definitions have been used by various authors. In the IMO all meteors of at least -3^{m} are regarded as fireballs. Extremely bright events (magnitude -17 or brighter) are designated as "superbolides".

focus: in an astronomical context, the focus of an elliptical orbit is the point where the sun is located. In geometry, an ellipse has two foci; astronomers call the focus without the sun the empty focus.

geocentric: Earth-centered.

heliocentric: Sun-centered.

horizon: a plane perpendicular to the line from an observer to the zenith. The great circle formed by the intersection of the celestial sphere with a plane perpendicular to the line from an observer to the zenith is called the astronomical horizon.

i: inclination of an orbit. The angle between an asteroid's orbit and the plane of the → ecliptic (or between a satellite's orbit and the planet's equatorial plane).

$\lambda_\odot$: → solar longitude.

long-period comet: a comet with an almost parabolic orbit and a period of revolution round the Sun exceeding 200 years. Some have orbital periods of millions of years.

magnitude: an arbitrary number, measured on a logarithmic scale, used to indicate the brightness of an object. If I_i is the brightness of star i amd m_i its magnitude, then $m_1 - m_2 = -2.5\log(I_1/I_2)$. Two stars differing by 5 magnitudes differ in luminosity by a factor of 100. One magnitude difference is the fifth root of 100, or a factor of about 2.512. The brighter the star, the lower the numerical value of the magnitude and very bright objects have negative magnitudes.

mass index: s – the number N of meteoroids having individual masses between m and $M + dM$ is $N = \text{constant} \times M^s$. The cumulative number of particles with masses greater than M is proportional to M^{1-s}. The → population index r can be converted into the mass index s. Assuming that the shape of the meteor light curve does not change over the magnitude range and based on a mass–luminosity relation published by Verniani, $s = 1 + 2.3\log r$.

meteor: the light phenomenon produced by a → meteoroid experiencing frictional heating when entering a planetary atmosphere; also used for the glowing meteoroid itself. If particularly large, it is

described as a → fireball.

meteoric: the adjectival form pertaining to meteor and meteoroid.

meteorite: a natural object of extraterrestrial origin (→ meteoroid) that survives passage through the atmosphere.

meteoroid: a natural small (generally sub-km; commonly 100μm to 10 m) solid object in an independent orbit in the Solar System.

meteoroid stream: stream of solid particles released from a → parent body (→ comet or → asteroid), generally through the influence of Solar radiation. The various ejection directions and ejection speeds of individual → meteoroids determine the width of a stream and the particles' distribution around the overall average orbit.

meteor shower: many → meteors appearing to radiate from a common point in the sky caused by the collision of the Earth with a swarm of meteoric particles.

micrometeorite: a small extraterrestrial particle that has survived entry into the Earth's atmosphere. The actual size is not rigorously constrained but is operationally defined by the collection procedure because small particles are more abundant than large ones. In practice, the micrometeorites being studied in the laboratory after collection in the stratosphere are rarely as large as 50μm.

minor planet: → asteroid.

nodes: the points at which the orbit of a planet, asteroid, comet or meteoroid crosses the plane of the → ecliptic. The object moves from south to north of the ecliptic at the ascending node, and from north to south at the descending node. The longitude of the ascending node is one of the six orbital elements and measures the angle between the ascending node and → vernal equinox, measured in the plane of the ecliptic.

ω: argument of perihelion or periapse for a planet or satellite. Angular distance (measured in the plane of a body's orbit in the direction of motion) from the ascending → node to the → perihelion point.

Ω: longitude of ascending → node. The angle between some line in the reference plane (usually the direction to the → vernal equinox) and the point where the body crosses the reference plane moving south to north.

orbital elements: six quantities that fully describe an orbit; along with the time, they specify the position of an orbiting body along its path. A typical set of orbital elements are: (1) → semimajor axis a; (2) → eccentricity e; (3) → inclination i; (4) longitude of the ascending → node Ω; (5) argument of periapse ω; and (6) the time of passage through periapse T.

parent body: a → comet or → asteroid which released → meteoroids, dust, and gas when approaching the inner Solar System for a potential → meteoroid stream.

Also used for the body on or in which a given meteorite or class of meteorites was located prior to ejection as ≈ meter-sized objects.

perihelion distance: q, distance of the least heliocentric separation for a body in an eccentric orbit; $q = a(1 - e)$.

persistent train: ⟶ train.

perturbation: the gravitational effect of one object on the orbit of another, if this effect is very small.

Poynting-Robertson effect: a dissipative force due to the anisotropic loss of momentum by a particle through re-radiation of solar energy. This causes aphelion collapse such that a circular orbit is soon attained; thereafter the particle spirals slowly toward the Sun. Small particles (below 1 cm) are most severely affected because the force (relative to solar gravity) varies as the reciprocal of its size.

prograde motion: motion in the same direction as the prevailing direction of motion. As viewed from the north, prograde motion is counter-clockwise, or west to east.

q: → perihelion distance.

Q: → aphelion distance.

radiant: the point where the backward projection of the meteor trajectory intersects the celestial sphere, or the backwards prolongation of the apparent trails of a given meteor as seen by observers at different locations.

right ascension: angular distance east of the → vernal equinox, as measured on the celestial equator.

semimajor axis: half the length of the major axis (long axis) of an ellipse; a standard element used to describe an elliptical orbit.

short-period comet: a → comet with an orbital period of < 200 years.

solar longitude: $\lambda_\odot$, angular distance along the Earth's orbit, measured from the → vernal equinox. It gives the position of the Earth at its orbit and

hence is more appropriate information on a meteor shower's maximum than the date.

standard epoch: a date and time that specifies the reference system to which celestial coordinates are referred. Prior to 1984 coordinates of star catalogs were commonly referred to the mean equator and equinox of the beginning of a Besselian year. Beginning with 1984 the Julian year has been used, as denoted by the prefix J, e.g., J2000.0.

sunrise, sunset: the times at which the apparent upper limb of the Sun is on the astronomical horizon; i.e., when the true zenith distance, referred to the center of the Earth, of the central point of the disk is 90°50′, based on adopted values of 34′ for horizontal refraction and 16′ for the Sun's semidiameter.

superbolide: → fireball.

train: light/material behind the meteoroid.
- *wake* – luminosity just behind the meteor head.
- *green train* – short-duration trains exclusively formed by the green oxygen line at 557.7 nm.
- *persistent train* – self-luminous, visible for tens of minutes after the meteor.
- *reflection/dust train* – not self-luminous; visible in twilight/daylight.

trajectory: path of a meteor in the Earth's atmosphere.

twilight: the interval of time preceding sunrise and following sunset during which the sky is partially illuminated. Civil twilight comprises the interval when the zenith distance, referred to the center of the Earth, of the central point of the Sun's disk is between 90°50′ and 96°, nautical twilight comprises the interval from 96° to 102°, astronomical twilight comprises the interval from 102° to 108°.

Universal Time (UT): the local mean time of the prime meridian. It is the same as Greenwich mean time, counted from 0 hour beginning at Greenwich (observatory) mean midnight.

vernal equinox: the intersection of ecliptic and celestial equator where the Sun is moving from south to north.

wake: → train.

Yarkovsky effect: the effect of rotation on the trajectory of a small particle orbiting the Sun (compare → Poynting-Robertson effect). If the orbiting body is rotating, there is a temperature variation over its surface, and it will reradiate the incident radiation anisotropically.

zenith attraction: the effect of the Earth's gravity on a meteoric body increasing the velocity and moving the radiant towards the zenith.

ZHR: Zenithal Hourly Rate – number of shower meteors corrected to standard conditions.

4.3 Journal abbreviations

A & A – Astronomy and Astrophysics
BAC – Bulletin of the Astronomical Institutes of Czechoslovakia
EMP – Earth, Moon, and Planets
JBAA – Journal of the British Astronomical Association
MNRAS – Monthly Notices of the Royal Astronomical Society

The International Meteor Organization

web site http://www.imo.net

Council

President: Cis Verbeeck, Bogaertsheide 5, 2560 Kessel, Belgium.
E-mail: cis.verbeeck@scarlet.be

Vice-President: Jürgen Rendtel, Eschenweg 16, 14476 Potsdam, Germany.
E-mail: jrendtel@web.de

Secretary-General: Robert Lunsford, 1828 Cobblecreek Street, Chula Vista, CA 91913-3917, USA.
E-mail: lunro.imo.usa@cox.net

Treasurer: Marc Gyssens, Heerbaan 74, 2530 Boechout, Belgium.
E-mail: marc.gyssens@uhasselt.be

Other Council members:

David Asher, Armagh Observatory, College Hill, Armagh BT61 9DG, Northern Ireland, UK.
E-mail: dja@star.arm.ac.uk

Geert Barentsen, University of Herfordshire, Hatfield AL10 9AB
E-mail: geert@barentsen.be

Javor Kac, Na Ajvov hrib 24, 2310 Slovenska Bistrica, Slovenia
E-mail: javor.kac@gmail.com

Detlef Koschny, Zeestraat 46, 2211 XH Noordwijkerhout, Netherlands
E-mail: detlef.koschny@esa.int

Sirko Molau, Abenstalstraße 13b, 84072 Seysdorf, Germany.
E-mail: sirko@molau.de

Jean-Louis Rault, Société Astronomique de France, 16, rue de la Vallée,
91360 Epinay sur Orge, France.
E-mail: f6agr@orange.fr

Paul Roggemans, Pijnboomstraat 25, 2800 Mechelen, Belgium
E-mail: paul.roggemans@gmail.com

Commission Directors

Photographic Commission: William Ward, School of Engineering, Rankine Building, Oakfield Avenue, Glasgow G12 8LT, Scotland, U.K.; E-mail: photo@imo.net

Radio Commission: Jean-Louis Rault, Société Astronomique de France, 16 Rue de la Valleé, 91360 Epinay sur Orge, France; E-mail: radio@imo.net

Video Commission: Sirko Molau, Abenstalstraße 13b, 84072 Seysdorf, Germany; E-mail: video@imo.net

Visual Commission: Rainer Arlt, Bahnstraße 11, 14974 Ludwigsfelde, Germany; E-mail: visual@imo.net

.

ISBN 978-2-87355-027-1